

Republique Algérienne Démocratique et Populaire

University of Boumerdès

Faculty of Engineering

Department of Electronic and Electrical Engineering

THESIS

Presented in Partial Fulfilment of Requirement of the

DEGREE OF MAGISTER

In Electronic Systems Engineering

By:

Abdelkader ZITOUNI

*An Integrated PC-based System for Characterising
Electronic Components*

Defended On July , 1999 before the Jury :

President	: Dr. L. REFOUFI	(U B, Faculty of Engineering, DEEE)
Supervisor	: Dr. H. BOURDOUCEN	(Sultan Qaboos University, Muscat, Oman)
Members	: Pr. A. FARAH	(MC-ENP)
	Dr. A. BELOUHRANI	(MC-ENP)

Dedications

To the memory of my brother *Reda* ,

To my lovely wife ,

To my parents, sister and brothers ,

I dedicate this modest work.

Table of Content

Acknowledgements	i
Abstract	ii
Chapter 1 : Introduction	1
Chapter 2 : Description of the measurement set	4
2.1. Introduction	4
2.2. Hardware Part Description	5
2.3. Software Part description	21
2.4. Examples of the implemented software capabilities	31
Chapter 3 : Electronic components models	34
3.1. Introduction	34
3.2. Passive Components models	35
3.2.1. The Resistor equivalent circuit	35
3.2.2. The Capacitor equivalent circuit	36
3.3.3. The Inductor equivalent circuit	37
3.3.4. Models for non linear capacitors and inductors	37
3.3. Active electronic components	38
3.3.1. PN junction diode and Schottky diode	38
3.3.2. Bipolar Junction Transistors (BJTs)	43
3.3.3. Junction Field Effect transistors (JFETs).....	52
Chapter 4 : Extraction methods of model parameters	57
4.1. Introduction	57
4.2. Method of Extraction of passive devices parameters	58
4.2.1. Method of Extraction of the Resistor Model Parameters	58
4.2.2. Method of Extraction of the Capacitor Model Parameters	60
4.2.3. Method of Extraction of the Inductor Model Parameters	61
4.2.4. Implementation of the routine of extraction.....	62
4.3.Extraction of diode model parameters	65
4.4. Extraction of JFET model parameters	69
4.5. Parameters extraction of BJT model.....	71
Chapter 5 : The integrated system testing	75
5.1. Introduction	75
5.2. Testing of passive devices	75
5.3. Testing of PN junction and Shottky diodes	81
5.4. Testing of junction field effect transistors	84
5.5. Bipolar junction transistor testing	86
Chapter 6 : conclusion	89
Appendix A	91
Appendix B	93
References	94

Acknowledgements

This thesis, although it bears the name of only one author, would not have been written without the support of many others. Dr H. Bourdoucen “maitre de conférence” offered me the opportunity to carry out the work described in this thesis. I would like to thank him for this and for all his help.

A large part of this work would not have been possible without the precious contribution of Mr A. Ouadi in solving many problems related to the implementation of the optimisation methods and also for the many fruitful discussions around the obtained results.

My sincere and deep gratitude is due to the president of the jury, Dr L. Refoufi and the members of the jury Pr. A. Farah and Dr. A. Belouchrani for their acceptance to evaluate this work.

Special thanks are also dedicated to Mr A. Achour for his supply with the thick film silicon resistors which permits to carry out very interesting results.

I wish also to thank the research department head Dr. M. Nourredine, and all the staff of library for making different materials under our disposal.

Finally, I would like to thank my friends and colleagues at the department of electronics for creating a friendly and good working atmosphere

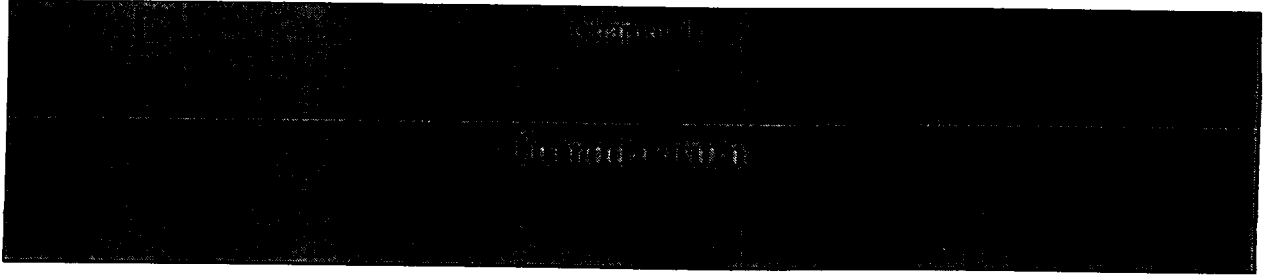
Abstract

The present work consists on the implementation of an integrated system controlled by an IBM compatible PC through an GPIB card.

The system gathers a set of HP model high quality measuring devices, the measurements of a large set of electrical parameters can hence be achieved automatically.

In addition, a set of MATLAB routines have been implemented to extract SPICE model parameters of a large set of passive and active electronic components. This allows a more accurate results to be obtained from simulation of electrical circuits.

Different methods of parameters extraction from measurement data have been tested, and satisfactory results are obtained.



As the electronic components industry continue to overcome rapidly many barriers, the characterisation tools used to understand its product behaviour must advance at the same speed. As an example, within the semiconductor field, many measurement instrument manufacturers such as Hewlett Packard (HP), have developed new sophisticated products and improve current equipment, to get high measurement resolution and hence precise semiconductor device parameters can be extracted. Furthermore, most of instruments are provided with interface buses to be remotely controlled by computer. Automated operations from measurement to analysis can thus be obtained. The IEEE bus (also known as; GPIB, GPIB or simply ASCII bus), which is used as an interface bus for the HP instruments, is one of the most popular buses used in the industry. It is a carefully defined instrumentation interfacing means, that simplifies the integration of measuring instruments and calculator or computer into a system.

This work is a description of an integrated PC-based system that takes full advantage of advanced features of the HP instruments to operate remotely via the IEEE bus in order to characterise accurately a wide set of passive and active components met in electronic industry as well as in research. The flow of data on the IEEE bus is completely monitored using a developed integrated software. Further, and in order to justify the need of such system, a set of routines for MATLAB environment have been implemented. These routines permit to extract SPICE model parameters of a large set of electronic devices including, passive elements (R, L and C) and active devices (diodes, BJTs and FETs).

The main feature of such product is its ability to carryout both measurement and analysis of electronic devices in a single unit. Conventionally two approaches are used in the testing of components supplied for industry:

- i) *Total system solutions*: they are integrated software and hardware systems, designed to maximise productivity [36]. The obtained results with this solution are extremely accurate, however it is a very expensive one. In addition a complete set is used for only one specific type of devices. This is why it is used in advanced technologies and associated complex problems.
- ii) *Low cost system solutions*: they are based on the use of suitably designed cards, which can be housed in the extension slots of the PC, in order to measure device parameters [37]. The main advantage of this solution is its low cost. But, it presents also low accuracy of measurements and, can not ensure measurement of complex devices which have more than two terminals such as, integrated circuits and even field effect transistors.

Our solution can be considered as a good compromise between the two above ones, since good accuracy is ensured with the use of high quality devices (HP models) with relatively low cost in comparison with the total systems. Furthermore, the system offers the ability to characterise a large spectrum of components from passive devices to active, discrete or integrated ones.

An interesting feature of our integrated system is the developed function library with the help of which the integrated software was built. This library groups the major functions used to control measuring devices that are included in an IEEE bus loop. Thus using the developed library the system can be enhanced with new devices with less programming effort.

The integrated system we have implemented can be helpful in many ways. For example, the fact that many electrical parameters of electronic devices can be accurately measured, make it dedicated for characterisation purposes. Probably the most interesting application of our system is the extraction of device model parameters. Indeed, as soon as models are developed there is always a need to determine model parameters experimentally from measurements. This means that there is a need for parameter extraction methods. For simple models with only one or two parameters, simple extraction schemes can be sufficient but for more complex models such as transistor models, parameter extraction can be a complicated matter. In today's semiconductor industry there are several different areas where parameter extraction algorithms are used. The different groups using the extraction algorithms have different requirements on them [31]. Below there is a compilation on the requirements from three groups using extraction algorithms, namely: design, production and process development groups. (see figure 1.1).

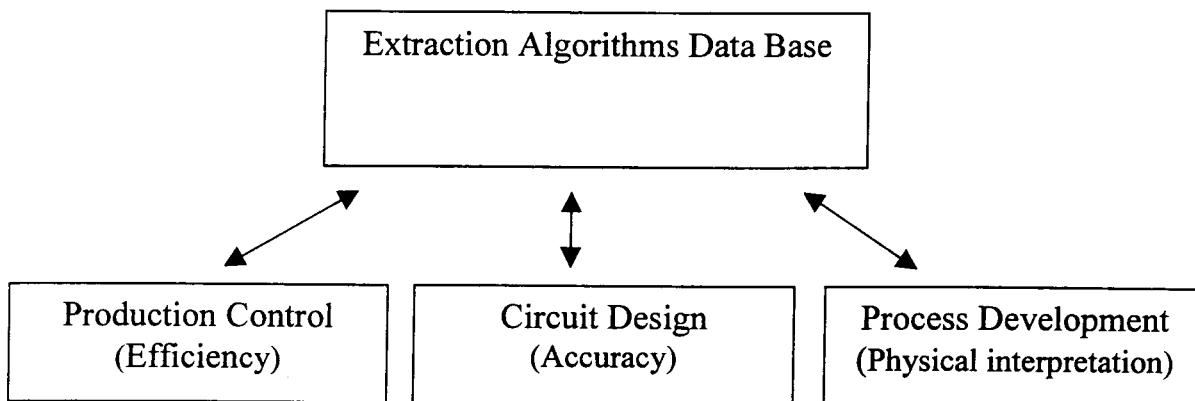


Figure 1.1. The requirements from different groups involved in design and manufacturing of integrated circuits.

Circuit design groups (such those in microelectronic field for instance) use circuit simulators during the design of integrated circuits to compare different implementations of logical or analog functions. The amount of simulation during the design phase of integrated circuits has increased with the complexity and the performance of the circuits. To speed up the design phase and keep cost low, it is of great importance that the circuits meet the performance specifications already the first time they are manufactured. Therefore reliable and accurate results from the circuit simulations are very important. To obtain reliable results, accurate device models are not enough, good parameters values for the model on which the simulation program is based, are also necessary to approximate the measured device characteristics as closely as possible. The only way known in current days to determine good parameters is, by

extracting them from measurement on real devices. Hence, the extraction algorithms can be regarded as a link between the manufacturing process and the circuit simulator. In such situations, good parameters can be defined as parameters which reproduce the device characteristics accurately.

Production groups use extraction algorithms for process monitoring. The most important features for these groups are efficiency, robustness and reliability. Therefore they usually use simple methods to determine a small number of parameters only to check if the process is within specifications.

Process development groups have increased their use of technology CAD (TCAD) tools with increased complexity of IC processes and devices. During the development of new processes these tools can be used for reducing the number of physical experiments. Hence money and time can be saved during the development phase. It is also easier to investigate the effects of process disturbances when other noise sources are eliminated. A TCAD-system consists of different types of process, device, and circuit simulators. The parameter extraction algorithm is a vital link between the device and circuit simulators. It is advantageous to use the same algorithm in the TCAD-system as well as when performing measuring on real devices since the same parameter definitions are then used in both cases.

With an extraction algorithm which meet the requirements from the groups involved in design and manufacturing of integrated circuits as well as process development many benefits would be realised. For instance, confusion about seemingly identical parameters can be avoided with a common extraction algorithm used by all groups. Another advantage is that information obtained by one group can also be useful for the other groups if the same definitions of parameters are used. Hence redundancies in work are eliminated. Right now, the best methods of parameter extraction still the ones based on optimisation techniques. They show a good agreement between measured and simulated device characteristics.

This thesis is organised in the following way: In chapter 2 a complete description of the developed integrated system hardware and software parts is given. Chapter 3 reviews the circuit models of the basic passive components and the SPICE models of the active devices; diodes, BJTs and JFETs. Rather than being a complete review, this chapter is considered as a reference material for the methods of parameters extraction presented in chapter 4. In chapter 4 the extraction methods (graphical and optimisation) of model parameters we have chosen to implement, are described in some details. Chapter 5 is intended to validate our integrated system by testing the implemented routines of parameters extraction, and some results and discussions are presented.

Chapter 2

Description of the Measurement Set

2.1. Introduction

Along the present chapter will be described in some detail each equipment included into our system. The whole system is shown in figure 2.1.1, all existing devices are Hewlett-Packard (HP) designed. In addition to their high performance and accuracy, those devices are provided with GPIB bus interface cards that make them remotely controlled by any IBM compatible computer. This last feature allows automated monitoring from measurement to analysis and hence, many electrical characterisation techniques of both passive and active electronic components are feasible with less effort.

The chapter includes also detailed description of the different developed software parts of our integrated system. The developed software supervises completely the flow of data on the GPIB bus and, the user has almost no contact with the measuring devices front panel.

The existing instruments are connected together through the GPIB bus and controlled by an IBM compatible PC. The hardware connections (see figure 2.1.1) were realised with the help of an GPIB interface card [1] housed into one of the PC extension slots and fully monitored by an installable DOS device driver. The GPIB bus (also known as, GPIB, IEEE or ASCII bus) which at the origin was used as an interface bus for the Hewlett-Packard (HP) instruments, is one of the most popular data buses used in industry. It is a carefully defined instrumentation interfacing means, that simplifies the integration of measuring instruments and a calculator or a computer into a system. Up to 15 instruments including the controller can be integrated using one interface card.

The HP model 4275A, the HP model 4140B as well as the HP model 4145B represent the heart of our system. These three devices are not only the most sophisticated of the system, but also they perform for themselves all characterisation techniques that will be presented in this work. The other devices are used as complement to the previous ones and are added to get more accurate measurements than the two HP models 4275A and 4140B are not dedicated for. For example, The HP model 3478A digital multimeter, can be used to get more precise measurements for the voltage values delivered by the HP model 4140B voltage sources, especially at low voltage ranges.

Our system is fully monitored by an IBM compatible computer such that, the user is able to perform all device settings and operations remotely from his computer desk, without acting on device front panels, except in some rare situations. For this reason all descriptions in this report will be restricted on automated operations.

The developed software supervises completely the flow of data on the GPIB bus and, is designed in such a manner that static and dynamic measurements are processed separately using two executable programs; STATIC.EXE and DYNAMIC.EXE, that are monitored by a main program IISCEC.EXE. An other program UTILS.EXE has been also added to include some useful utilities such as, translation of saved measurement data to some data handling software formats like MATLAB, where they are processed to give useful electronic component parameters in a very easy and fast way.

Other kind of measurements that we have called "Charge measurements", are obtained also separately because of the specific field they belong to, even if basically they

are based on DC current measurement. In fact this kind of measurements is related to the well known “Charge Pumping Technique” [2] and other similar techniques of MOS structures characterisation, such as the “Charge Extraction Technique” [3].

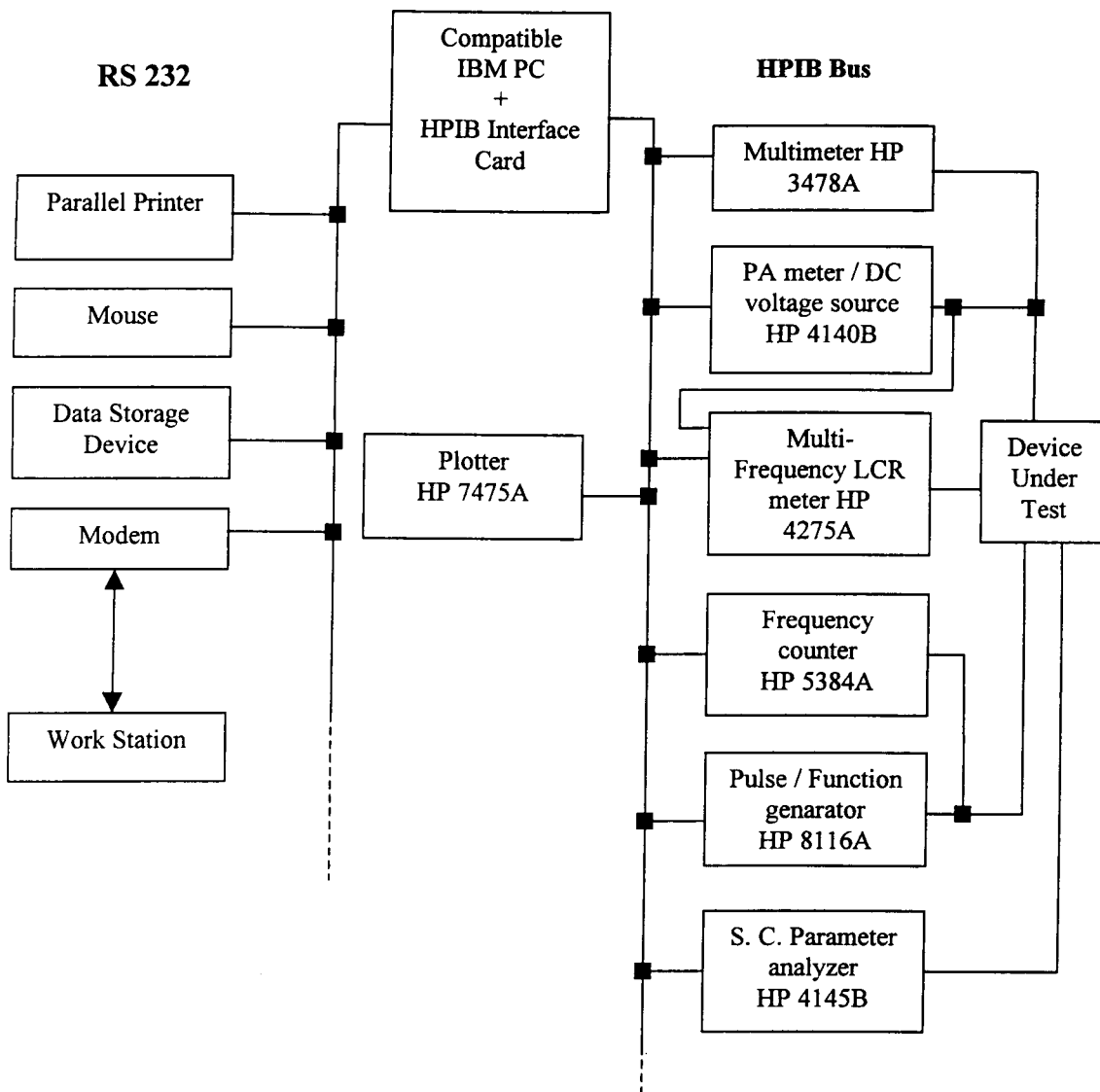


Figure 2.1.1 The Hardware configuration

2.2. Hardware Part Description

2.2.1. The HP model 4140B pA meter / DC voltage source

The HP model 4140B pA meter/DC voltage source includes for itself a high stability pico ammeter (pA meter) with one fA (10^{-15} A) resolution, coupled with two programmable DC voltage sources, labelled respectively VA and VB, figure 2.2.1.1 Wide range of usability is thus ensured in many application fields.

The HP model 4140B pA meter has a basic accuracy of 0.5% over wide measurement ranges ($\pm 0.001 \times 10^{-12}$ A to $\pm 1.999 \times 10^{-2}$ A) enabling stable current measurement at 10^{-15} A (± 1 count), this is achieved by employing a new unique, variable, digital integration method [4]. This stable and fast (less than 35 ms at 1nA) measurement technique is very useful not only for small leakage currents measurements of semiconductor devices and field effect structures [5], but also for making insulating resistance and leakage, current absorption measurement of capacitance and insulation materials.

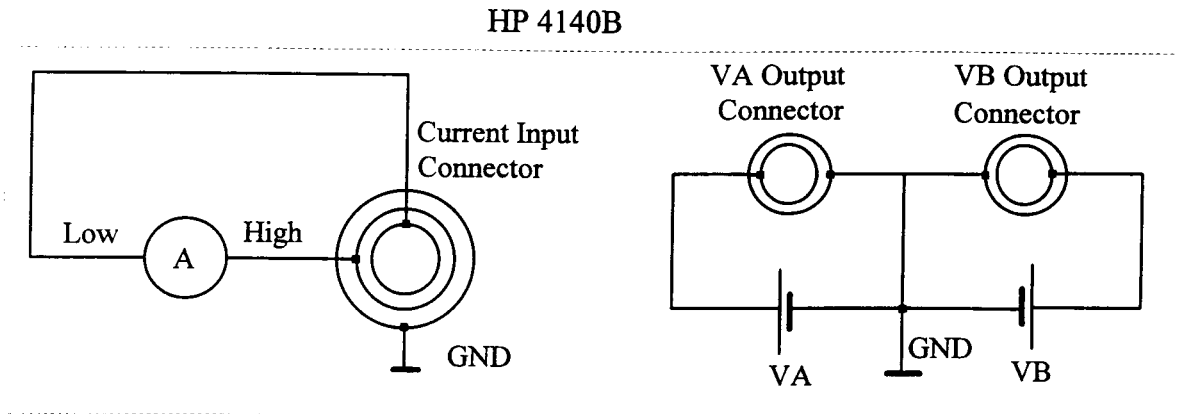


Figure 2.2.1.1 Equivalent Circuit of HP 4140B.

One of the two programmable DC voltage sources (VA) can operate not only as a simple programmable DC voltage source, but also as a single or double unique staircase and accurate single or double ramp generator, figures 2.2.1.2. The DC voltage source has an output range of ± 100 V in 100 mV steps or ± 10 V in 10 mV steps and, the ramp rate can be set from 0.001 V/s to 1 V/s at 0.001 V/s resolution. In addition each DC voltage source (VA and VB) has a current limiter which can be set to 100 μ A, 1mA or 10mA to avoid damaging the device under test by excessive current.

A key capability of the HP model 4140B is its ability to make accurate current-voltage (I-V) and capacitance-voltage (C-V) measurements which make it an excellent characterisation tool in the microelectronics area [4,6]. The measurement timing can be automatically synchronised between the DC voltage source and the pA meter section. The start, stop and step voltage values can be set from -100 V up to +100 V at 100 mV resolution and from -10 V to +10 V at 10 mV resolution. The hold time and step delay time figures 2.2.1.2, can also be easily set depending upon the characteristics of the material being tested.

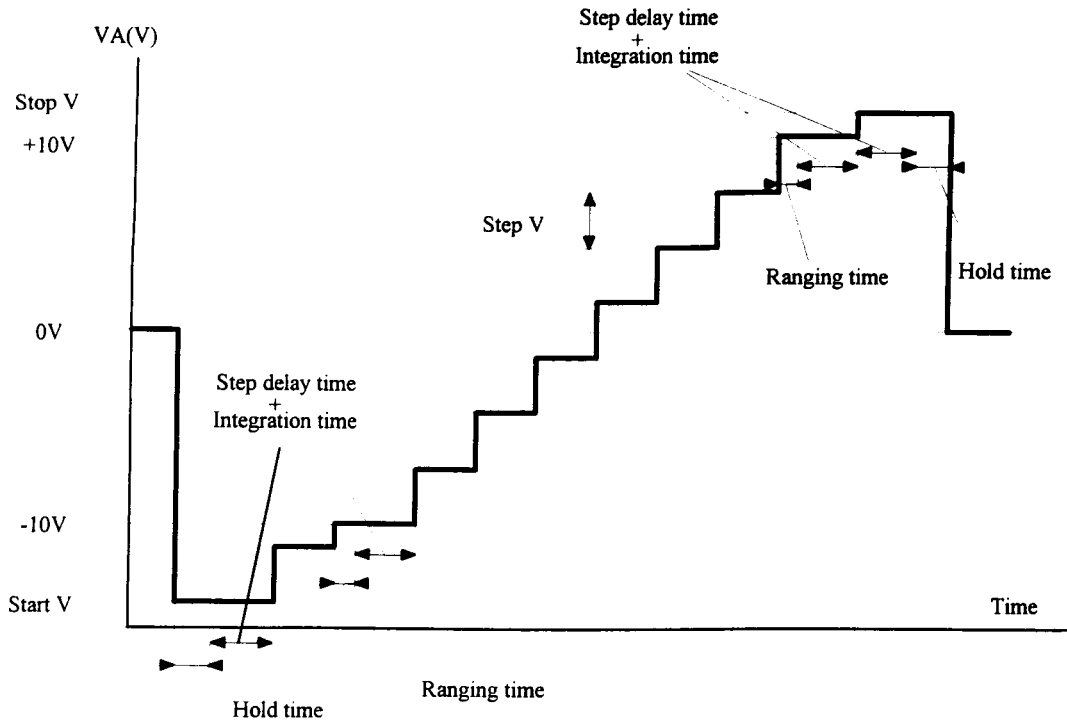


Figure 2.2.1.2.a. (I-V) Measurement with single staircase wave.

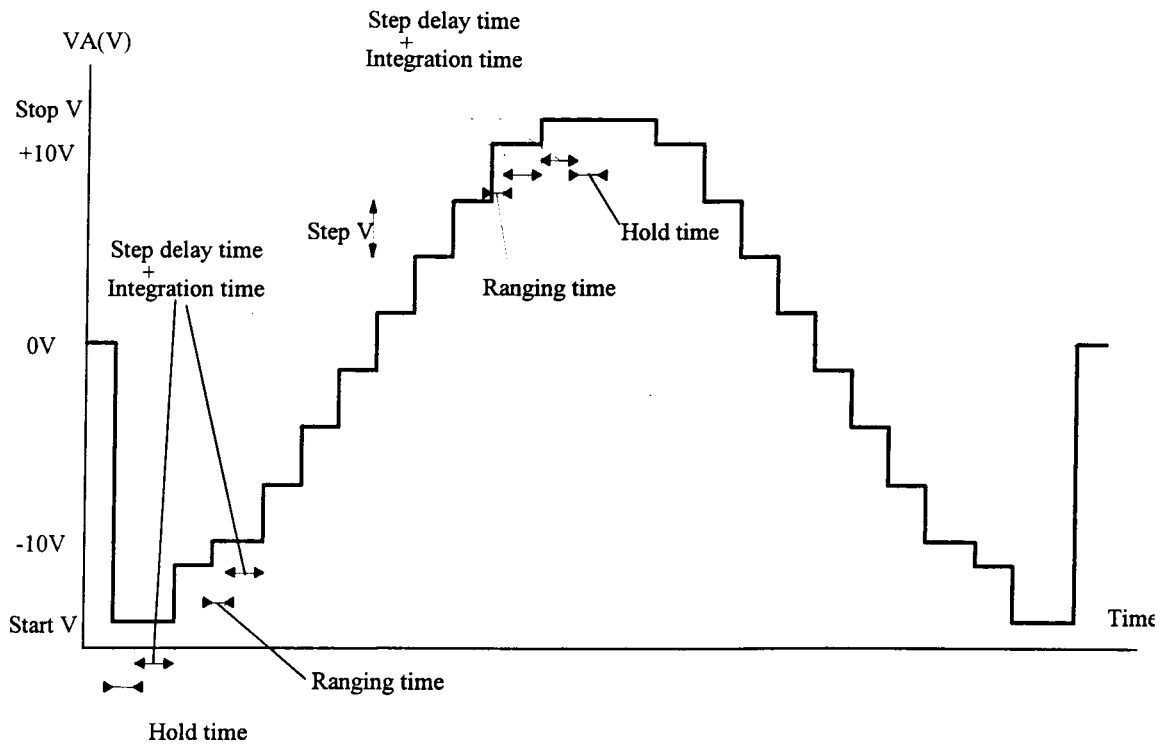


Figure 2.2.1.2.b. (I-V) Measurement with double staircase wave.

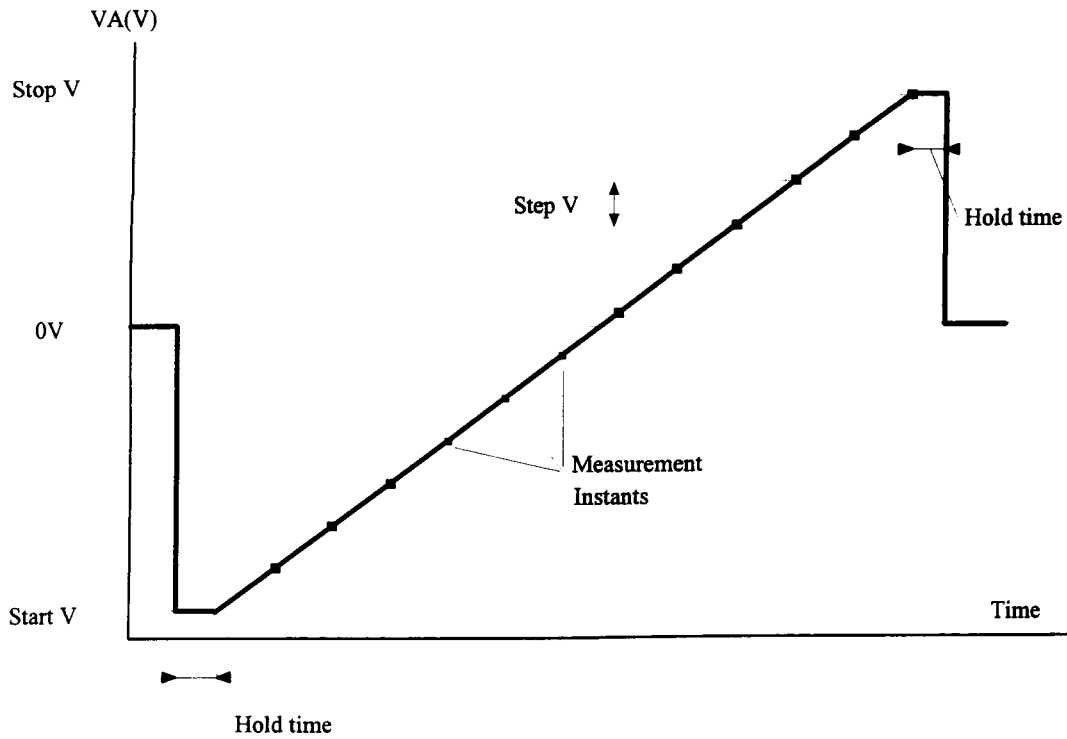


Figure 2.2.1.2.c. (I-V) Measurement with single ramp wave.

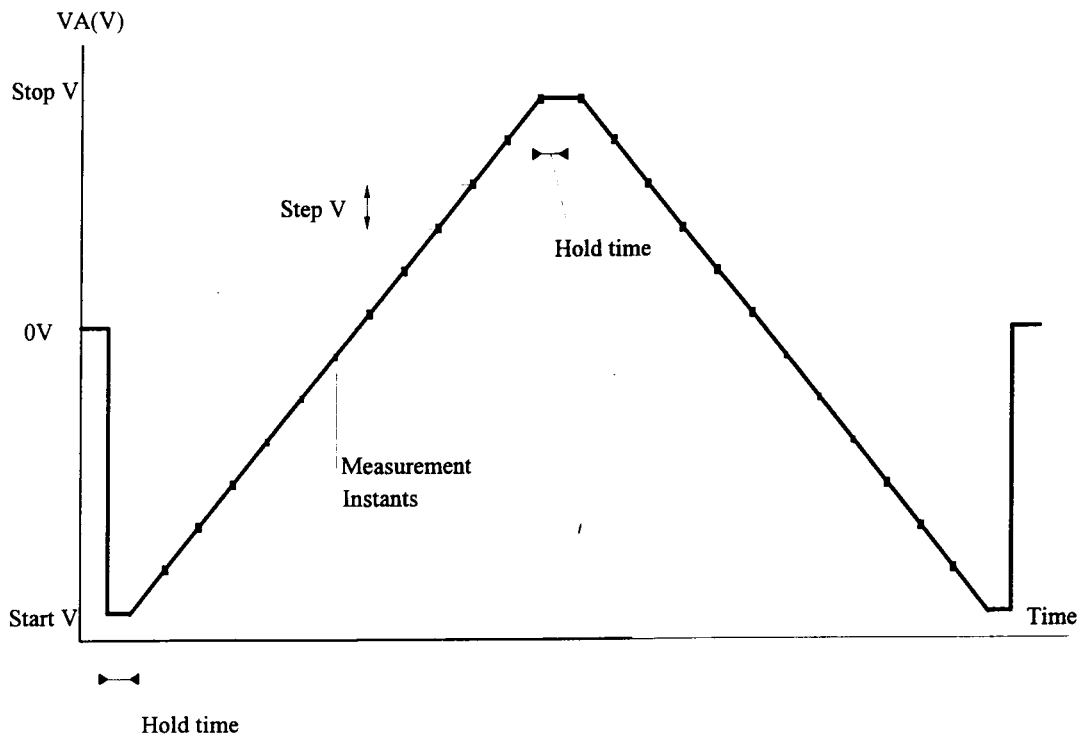


Figure 2.2.1.2.d. (I-V) Measurement with double ramp wave.

The Static characteristics of semiconductors, diodes and Field Effect Transistors (FET's), the analysis of Metal-Oxide Semiconductors (MOS) construction and the measurement of threshold voltages of FET's can be made easily, quickly and efficiently. The quasi static C-V measurement are performed using the well-known voltage ramp method [5] according to the following formula :

$$C = \frac{I \text{ (measured current)}}{dV/dt \text{ (voltage ramp rate)}} \quad (2.2.1.1)$$

This type of measurement is made possible because both the desired setting of the ramp voltage and the capacitance measurement are totally synchronised.

The ramp voltage value is displayed at measurement point simultaneously with the appropriate calculated capacitance value in the range from 0.0 pF to 1999 pF. In addition percent change of the capacitance can be displayed. For this purpose, a reference value from 0.1 pF to 1999 pF can be chosen by the user and stored into the device memory.

The HP model 4140B employs certain particular functions that make the best use of the intelligence capability of its microprocessor. For example, its zero off set current capability cancels leakage current of test leads and fixtures and, its zero off set capacitance capability cancels stray capacitance of test leads and fixture for accurate current or capacitance measurements.

Table 2.2.1.1 summarises the correlation between the instrument functions and DC voltage sources while, on table 2.2.1.2 are shown the integration times related to the different current ranges.

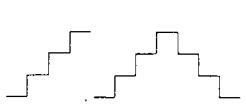


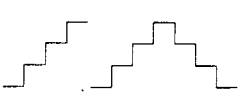


Function	VA source			VB source
	Staire case wave	Ramp wave	DC source	DC source
(I-V) measurement				
(C-V) measurement				
(I) measurement				

Table 2.2.1.1 HP 4140B measurement functions: I, I-V, C-V.

Two separate voltage sources are available:

VA : ± 100 V, function generator/programmable source.

VB : ± 100V, programmable DC voltage source.

Range (A)	Integration Time (mS)		
	Short	Medium	Long
$10^{-12} \sim 10^{-10}$	20	80	320
10^{-11}	80	320	1280
10^{-12}	160	640	2560

Table 2.2.1.2 Correlation between the current range and integration time.

2.2.2 The HP model 4275A multi-frequency LCR meter

The HP model 4275A multi-frequency LCR meter is a high performance, fully automatic test instrument designed to measure the various component parameter values of an impedance element in the relatively high frequency region (10 KHz to 10MHz). It is able to measure inductance (L), capacitance (C), resistance (R), dissipation factor (D), quality factor (Q), conductance (G), susceptance (B), reactance (X) and, in addition, the absolute value of the vector impedance ($|Z|$) as well as the phase angle (θ), over a wide range with high accuracy and speed. This is achieved by using the four terminal pair configuration measurement figure 2.2.2.1, which permits easy, stable and accurate measurements and avoids the measurement limitations that are met in ordinary terminal methods such as, mutual inductance, interference of the measurement signals and unwanted residual factors [7].

The wide range measurement capabilities of the HP model 4275A are enhanced by the 10 spot test frequencies, which have accuracy of 0.01 % and selectable from 10 KHz to 10 MHz in a 1-2-4-10 sequence.

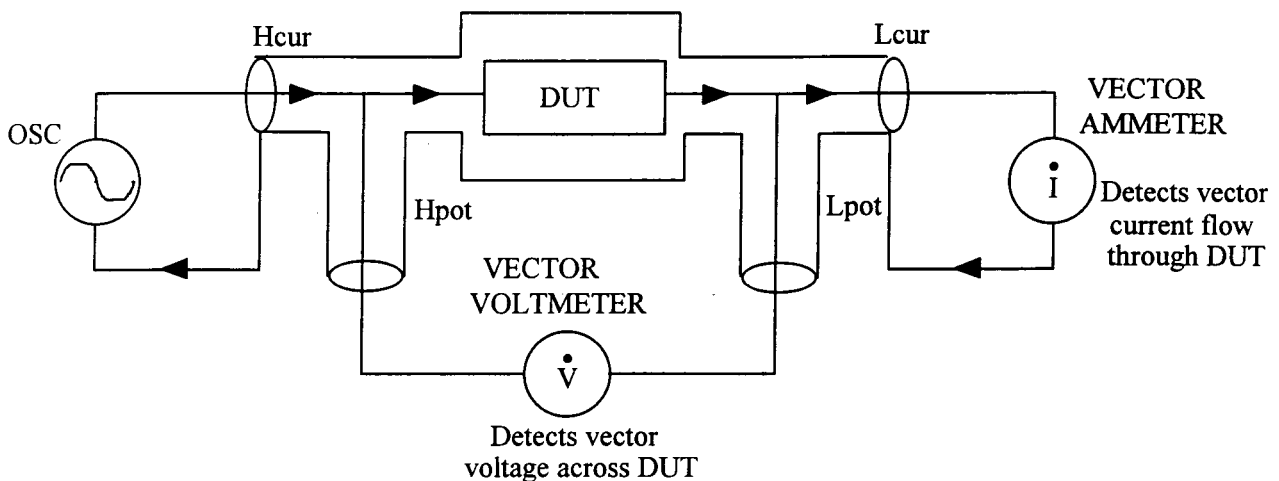


Figure 2.2.2.1 The four Terminal Pair Measurement Principle.

The test signal level provided by an internal sinusoidal oscillator, can be flexibly set at the desired amplitude within the range of 1 mV to 1 V rms by front controls.

The multi spot test frequency and test level control functions featured in the HP model 4275 A , make it a truly versatile instrument which can respond to the diverse measurement requirements in research, circuit design and production testing, because they

permit measuring the device to be tested under the practical test conditions at which it actually operates. The other obvious advantage of the variable test signal capability is that it becomes easy to measure non linear impedance elements whose parameters are strongly dependent on their operating conditions such as, inductors and semiconductor devices. Most significantly, the model 4275A can be of particular help in the experimental assessment of devices in the semiconductor testing field [7,5].

The measuring range for capacitance is from 0.001 fF (femto Farad = 10^{-15} Farad) to 199.99 μ F, for inductance from 0.01 nH to 199.99 H and, for resistance and impedance it is from 0.01 m Ω to 19.999 M Ω , all of which are measured with a basic accuracy of 0.1% to 5 %, depending on test signal level and operating frequency and, at a typical measuring speed of 140 to 180 milliseconds. The flexibility of the model 4275A is further enhanced by its capability of performing both parallel and series equivalent circuit measurement of the device to be tested. Either dissipation factor , quality factor , equivalent series resistance , conductance , reactance , susceptance or phase angle can be selected in addition to the choice for L, C, R or $|Z|$ measurement. The measuring range for dissipation factor is from 0.00001 to 9.9999, for quality factor it is from 0.01 to 9000, from 0.01 m Ω to 19.999 M Ω for the equivalent series and reactance, from 0.01 nS to 19.999 S for susceptance and the phase angle can be measured from $\pm 0.001^\circ$ to $\pm 80.000^\circ$.

The wide range capability of the HP model 4275A, enables a measurement range from that of small capacitance values such as ceramic chip capacitors and semiconductor junction capacitors, to that for high capacitance, such as the measurement of electrolytic capacitors to be covered. The high resolution measurement capability enables the measurement of an extremely low dissipation factor such as that of polystyrene capacitor. A wide range of inductance measurements, from the inductance of a high frequency coil to that of an output transformer, can be made at suitable test frequencies. The wide resistance range permits measurements for low value cable conductor resistance through those for high resistance solid resistors.

The model 4275A employs certain unique functions which make the best use of the intelligence capability of its microprocessor. Two functions execute capacitance, inductance, resistance and impedance deviation measurements. These functions make possible the memorising of measured value as a reference value such that the subsequent display is the measurement minus the reference value or, the percentage that the measurement deviates from the reference. The reference value is obtained and memorised from the preceding measurement. More than this, a digital offset adjustment function measures residual capacitance, inductance and resistance inherent to the test fixture used and offsets the effect of these parasitic impedance to zero, with respect to the measured values. An appropriate offset compensation quantity is automatically calculated every time a measurement is taken. Any measurement error due to the test fixture is therefore automatically eliminated for stray capacitance up to 20 pF, residual inductance up to 2000nH, resistance up to 0.5 Ω and conductance up to 5 μ S.

Table 2.2.2.1 summarises the specific measuring range of each measurable electrical parameter combinations according to the adopted circuit mode. All parameter formulas for measurement functions are listed on table 2.2.2.2.

Electrical parameter	Measuring range
Capacitance (C)	0.01 fF - 199.99 μ F
Inductance (L)	0.01 nH - 199.99 H
Impedance (Z), Resistance (R) and Reactance (X)	0.01 m Ω - 19.999 M Ω
Dissipation factor (D)	0.00001 - 9.9999
Quality factor (Q)	0.01 - 9000
Conductance (G) and Susceptance (B)	0.01 nS - 19.999 S
Impedance vector angle (θ)	$\pm 0.001^\circ$ - $\pm 100.000^\circ$

Table 2.2.2.1 Measuring ranges of different electrical parameters.

In order to select the most suited circuit mode for his measurement, the user should know that an impedance element can be represented by a simple equivalent circuit which is comprised of resistive and reactive elements each connected in series or in parallel with the other, Figure 2.2.2.2. Three circuit modes are available in HP model 4275A, the series mode, the parallel mode and the automatic mode. When the user select the automatic mode, the 4275A will automatically select either parallel or series equivalent circuit mode as appropriate to the range and function settings. Parameter values of a component measured in parallel equivalent circuit and that measured in series equivalent circuit are different from each other. The difference in measured values is related to the loss factor of the sample to be measured. Obviously, if no series resistance or parallel conductance is present, the two equivalent circuits are identical. However, a sample value measured in a parallel measurement circuit can be correlated with that of a series circuit by a simple conversion formula which considers the effect of dissipation factor. Table 2.2.2.2 shows the relationships of parallel and series measurable parameters for given dissipation factor. For example, a parallel capacitance (C_p) of 1000 pF with a dissipation factor of 0.5, is equivalent to a series capacitance (C_s) of 1250 pF with identical dissipation factor. As it is indicated in figure 2.2.2.2, the dissipation factor remains the same in both equivalent circuit representations. The measurement circuit used should be the one that approximates the equivalent circuit of the sample to be measured. However, there is no convenient criteria for reasonably selecting the appropriate measurement circuit for general components. Usually, a series measurement circuit is employed for the measurement of a low impedance sample and a parallel measurement circuit for a sample of high impedance. For example, in a low capacitance sample such as a ceramic capacitor,

parallel conductance is the major contributor to loss. On the other hand, for a high capacitance sample such as an electrolytic capacitor, the equivalent series resistance consisting of lead resistance, electrode resistance, dielectric loss, etc., is the main factor which contributes to the loss of the component. For middle range impedance, this reasoning still applies, but the effects are less pronounced. An empirical method of choosing the appropriate measurement circuit is to infer the actual equivalent circuit of the sample from the results of a trial measurement. Dependency of the dissipation factor (quality factor) upon test frequency offers a theoretical basis for such inference. The loss factor of series capacitance loss increases at higher frequency. The parallel loss of a capacitor will exhibit the opposite tendency. Also, for inductors, the equivalent circuit can be deduced by a similar course of reasoning. Therefore, the measurement circuit appropriate to the sample, can be determined by comparison of dissipation factor values obtained at the desired test frequency to the selected test frequency.

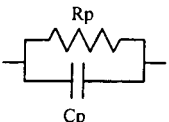
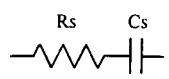
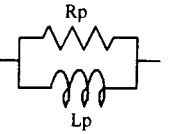
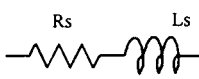
Circuit Mode		Dissipation Factor	Conversion to other modes
C		$D = \frac{1}{2 \pi f C_p R_p} = \frac{1}{Q}$	$C_s = (1 + D^2) C_p$ $R_s = \frac{D^2}{1 + D^2} R_p$
		$D = 2 \pi f C_s R_s = \frac{1}{Q}$	$C_p = \frac{1}{1 + D^2} C_s$ $R_p = \frac{1 + D^2}{D^2} R_s$
L		$D = \frac{2 \pi f L_p}{R_p} = \frac{1}{Q}$	$L_s = \frac{1}{1 + D^2} L_p$ $R_s = \frac{D^2}{1 + D^2} R_p$
		$D = \frac{R_s}{2 \pi f L_s} = \frac{1}{Q}$	$L_p = (1 + D^2) L_s$ $R_p = \frac{1 + D^2}{D^2} R_s$

Table 2.2.2.2 Correlation between Parallel and series circuit modes.

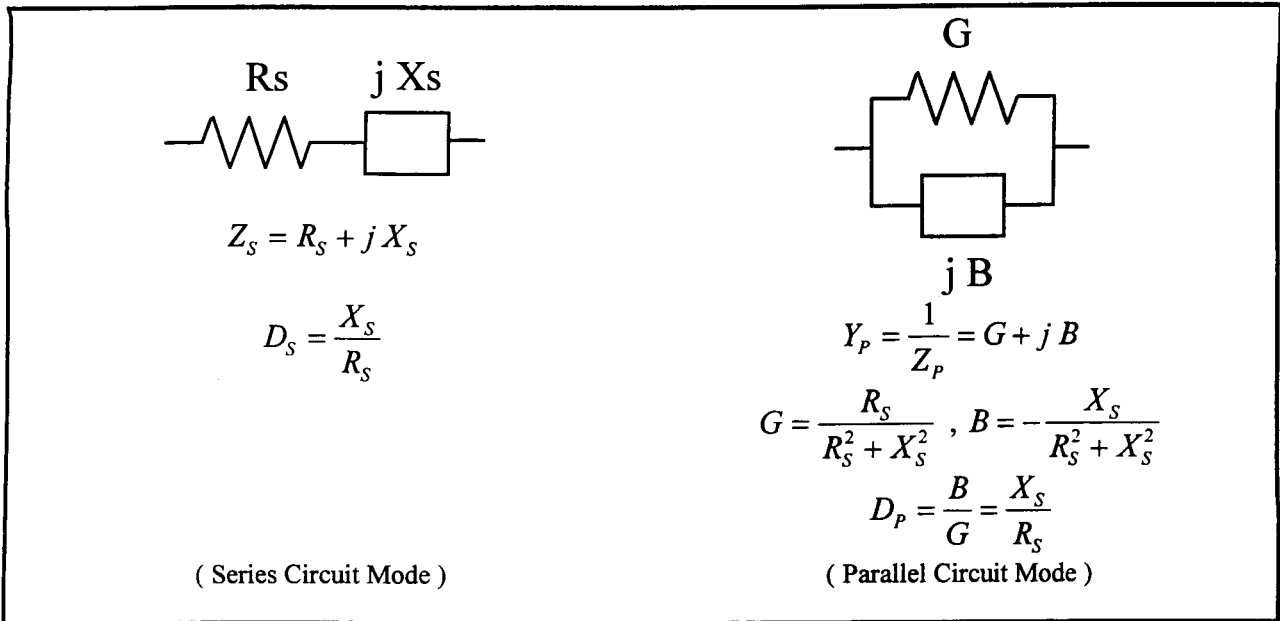


Figure 2.2.2.2 The equivalent impedance in both Series and Parallel circuit modes. When the conditions for the above equations are satisfied, the parallel and series circuits have at a particular frequency point the same equivalent impedance and the same dissipation factor.

2.2.3 The HP model 8116A pulse/function generator

The HP model 8116A pulse/function generator [8], can produce three output wave forms, sine wave, square wave and triangular wave in addition of a pulse output. Various wave parameters can be set by the user, amplitude (16 Vp-p into 50 Ω and 32 Vp-p into high impedance), duty cycle (0% to 100%), output frequency (from several milli-Hertz to 50 MHz), high level and low level output, output signal offset, pulse width and so on.. In addition, many trigger modes are available (See table 2.2.3.1) as well as control modes (see table 2.2.3.2). In external triggering modes a connector is available to receive the external signal. The triggering level can be set from -10 V to +10 V with an appropriate level selector. An other connector is also available to receive the input signal used in the different control modes. Table 2.2.3.3 indicates the permitted combinations of control modes, trigger mode and output wave form.

The user will find this versatile device very useful in some applications such as for instance, "The Charge Pumping " technique used in MOS devices characterisation area [2].

Output mode	Explanation
NORM	In normal mode a continuous output waveform is generated.
TRIG	In trigger mode each active input edge triggers a single output cycle.
GATE	In gate mode the active level of the external input signal enables output cycles. The first output cycle is synchronous with the active trigger slope. the Last output cycle is always completed.
E.WID	In external width mode, which is only valid with pulse waveform, the external input signal is shaped to determine output pulse width. This mode can be used for pulse recovery.
I.SWP	In internal sweep mode the instrument repeatedly sweeps the output frequency logarithmical between specified start and stop frequencies. The sweep time per frequency decade is selectable between 10 ms and 500 s in intervals in the ratio 1:2:5.
E.SWP	In external sweep mode an external trigger initiates a single sweep cycle. A second trigger is required to reset the instrument to the start frequency
I.BUR	In internal burst mode the instrument repeatedly gerates a specified number of output cycles (in the range 1 to 1999). The time between bursts can be selected in the range 100 ns to 999 ms
E.BUR	In external burst mode an external trigger initiates an output burst

Table 2.2.3.1 The different output modes available with the HP model 8116A.

External Trigger Control	Explanation
Trigger Slope	Select a positive or negative trigger slope.
Trigger level	The trigger level can be varied in the range ± 10 V.
Manual Trigger	Pressing the MAN key will simulate the external trigger signal.
Single Cycle	Pressing the 1 CYCLE key will initiate a single output cycle in GATE, I.BUR and E.BUR modes.

Table 2.2.3.2 Control of External Trigger mode.

Mode	NORM	TRIG	GATE	E.WID	LSWP	E.SWP	LBUR	E.BUR
FM	•	•	•	✗	•	•	✗	•
AM	•	•	•	⏏	•	•	✗	•
PWM	⏏	⏏	⏏	✗	⏏	⏏	✗	⏏
VCO	•	•	•	✗	✗	✗	•	•

•	All waveforms.	✗	In valid combination.
⏏	Pulse waveform only.	✗	All waveforms except pulse.

Table 2.2.3.3 The permitted combinations of control modes, trigger mode and output wave form of the HP model 8116A.

- In frequency modulation mode **FM**, the output signal frequency can be modulated to a maximum of $\pm 5\%$ of the programmed value by applying a control voltage in the range ± 6 V.
- In amplitude modulation mode **AM**, the output signal amplitude can be modulated from 0 to 100% using a ground-symmetrical control voltage in the range ± 2.5 V. Double side band suppressed carrier (DSBSC) is obtained using a control voltage in the range +2.5 V to -7.5 V which gives 200% modulation.
- In pulse width modulation **PWM**, the pulse width of the signal output can be controlled using a control voltage in the range ± 6.5 V. There are 8 non-overlapping pulse width ranges available: (10ns-100ns, 100ns-1 μ s, 1 μ s-10 μ s, 10 μ s-100 μ s, 100 μ s-1ms, 1ms-10ms, 10ms-100ms, 100ms-1s).

2.2.4 The HP model 5384A frequency counter

The HP model 5384A frequency counter [9] is a minicomputer based instrument dedicated for accurate frequency and time period measurements, over a relatively wide frequency range (from 10 Hz to 225 Mhz). The input signal to be measured can be applied through BNC connectors located on the front panel of the device. Two input channels labelled "A" and "B" are available. One may set either the trigger level of channel "A", or adjust the input attenuation of channel "B".

Through channel "A" frequency measurements are possible in the 10 Hz to 100MHz range, and a 100 KHz low pass filter can be toggled in or out of the channel signal, and thus measurements in the 10 Hz to 100 KHz frequency range can be enhanced by eliminating low frequency noise signals.

On the other hand, channel "B" ensures high frequency measurements (50 MHz to 225 Mhz) with the possibility to attenuate the input signal.

Mainly, this device was included into our system to get accurate measurements of frequency signals that may be specially produced by the HP model 8116A pulse/function generator (see the preceding section).

2.2.5 The HP model 3478A digital multimeter

The HP model 3478A digital multimeter, is a very powerful bench instrument equally in the laboratory or production area. It has the capability of measuring DC or true rms currents, DC and AC voltages and resistance, over a relatively wide ranges [10]. The model 3478A is also featured with many useful options.

The most important option provided with the HP model 3478A is the "AUTO ZERO" capability, which once turned on insures the user that any offset errors generated internally (Thermal effect in particular) are continuously nulled with each reading, this renders the most accuracy. There are however, many applications where speed is critical, disabling the Auto Zero mode is therefore advantageous. Furthermore, the HP 3478A input circuitry remains in a completely static state with Auto Zero off. This is useful when making measurements in extremely high impedance circuits, where the internal switching transients of the HP 3478A may affect the reading accuracy. With the Auto Zero feature enabled (this is the default state at power turn-on) the HP 3478A takes two measurements per reading : a "Zero" measurement and a measurement of the input voltage. The actual reading is the algebraic difference between the two measurements. The HP 3478A makes the "Zero" measurement by disconnecting the multimeter's input terminals, and then shorting the internal input circuitry to circuit common. It then switches back for an input voltage measurement. All switching is internal and is automatic. In conclusion, Auto Zero feature of the HP model 3478A is very useful for making accurate measurements in relatively low impedance circuits. It should be turned off when high measurement speed is needed (the internal reading rate nearly doubles). The thermal stability of the measurement environment is the most important factor in deciding whether or not to turn Auto Zero off. By simply keeping the temperature of the 3478A at a fixed value, we may turn Auto Zero off without adverse effects.

An other interesting feature of the model 3478A is its "4-wire Ohms" resistance measurement capability. This function alleviates the errors caused by the effects of test lead resistance. Figure 2.2.5.1 illustrates this point. A comparison between the classical "2-wire Ohms" and the 4-wire Ohms methods, shows that the current through the unknown resistor is the same regardless of lead resistance, and the voltmeter in 4-wire Ohms method measures only the voltage across the resistor, not across the combined lead resistance as in 2-wire Ohms method. The 4-wire resistance measurements are essential when highest accuracy is required, or when long lead lengths are present.

It is also important to indicate that temperature measurement is possible using the HP model 3478A multimeter. By setting the device for either 2-wire Ohms or 4-wire Ohms measurement, and using a thermistor as unknown resistor, temperature measurements are hence feasible, provided that necessary electrical parameters of the thermistor are available. For example, the 44007 thermistor type which exhibits a 5 K Ω resistance at 25 °C, is very suited for temperature measurements over the -80°C to 150°C range. More than this, the fact that the HP model is remotely controlled by a computer, makes the temperature measurements through a thermistor very easy, the user does not care about the non linear behaviour of the thermistor, since the temperature value is adjusted using a simple formula through the computer according to the chosen thermistor model. The

calculated temperature value can even be displayed on the HP 3478A LCD display using the GPIB bus, since as it is the case for the HP 5384, ASCII text messages can be placed on the device LCD display.

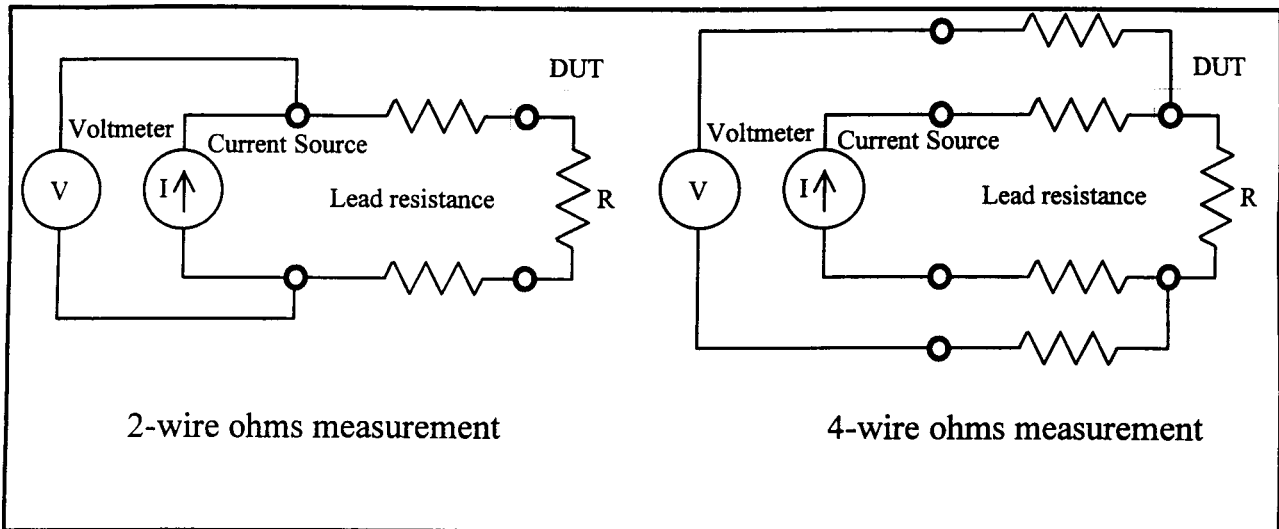


Figure 2.2.5.1 The 4-wire technique principle.

The HP model 3478A digital multimeter has been included in our system, mainly to obtain more accurate voltage measurements produced by the HP model 4140B voltage source especially at low voltage ranges. However, the user may easily find other useful applications of this powerful device.

2.2.6. The HP model 4145B Semiconductor Devices Analyser

The HP model 4145B Semiconductor Parameter Analyser [11] is a fully automatic, high performance, programmable test instrument designed to measure, analyse, and graphically display the DC characteristics of a wide range of semiconductor devices such as diodes, bipolar transistors, field-effect transistors, wafer, integrated circuits, etc. Main applications include computer-aided design (CAD) of integrated circuits, new device evaluation, material evaluation, component selection for circuit design, incoming/outgoing inspection, semiconductor process control, and quality assurance.

The HP model 4145B is equipped (see figure 2.2.6.1) with four programmable Source/Monitor units, labelled (SMU), two programmable voltage source units, labelled (Vs), two voltage monitor units, labelled (Vm), a fully interactive graphics display, removable flexible-disc storage, softkeys, full arithmetic keyboard, and GPIB capabilities.

For device simulation and characteristics measurements, the HP model 4145B has eight channels. Channels 1 through 4 are Source/Monitor units (SMU); channels 5 and 6 are voltage source units (Vs); and channels 7 and 8 are voltage monitor units (Vm).

Each SMU channel has three modes of operation (figure 2.2.6.2): mode (V); voltage source/current monitor, mode (I); current source/voltage monitor, and mode (COM);

common mode, that is the channel is considered as a reference node. Both source voltage and source current can be held constant or swept linearly or logarithmically. In the (V) mode each (SMU) can be programmed to deliver DC voltages from 0V to $\pm 100V$ over three ranges: 0V to $\pm 19.999V$, $\pm 20V$ to $\pm 39.998V$ and $\pm 40V$ to $\pm 100V$ with resolution of 1mV, 2mV and 5mV respectively. In the (I) mode each (SMU) can be programmed to output currents from $\pm 1pA$ to $\pm 100mA$ over nine ranges, with a resolution of 1pA max. Note that current measurement resolution is 50fA max, depending on the current range. Current through the sample in the (V) mode and voltage across the sample in the (I) mode can be limited to prevent damage to the sample under test.

- The two (Vs) channels are programmable voltage sources. Output voltage can be as desired held constant or linearly or logarithmically swept from 0V to $\pm 20V$ with a maximum resolution of 1mV. The voltage sources are in particularly useful in situations where many bias and voltage sources are required.
- The (Vm) channels are used to measure voltages up to $\pm 20v$.

Of the six source channels (four (SMU) and two (Vs)), any combination of three can be automatically swept in linear or logarithmic staircase manner within the range of each channel. Hold times from 0 to 650s as well as delay times from 0 to 6.5s can be set. In a multi-channel sweep set-up, one channel functions as the main sweep channel and is referenced as (VAR1). One of the other channels can be swept subordinately to the main channel in two different manners: The first one is the linear staircase sweep (VAR2) in accordance to the user defined start, step and number of steps values. (VAR2) source channel output is incremented one step each time the (VAR1) source channel completes one sweep. The second manner (VAR1') is the staircase sweep synchronised with the (VAR1) sweep, in accordance to the user specified fixed ratio or offset value. (VAR1') output is calculated as:

$$\begin{aligned} \text{VAR1}' &= (\text{ratio}) \times \text{VAR1} \text{ or} \\ \text{VAR1}' &= (\text{offset}) + \text{VAR1} \end{aligned}$$

The other (SMUs) not swept may be used as constant current or constant voltage sources.

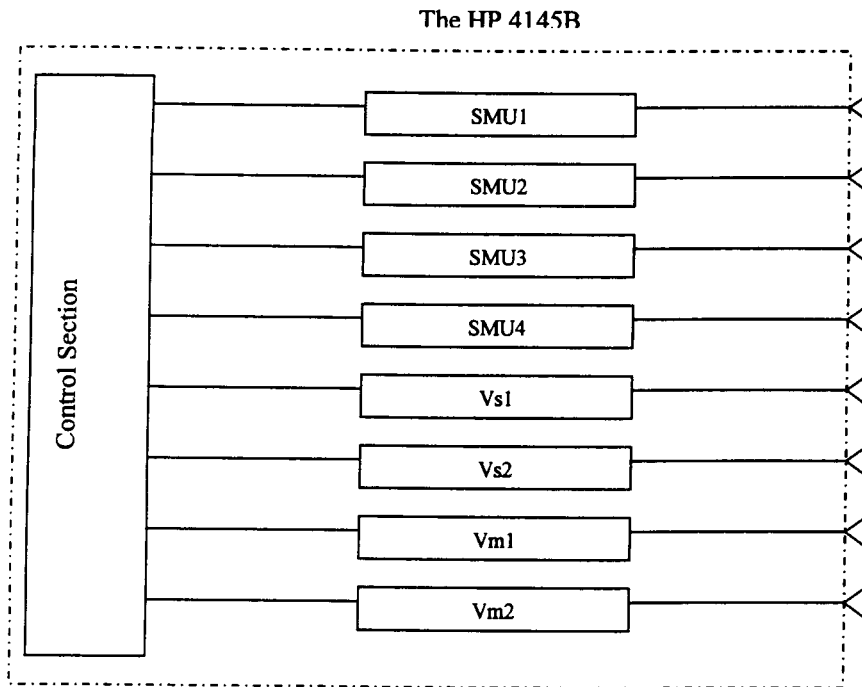


Figure 2.2.6.1 Source and Measurement Channels of The HP model 4145B

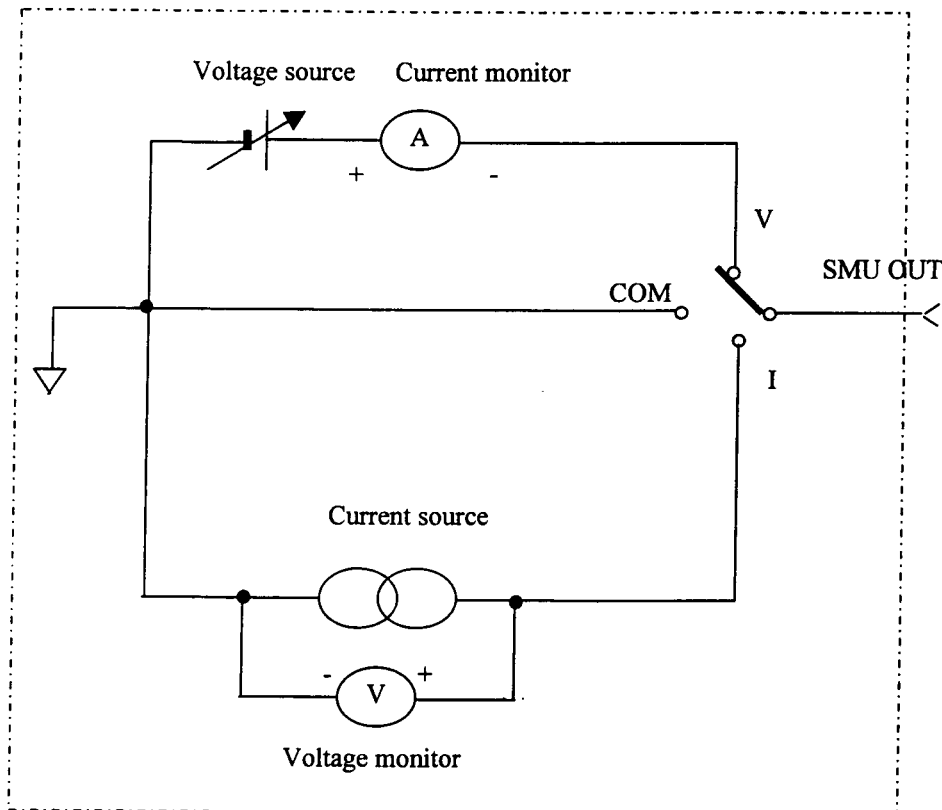


Figure 2.2.6.2 Simplified circuit diagram of one of the four SMUs

2.3. Software Part Description

2.3.1. General overview

The integrated software has been developed mainly using two principal files provided by the installable device driver the PRO488.

The CONTROL file, is used as a "pipe" through, which the ASCII character string commands are sent to the HP equipment. It is by this mean that each measuring instrument, when addressed, can process commands that are sent to it through the bus. In addition, the integrated software exploits the intelligence of HP instruments to great extent by using the TRIGGER mode feature. Indeed, many HP instruments (such as the model 4140B) have the capability to be pre-programmed in order to see them perform their individual actions simultaneously or in sequence, depending on the current application. The CONTROL file can also operate as an output file to read the bus status string. Bus errors may thus be detected.

The second file, DATA file, is used to collect device measurements to be processed by the controller. Each device is able to produce an ASCII string as formatted output data, that contains measurement information such as, data status (normal data, overflow, underflow, . . .), measurement function (current-voltage measurements, capacitance-voltage measurements, capacitance with dissipation factor measurements, . . .) and so on. The output data needs then, to be filtered to get meaningful outcomes. The software's run time is presented in figure 2.3.1.1.

At the first step the user should decide depending on his application, which program to run; STATIC program , DYNAMIC program or CHARGE program. For example, STATIC program includes a set of static measurements that are: current measurements (I), current-voltage measurements (I-V) and quasistatic capacitance-voltage measurements (C-V). All of these measurements are performed by a unique device the HP model 4140B pA meter DC voltage source. On the other hand, DYNAMIC program gathers all parameter combinations measurements that the HP model 4275A multi-frequency LCR meter can perform. It is interesting also to note that, by combination of HP 4140B with HP 4275A, it is possible to carry out other type of measurements such as, multi-frequency capacitance-voltage (C-V) characteristics of MOS structures. The user has just in this case, to connect directly through a BNC cable the programmable voltage source VA of the HP model 4140B to one of the rear panel (ext) connectors of the HP model 4275A, that have been provided to receive external biasing DC sources. One connector can receive external voltage values in the ± 35 volts range ,while the other is able to receive values up to ± 100 volts.

In the second step, the corresponding instrument settings must be defined. At this stage, the user is completely assisted such that any setting error is automatically detected and pointed out. Command strings are thus obtained and are ready to be sent to the appropriate devices.

In the third step, the user can run the measurement procedure, which consists then, of sending command strings to the corresponding instruments, by writing them to the CONTROL file. Here, two modes are available depending on the desired operating speed. the DIRECT mode, where data strings read from the DATA file are taken and displayed simultaneously as measurements are taken, or the INDIRECT mode, where the data strings are first stored in a memory buffer and displayed when desired. Obviously, the last mode is the most suited if high speed measurements are required.

Once data measurements are obtained, the user can either save them, print them or plot them. This step is the last when using STATIC , DYNAMIC or CHARGE program. The UTILITIES program can be run after when desired to convert saved data into a convenient format in order to use them for his data processing software.

We have also include in our system a set of MATLAB programs in order to get parameters of certain type of devices (see chapter 4). The user can use those parameters extracting routines directly if they match his application or consider them as initial bloc to build his own ones.

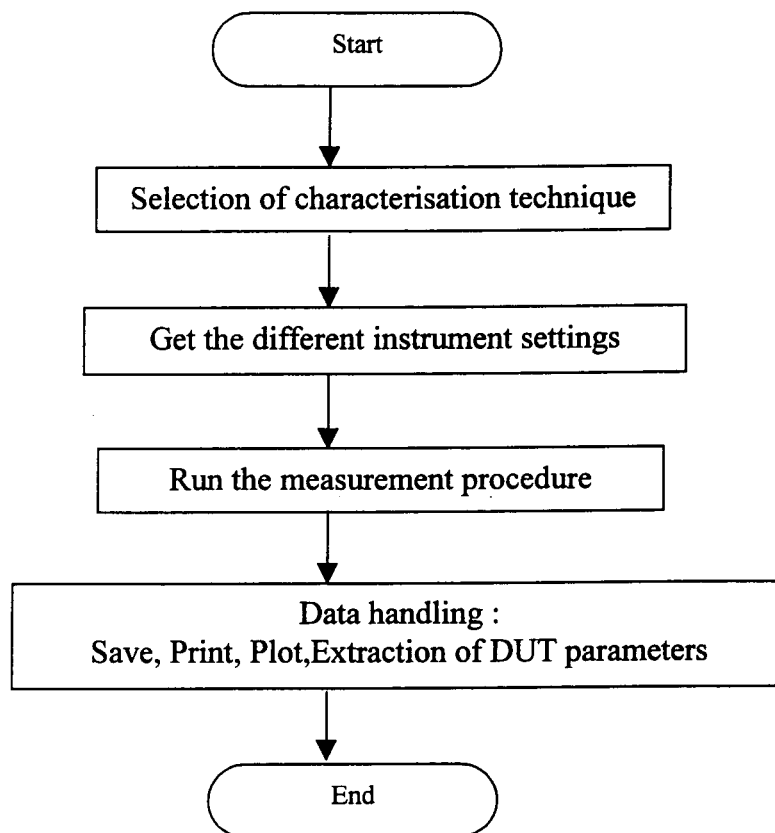


Figure 2.3.1.1 The integrated software sequence.

3.2. The PRO488 installable device driver

In general, a DOS device driver is a piece of software that loads at PC power uptime. It is this way that DOS uses to add new facilities or devices without it being necessary to write the whole operating system. A DOS device driver is hence, a method of allowing the standard personal computer to communicate with any type of interface or device using existing commands.

PRO488 [12] is an "installable" device driver, it can redirect the output of existing programs to the HPIB port. Just because an IEEE 488 interface has been added to the computer, it does not require a whole new programming language to make it work. The PRO488 device driver allows the PC to consider the IEEE interface card as a standard file or port. The device driver makes the PC's IEEE 488 interface compatible with the PC's operating system. All the standard DOS commands can now be used with the IEEE interface card. Once the device driver is installed, files can be copied to or loaded from the HPIB bus, control information can be sent to the bus, data can be read from or written to the bus etc. In fact, all normal DOS operations can be performed on IEEE devices. Detailed information on the installation of PRO488 is given in appendix A.

2.3.3. Description of the developed function libraries

Two Turbo Pascal function libraries have been developed; **PRO488.TPU** and **COMMON.TPU**, in addition to a third one **IEEEDEV.TPU** a modified version of the one provided with the software package that comes with PRO488 device driver.

There are two main reasons that make us implementing these units. Firstly, all HPIB interfaced devices can recognise two kind of commands; universal commands that act on any measuring device. Among such command we can state for example, the CLEAR command, the REMOTE command and so on. The second type of commands are device dependent commands, that are ASCII strings dedicated to act on a specific device in the set, the other devices can not respond (or respond wrongly) to such commands. The W1 string command for example , can be recognised only by the HP model 4140B and will make it starting automatically its voltage sweep. Universal commands may be found in any HPIB bus reference manual, while device dependent commands of a specific device can be found only in its operating manual delivered by the manufacturer. As described previously, both universal and device dependent commands are performed by writing to or reading from the CONTROL and the DATA files provided by the installable device driver. Hence, the user should have special background in manipulating files through the programming language he is using (Turbo Pascal in our case), as well as some experience in processing errors an messages that may result from the measuring devices. This will make the obtained programs very large and difficult to write and debug, especially for complicated applications.

The second reason of developing such units is, that our system may be extended with new equipment. Hence, extra source code will be added to include their control into the system. The existing functions will be thus of great help to carry out such extension. Of course we are not claiming that integrating new devices into the current system is a

straight forward operation, using the library functions. However, we may imagine the huge task that will result without them. Figure 2.3.3.1 shows an example of use of one of these functions, the **REMOTE** function.

The set of functions provided in the PRO488.TPU Turbo Pascal unit can be used to perform the majority of tasks that a user may meet in controlling measuring devices through the HPIB bus. This is achieved by just writing the function name with its specific parameters if any, without manipulating any file or processing any resulting error. More than this, each function returns an integer number which can be consulted to detect any function manipulating error. Table 2.3.3.1 summarises the PRO488.TPU unit function names, with their corresponding actions. All functions are of type BYTE. On table 2.3.3.2 a descriptive list of possible error codes that may be generated by a function is presented.

```

Program Example_of_using_PRO488.TPU_functions;

{This example shows how to put a device in remote control, through the developed }
{function REMOTE. In this example the device address is assumed to be 12.      }

USES
    PRO488;

Var
    error           :Byte           ;
    device_address  :AddrType       ; {This data type is defined in the PRO488 unit }

BEGIN
    device_address := 12           ;
    error := REMOTE(device_address) ; {Puts the device of address 12 in remote control}
    if error <> 0 then writeln('Error Occurred') ; {error =0 means that no error occurred }
END.

```

Figure 2.3.3.1 Example of use of a PRO488 library function.

In COMMON.TPU developed library are grouped some useful functions and procedures that can be used to facilitate the interaction between the user and the computer. Our software user interface has been developed mainly with the help of this unit.

The IEEEDEV.TPU implements two routines; the procedure AssignIeee and the function ReBuffer of type Boolean. The former, AssignIeee, is used instead of the standard Assign procedure for the files IEEEEDATA and IEEECTRL. All other I/O on these files is done using the standard routines such as, Read and Readln, Write and Writeln, Reset, Rewrite, Close etc. See appendix B for more detail.

Function name	Description
SEND (address:AddrType;command:String)	Function used to Send HP-IB string command to a device. address is the device address (1-15). command is the command string, maximum length is 255 characters.
GET (address:AddrType;Var data:String)	Function used to Get data from a device. address is the device address (1-15). data is the data string, maximum length is 255 characters.
CLEAR(address:addrtype)	Function used to Clear a device. address is the device address (1-15).
CLRALL	Function used to Clear all devices.
TIMEOUT(value : Integer)	Function used to Set bus Time Out . value is the time out value (1-15).
RESETALL	Function used to Reset the bus.
EOI (bytechar,status:Integer)	Function used to define the End Or Identify Byte. bytechar is the EOI byte (0-255). status is the byte status (ON: Enabled , OFF: Disabled).
EOS (bytechar,status:Integer)	Function used to define the End Of Sequence terminator. bytechar is the EOS byte (0-255). Status is the byte status: ON : Data Sent Terminated when EOI bus ligne is set true. OFF: Data Sent Terminated when bytechar matched.
REMOTE(address:addrtype)	Function used to put a device in the Remote mode. address is the device address (1-15).
LOCAL(address:addrtype)	Function used to put a device in the Local mode. address is the device address (1-15).

Table 2.3.3.1. List of the PRO488 library functions.

Error Code	Description
0	No Error Occured
1	I/O Error
2	Address Vaue Out Of Range
3	Time Out Value Out Of range
4	Illegal Character Byte
5	Illegal Status Byte

Table 2.3.3.2. Error Codes Generated by The PRO488 Library functions.

2.3.4. Description of the different software components

2.3.4.1. The IISCEC.EXE main program

The IISCEC main program, is the first executed of the whole software. It manages the other programs by sending to them special information about the content of the environment variables (see the CHAR.BAT batch file later). When executed the screen presented in figure 2.3.4.1 appears to the user. This is the main menu. By just typing the corresponding number on keyboard, the user is able to run the STATIC program, the

DYNAMIC program, the UTILITIES program or simply QUIT the MAIN program. If one of these programs does not exist in the current directory or if an error occurs in running it, an explanatory message appears at the screen bottom to inform the user.

2.3.4.2. The STATIC.EXE program

The STATIC program can be executed by the user through the IISEC main program. It includes all current (I), current-voltage (I-V) and capacitance-voltage (C-V) measurements. All of these measurements are done by the HP model 4140B pA meter/DC voltage source instrument. The screen shown in figure 2.3.4.2.1 appears when the STATIC program starts. The user can select one of the four menu items by typing the corresponding number on the keyboard. Here is a brief description of each of them.

a) SETUP item

This item includes all operations that are related to the device setting. The user can load an existing setting or create a new setting by defining device function, range, parameters etc. (see description of the HP model 4140B device in previous chapter). The user can also save or show the content of the current setting. If the user define and save a set-up with DEFAULT as name, this one will be automatically loaded each time the static program starts. This feature is of great help especially when the same application is repeated for many times. Figure 2.3.4.2.1 shows the STATIC program in the setup definition.

b) Run item

Once a setting is defined, the user is allowed to run its measurement sequence, either in the direct mode (On line item) or the indirect mode (Buffered item) as described in the previous General overview section. If the direct mode is selected the data measurements are printed on screen as soon as they are obtained, in the form of a convenient tableau.

b) Utilities item

Some data utilities are grouped in this item such as, loading previously saved data measurements, saving current data, printing data on parallel printer, on HP 2631G printer, on screen or to a file, and plotting data on an the HP 7475A plotter or on screen.

d) Quit item

Choosing this item causes exiting STATIC program and backing to the IISCEC main program. Before that, if new setting or data is not saved a warning message appears on the screen bottom to prevent the user. Thus a chance is given to avoid setting or data loss before actually quitting.

2.3.4.3. The DYNAMIC.EXE program

As it is the case for STATIC program, the DYNAMIC program is executed by the user through the IISCEC main program, and is intended to all electrical parameter measurements obtained using the HP model 4275A multi-frequency LCR meter. (See description of HP 4275A in previous section). In addition, parameter measurements of

biased device under test are possible by making a link between the HP 4275A and the HP 4140B VA voltage source output. An example of DYNAMIC program at a measurement procedure is presented in figure 2.3.4.3.1. The DYNAMIC program is similar to the STATIC program in its structure except when defining a new setting in setup item, where the user is asked to define parameters of both HP model 4275A and HP model 4140B. However, the HP 4140B setting is restricted of course to the VA voltage source only. All others items are the same as of the STATIC program.

2.3.4.4. UTILS.EXE program

The utilities program is also executed through the IISCEC main program. This program gathers some useful utilities the user may need to carry out his application in a convenient way. The set of utilities concerns operations on both system hardware and saved measurement data.

a) Hardware utilities

If the user select the hardware utilities, he will be asked to chose one among a set of existing HP instruments present in a numbered list. After that, an other list related to the selected device appears. This list contains a set of useful checking tests that concern the selected device. The user will see a test procedure running by just typing its corresponding number on the keyboard. It is recommended to test the devices related to a given application, before starting the measurement sequence. By this way, the user may detect any device malfunction and hence, avoid corrupted data to be obtained later. Testing a device using hardware utilities may give to the user explanations about run time failures that can occur during execution of either STATIC or DYNAMIC program.

b) Data translation utilities

Currently large number of powerful data handling commercial software are available in the market. MATLAB and HARVARD GRAPHICS are two examples of existing software at our departement. Hence, it will be very useful (and may be necessary) to implement pieces of program for data translation purpose, in order to allow the user processing his measurement data using the various facilities provided by these software packages and thus, carry out his results in a pleasant manner. The data translation utilities have been developed to reach this goal.

In data translation utilities, the user can select either translation of STATIC data measurements (obtained using the STATIC program) or to DYNAMIC data measurements (obtained using the DYNAMIC program). In both cases, the user should indicate if data translation is to MATLAB format or to ASCII format which is recognised by most of data handling software. He will be asked after that to select one file (source file) from a numbered list of existing data files, and second, to give a name for the translated file (target file). Pressing on the Enter key without typing any character, will keep the source file name as a name for the target file, but with the .DAT extension. At the end of each data conversion, a message appears to the user to inform him about the success of the translation procedure. Translated files are stored in a disk directory which can be defined previously by the user (see next section).

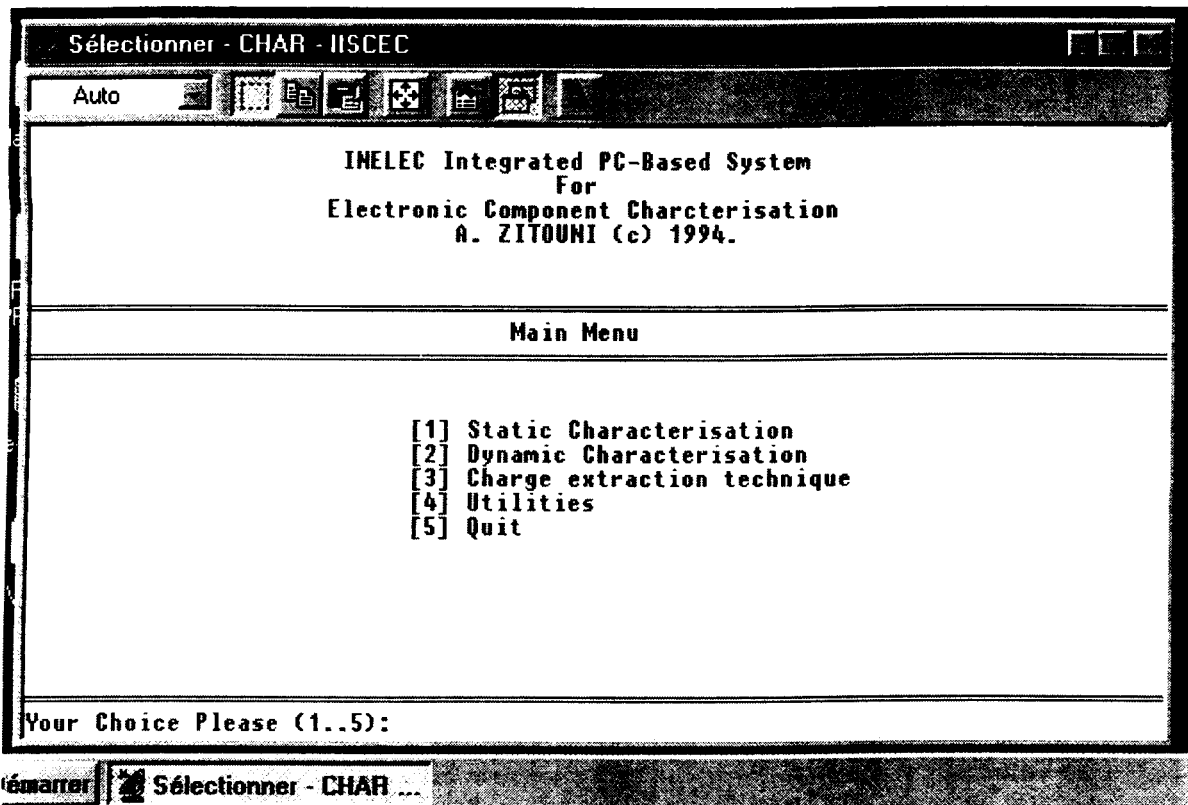


Figure 2.3.4.1 The IISCEC.EXE Starting screen.

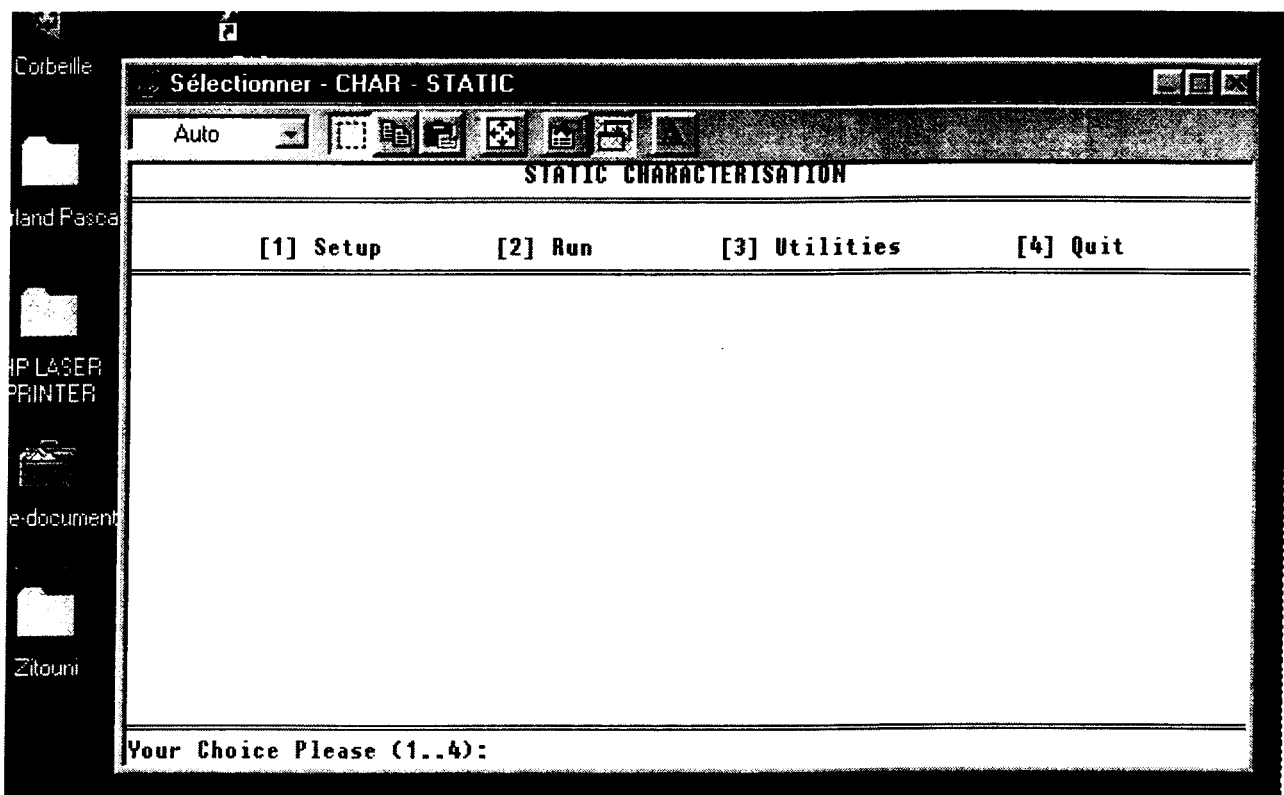


Figure 2.3.4.2.1 The STATIC.EXE starting screen

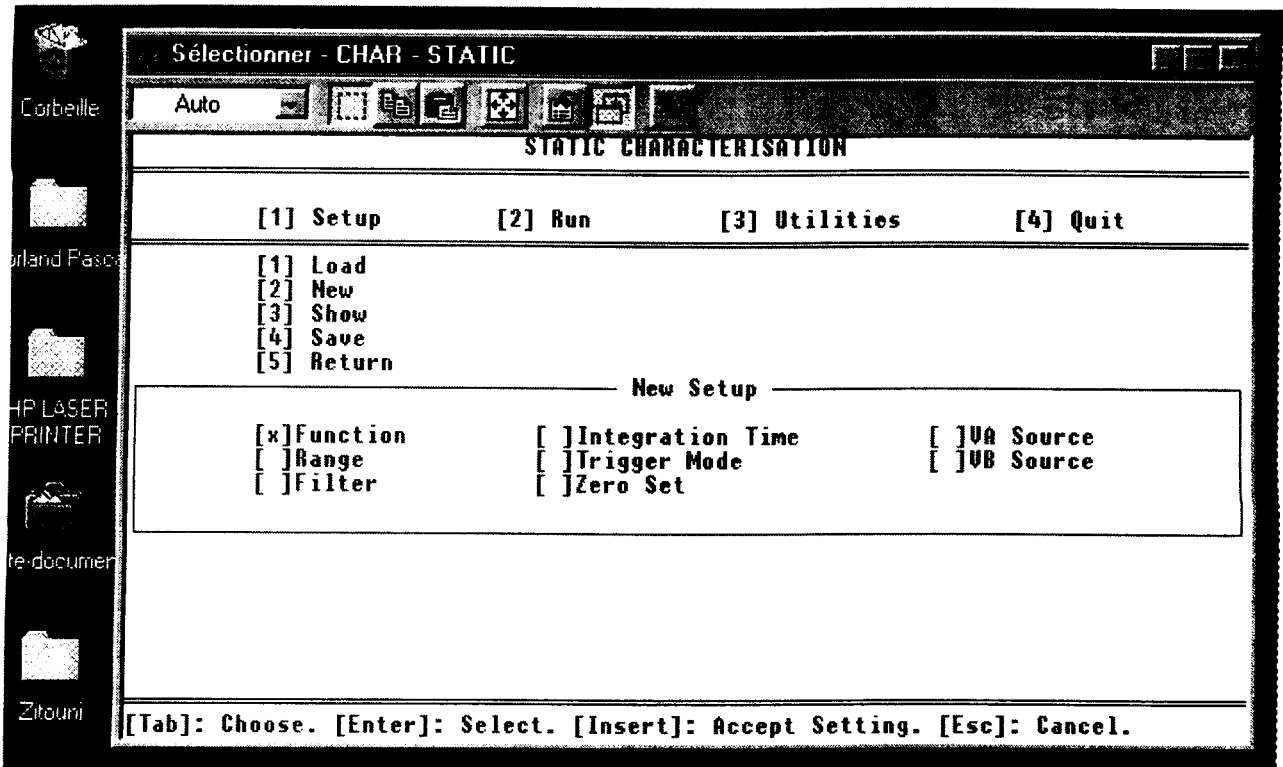


Figure 2.3.4.2.2 Setup definition.

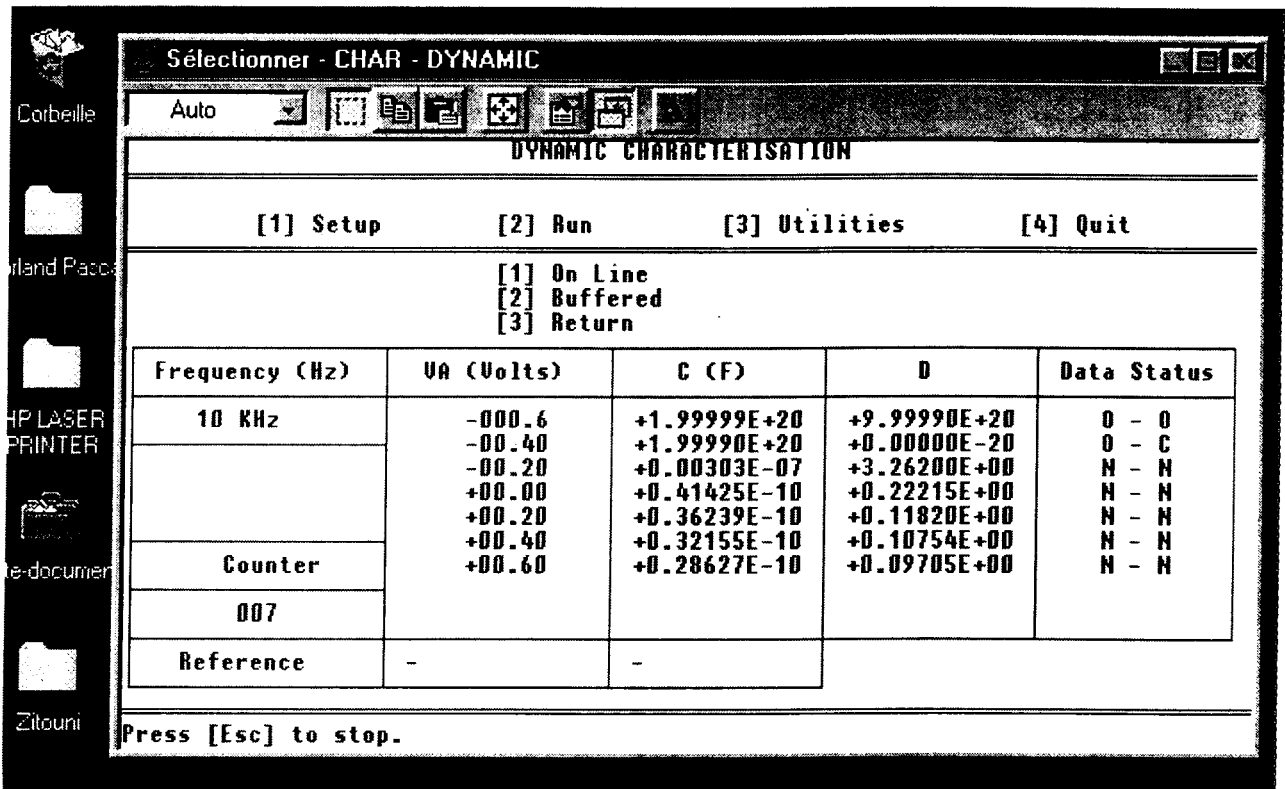


Figure 2.3.4.3.1 The DYNAMIC.EXE during measurement procedure

2.3.5 The CHAR.BAT batch file

As described before, the IISCEC main program manages both static and dynamic measurements by executing (depending on the user choice) the corresponding program ; STATIC program or DYNAMIC program. It has been also indicated that when executing these programs, IISCEC main program sends to them the content of some environment variables. Some of these environment variables are related to the installable device driver which manages the integrated interface card input output operations, while others are related to disk directories definition.

2.3.5.1. Variables related to the installable device driver

There are two variables used to define the name of each of the main files provided by the installable device driver PRO488, CONTROL file and DATA file. These two variables are CTRLFILE and DATAFILE. The content of the first one should be exactly equal to the second parameter added to the DEVICE=PRO488.SYS line in the CONFIG.SYS system file. The second variable contains the third parameter (see the description of the PRO488 device driver in previous section). If neither control file name nor data file name is specified in the DEVICE=PRO488.SYS line, then CTRLFILE variable should be set to IEEECTRL and DATAFILE variable to IEEE DATA, which are taken by the device driver as default file names.

2.3.5.2. Variables related to disk directory definition

Since the integrated software has been designed so that static measurements are separated from dynamic measurements, it is convenient then, to separate saved files for both instrument settings and measurement data of STATIC program from those of DYNAMIC program. This will likely prevent the user from losing time in searching for his saved data files through system disk, knowing that their number is supposed to increase along the use of the software.

To save instrument settings, the user can define appropriate directories by setting two environment variables ; STATICSTP for STATIC program, and DYNAMICSTP for DYNAMIC program. Similarly by setting the STATICDATA variable for STATIC program and the DYNAMICDATA for DYNAMIC program, the user is able to define his saved measurement data directories.

In addition, two other variables can be used to define translated measurement data files directory using the translation utility, as well as the directory for files that result from the "print to file" option in the "print data item". Thus, TRANSDATADIR variable holds the directory name for translated measurement data, while TEXTDIR variable contains the directory name of data printed to files.

2.3.5.3. The content of CHAR.BAT file

To define the previously mentioned variables, the user can use the SET DOS command. However and especially for less experienced users, we have created a batch file CHAR.BAT, in order to set all environment variables. The user has just to run the CHAR file in the DOS prompt, the bath file will do the rest for him. That, is defining the

concerned DOS variables and run the IISCEC program. It is recommended in particular for less experienced users, to run the integrated software using this way rather than running IISCEC program directly. In figure 2.3.5.3 is listed a typical CHAR.BAT batch file. In this example, all executable programs; IISCEC.EXE, STATIC.EXE, DYNAMIC.EXE, UTILS.EXE as well as CHAR.BAT are located in C:\CHAR directory. Instrument settings related to STATIC program will be saved in C:\CHAR\SETUP\STATIC directory while those related to DYNAMIC program will be saved in C:\CHAR\SETUP\DYNAMIC directory. In like manner the user will find his data measurements associated to STATIC program at C:\CHAR\DATA\STATIC directory and those associated to DYNAMIC program at C:\CHAR\DATA\DYNAMIC directory. The C:\CHAR\TEXTS directory contains files produced by the "print to file" option of data measurements, and finally, the C:\CHAR\TRANSDAT directory is the directory where translated data will be saved. We must notice here, that the DOS environment memory space may not be sufficient to define all these variables. In this case it is necessary to increase the amount of DOS environment memory space using the SHELL command in CONFIG.SYS system file.

```

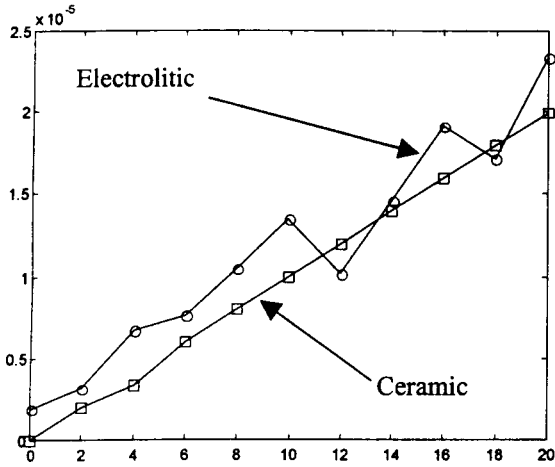
REM Variables definition :
SET CTRLFILE=IEEECTRL
SET DATAFILE=IEEEEDATA
REM Directories definition :
REM SETUP Directories :
SET STATICSTP=C:\CHAR\SETUP\STATIC
SET DYNAMICSTP=C:\CHAR\SETUP\DYNAMIC
REM DATA Directories :
SET STATICDATA=C:\CHAR\DATA\STATIC
SET DYNAMICDATA=C:\CHAR\DATA\DYNAMIC
REM Translated Data Directory :
SET TEXTDIR=C:\CHAR\TEXTS
SET TRANSDATADIR=C:\CHAR\TRANSDAT
IF NOT EXIST IISCEC.EXE GOTO CLEAR
IISCEC.EXE
:CLEAR
SET CTRLFILE=
SET DATAFILE=
SET STATICSTP=
SET DYNAMICSTP=
SET STATICDATA=
SET DYNAMICDATA=
SET TEXTDIR=
SET TRANSDATADIR=

```

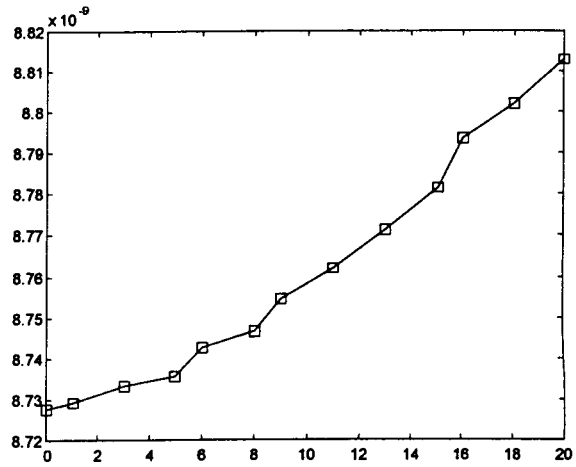
Figure 2.3.5.3 A typical example of CHAR.BAT file.

2.4. Examples of the implemented software capabilities

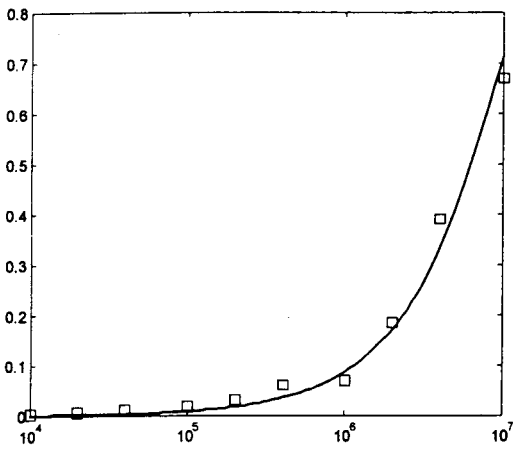
The implemented software has been tested on a large set of measurements and some results are shown on figures 2.4.1 and 2.4.2. Further, the system was used in the achievement of several research works as well as under graduate projects as a measurement tool, and, the users found it very helpful and reliable [13,14,15].



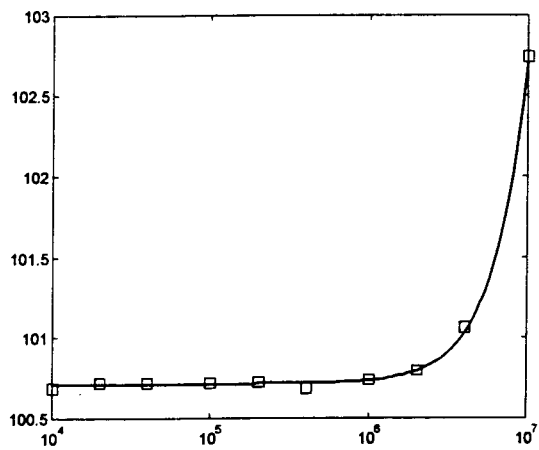
(a) Leakage current in the dielectric



(b) Capacitance as function of applied voltage

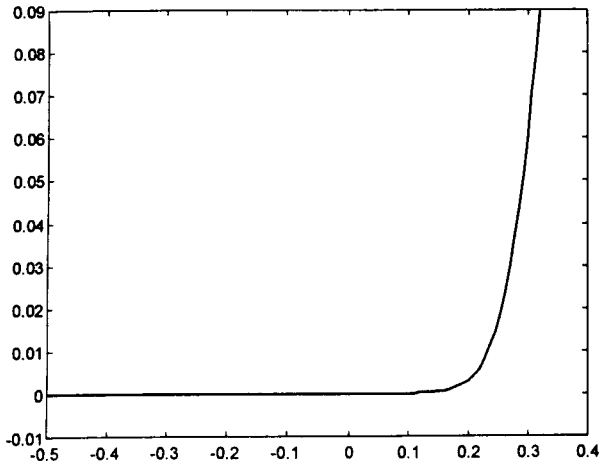


(c) Resistor impedance phase as function of frequency

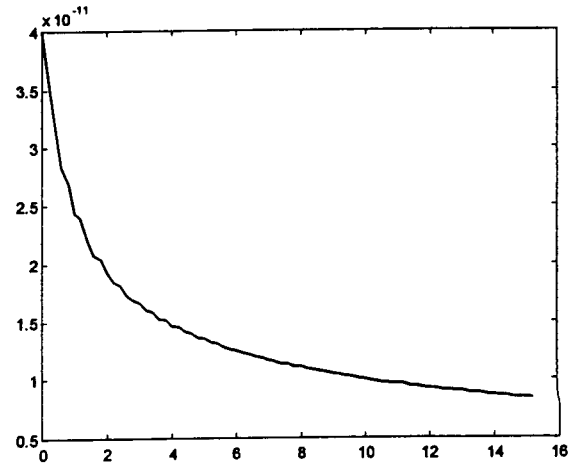


(d) Resistor impedance magnitude as function of frequency

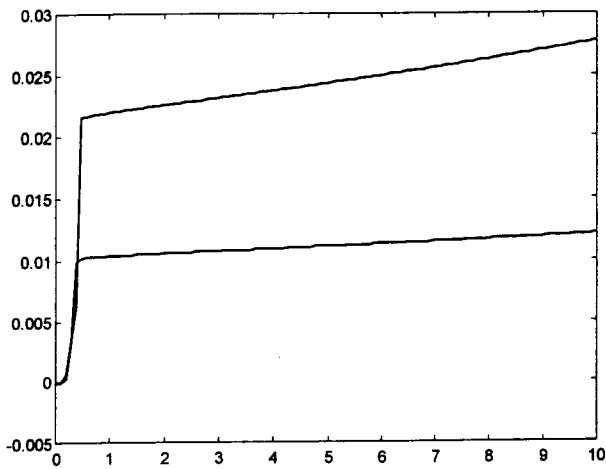
Figure 2.4.1 Example of measurements on passive components



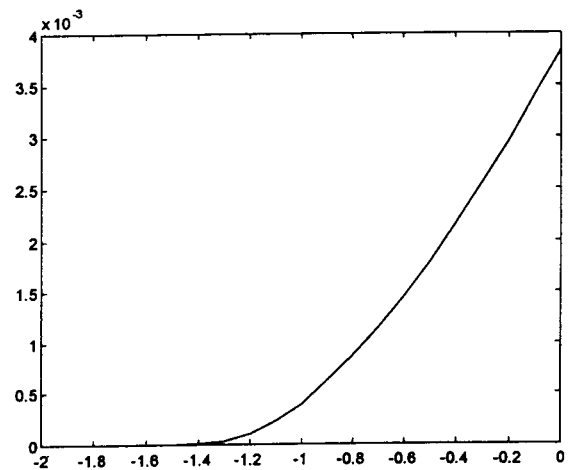
(a) Schottky diode I-V Characteristics



(b) reverse biased junction diode C-V characteristics



(c) BJT I_c - V_{ce} characteristics



(d) JFET I_d - V_{gs} characteristics

Figure 2.4.2 Example of measurements on active devices

Chapter 3

Electronic Components Models

3.1. Introduction

Modelling can be defined as mathematical representation of some or all the properties and characteristics of a device, system, object, process, etc. The accuracy of a model resides in its ability to explain the behaviour of the device in many modes of operation. It can be seen also as the completeness in studying various phenomena related to the device, so the more properties represented by the model the more accurate it will be and then the more complex it will become. Thus in constructing a satisfactory model we are faced with many trade-offs [17].

In electronic industry, the attractive face of modelling is that in order to run an experiment for a device in a specific operating conditions, it is not necessary to perform real experiment, we have just to represent all the properties of our device in a suitable model then, run the experiment by a software program such as SPICE. Hence, modelling helps understanding the device which leads to a better use of it in designing electronic circuits. Modelling sometimes is a necessary result as technology advances. In the case of semiconductor devices technology for example, the need of modelling comes from rapid development in their technology and also because of the behaviour of the small scale devices which do not follow the well understood pattern of their large counterparts [17]. Since models are main parts of simulating programs then, modelling contributes strongly in predicting the behaviour of a device in a specific operating conditions, so that both time and money are saved in electronic devices fabrication.

Therefore, parallel to the development of the device itself, a continuous development can be seen in the modelling of the electronic devices. Nowadays a wide variety of different types of device models exist. They all give a more or less accurate description of the terminal characteristics of the device. Most of them are at different levels of sophistication depending on the physical process of interest. In fact the following approaches can be distinguished [18]:

1. Numerical physical modelling: numerical or Monte Carlo methods for solving semiconductor equations on a discrete geometrical mesh.
2. Analytical physical modelling: analytical methods to solve the semiconductor equations. The solution is generally applicable to all regions of operation.
3. Compact analytical modelling: piece wise analytical solutions of the semiconductor equations valid in a limited range of conditions. Several (optimisation) parameters, which have usually a physical meaning, are necessary.
4. Empirical modelling: analytical expressions, not (directly) based on physics, which are fitted through measurement data by an optimisation process. The parameters of these models usually have no physical meaning.
5. Table modelling: look-up tables of measured data with inter- and extrapolation methods for obtaining the characteristics at any bias condition.

Each of these models has its distinct advantages and disadvantages. These will be discussed briefly, but this section is in no way meant to be exhaustive.

The most sophisticated type of model arises from the numerical physical approach. In particular with Monte Carlo modelling the relation to real physical process. With numerical solution of the semiconductor equations several physical processes occurring on the atomic scale are treated as macroscopic quantities. The advantage of

this type of models is its close relation to physics and the insight gained by the possibility to study processes occurring inside the device. The main disadvantage is its (relatively) long computation time, which in most situations, is too long for circuit simulation purposes. Therefore the above is mainly used for improving device design.

The next type (2) can be closely related to physics, but usually yields implicit relations. Therefore iterative procedures are needed within the device model to evaluate useful model quantities. This has to be done for each iteration in the solution process of the circuit simulator. Therefore these models are rather time consuming.

The types (4) and (5) can both be very fast and accurate, but offer little physical insight. In addition, the results are limited to the measured series of device data and adaptation for different devices is difficult and, therefore they are rarely used for design purposes.

The compact models (3) seem to give a good compromise between the advantages and disadvantages of most of the other categories. They are based on the physical processes occurring in the device and yield explicit (relatively simple) model equations, however at the cost of appropriate approximations. This is accomplished by splitting the operation range in several distinguished regions. For each region appropriate assumptions can be made and explicit model equations can be derived, which are applicable in that region. The prize to be paid is that the solutions have to be matched at the transition from one region to another. This can be generally achieved either by choosing the point of transition such that a differentiable transition arises naturally, or by a mathematical smoothing function. This is a dangerous pitfall and may lead to non-physical behaviour. Therefore the number of different modelling regions has to be minimised.

The following sections deal with the electrical approximating models of the basic passive and active electronic components that are often met in electrical engineering, that are: Resistors, Capacitors, Inductors, diodes, BJTs and JFETs. Because SPICE (Simulation Program with Integrated Circuit Emphasis) program [19] is used world-wide as an essential computer-aid for circuit design, the models we have chosen to approximate the behaviour of the basic electronic active devices are those on which SPICE program is based.

3.2. Passive Components models

Passive components exists commercially under different types depending on their construction details (fabrication method, material employed ...). Hence, the models that have been developed in order to approximate the electrical behaviour of these devices take this fact in to high consideration. As a result, to each type of component is associated an equivalent circuit provided that the considered device is linear. This circuit consists of a combination of the three pure elements (resistor, capacitor and inductor). Extra effects such as non linearity (change of device characteristics with respect to the applied voltage or current) and temperature, are generally modelled with mathematical equations.

3.2.1. The Resistor equivalent circuit

An ideal resistor is a two terminal device that obeys to the well known Ohm's law; $v = R i$, figure 3.2.1.a . v is the electrical voltage across the element, i is the

electrical current through it an R a constant parameter called the electrical resistance of the element and expressed in Ohm or (Ω). In practice no such device exists and is rather approximated with the circuit of figure 3.2.1.b [20].

In this circuit, the resistance R_p represents the resistance that normally the device takes if it is a pure one. The inductor L represents inductive effects due to the type of fabrication and the presence of connecting lead wires, these effects can be relatively important in the wire-wound resistors. The capacitance C is present because it is known that each pair of conductor for which it is applied a difference of potential gives rise to a capacitance, this effect is not localised but rather distributed in the volume occupied by the component, this is why C is placed in parallel with R and L .

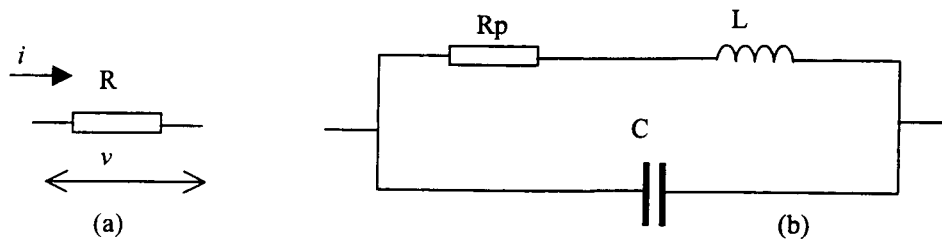


Figure 3.2.1 The Resistor Equivalent Circuit. (a) The ideal Resistor. (b) The real Resistor

3.2.2. The Capacitor equivalent circuit

For an ideal capacitor the current through the element and the voltage across it figure 3.2.2.a. are related by the following equation; $i = C \frac{dv}{dt}$, in which, C is a constant parameter called the capacitance of the element and given in Farad (F). In the case of a real capacitor the equivalent circuit of figure 3.2.2.b is proposed [20].

In this circuit, the capacitance C is the one that the capacitor takes if it is a pure element. The resistance R_s is a series resistance that represents the resistive effects due to conducting material used for the device fabrication. The resistance R_p models the leakage currents through the dielectric material. The inductance L is present to model any inductive effect due to the conducting connections and the form of the electrodes. Its effect appears at high frequency values where the impedance magnitude of the component increases instead of decreasing.

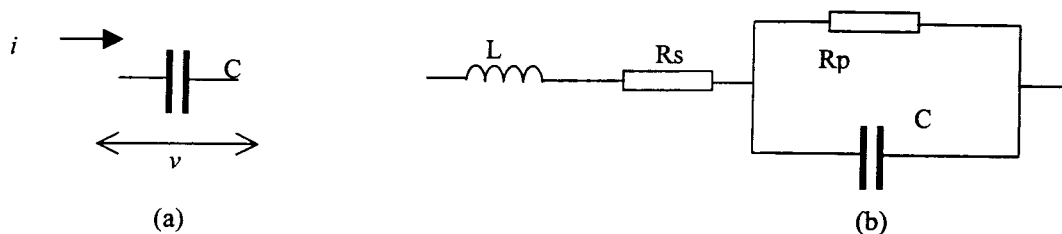


Figure 3.2.2. The Capacitor Equivalent Circuit. (a). (b) The ideal Capacitor The real Capacitor

3.2.3. The Inductor equivalent circuit

An ideal inductor is a two terminal device for which the current to voltage relationship is given by $V = L \frac{di}{dt}$, figure 3.2.3.a. L is a constant parameter known as the inductance of the element and expressed in Henry (H). Practically the circuit of figure 3.2.3.b is used to model a real inductor [20].

In this circuit, the inductance L is the inductance value that the device takes if we assume it to be a pure one. The resistance R_s is the series resistance of the wire from which the inductor is fabricated. C is known as the inter-winding capacitance and is due to the adjacent and the non adjacent windings. The resistance R_p models losses of both hysteresis and Foucault currents.

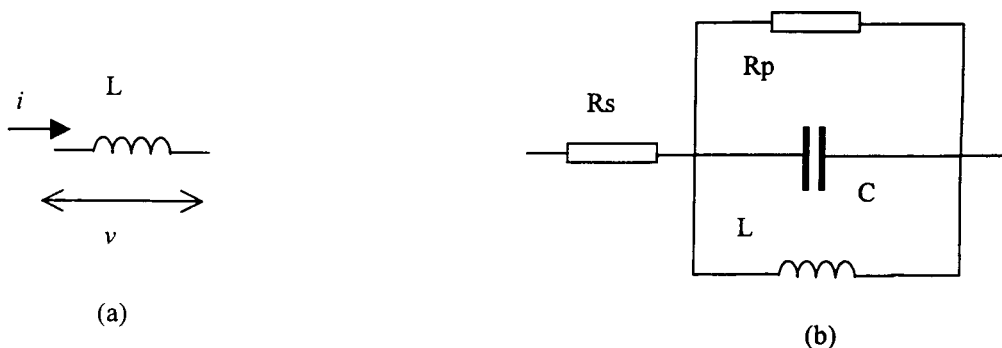


Figure 3.2.3 The Inductor Equivalent Circuit. (a) The ideal Inductor. (b)The real Inductor

3.2.4. Models for non linear capacitors and inductors

a. Non linear capacitors

In general the capacitance parameter of a capacitive element varies with the applied voltage V . This variation is modelled using the following equation [21]:

$$C(V) = C_0 + C_1V + C_2V^2 + \dots + C_nV^n \quad (3.2.4.1)$$

Where $C_0, C_1, C_2, \dots, C_n$ are constant parameters that model the phenomenon. Usually higher order terms are neglected so that equation (3.2.4.1) can be simplified to [21]:

$$C(V) = C_0 + C_1V + C_2V^2 \quad (3.2.4.2)$$

b. Non linear Inductors

As it is the case for the non linear capacitor, the inductance of an inductive element depends generally on the value of the current I that flows through it, according to the following equation [21]:

$$L(I) = L_0 + L_1I + L_2I^2 + \dots + L_nI^n \quad (3.2.4.3)$$

Where $L_0, L_1, L_2, \dots, L_n$ are constant parameters that model the phenomenon. Usually higher order terms are neglected so that equation (3.2.4.3) can be simplified to [21]:

$$L(I) = L_0 + L_1I + L_2I^2 \quad (3.2.4.5)$$

3.3. Active electronic components

Active electronic components are more difficult to model, because the theory involved to build equivalent circuit models, requires a good background in physics and technology of semiconductor structures. Many excellent references are available in this area [22,23,24], and deep details on the theory of semiconductor devices is beyond the scope of the present work. This is why brief description of the models that will be presented later is given only when necessary.

3.3.1. PN junction diode and Schottky diode

The resulting model of PN junction and Schottky diode comes from the analysis of the simple monodimensional PN structure shown in figure 3.3.1.a. Where the following simplifying assumptions are supposed to be valid [22].

1. The uniform doping and electrical neutrality in the P and N type regions as shown in figure 3.3.1.b, where N_A is the acceptor concentration in the P type region and N_D is the donor concentration in the N type region.
2. The abrupt depletion-layer approximation: The built-in potential and applied voltages are supported by a dipole layer with abrupt boundaries, and outside the boundaries the semiconductor is assumed to be neutral.
3. The Boltzmann approximation: Throughout the depletion layer, the Boltzmann relations are valid.
4. The low-injection assumption: The injected minority-carrier densities are small compared with the majority-carrier densities.
5. No generation current exists in the depletion layer, and the electron and hole currents are constant through the depletion layer.

a) Static Model

from the previous assumptions, the DC characteristics of the ideal diode can be derived as:

$$I_D = I_S \left(e^{\frac{V_D}{V_T}} - 1 \right) \quad (3.3.1.1)$$

Where,

I_D and V_D are respectively the current through the diode and the voltage across its terminals according to the polarity convention of figure 3.3.2.

V_T the Thermal potential $V_T = kT/q$ ($V_T = 25.86\text{mV}$ at $T = 300\text{K}$).

($k = \text{Boltzmann constant} = 1.38 \times 10^{-23} \text{ J/K}$ and, $q = \text{electronic charge} = 1.602 \times 10^{-19} \text{ C}$).

I_S is what it is known as the diode saturation current.

The ideal diode model described by equation (3.3.1.1) suffers from several limitations, that make the experimental results for most junction diodes presenting discrepancies from calculated ones. These limitations are due to several mechanisms including [22]:

1. Carrier generation-recombination in the space-charge layer.
2. High-level injection.
3. Voltage drop associated with the electric field in the neutral regions
4. Internal breakdown associated with high reverse voltage.

- The first effect can be modelled by the following expression:

$$I_D = I_S \left(e^{\frac{V_D}{nV_T}} - 1 \right) \quad (3.3.1.2)$$

Where n , the emission coefficient, is usually about 2 [25].

- The second effect and the third one are modelled by introducing an ohmic resistance r_s in series with the ideal diode so that, the actual voltage drop across the diode terminals becomes:

$$V'_D = r_s I_D + V_D \quad (3.3.1.3)$$

Where I_D is given by equation (3.3.1.2).

- The last effect is what is known as Zener breakdown [23] and is modelled for negative values of V_D by the following equation[25]:

$$I_D = -I_S \left(e^{-\frac{V_B + V_D}{V_T}} - 1 + \frac{V_B}{V_T} \right) \quad (3.3.1.4)$$

Where V_B , is a positive parameter known as the breakdown voltage.

Hence, a complete description of the static diode model, requires the knowledge of a set of parameters that are: I_S , n , r_s , V_B . The current to junction voltage relationship can hence be obtained in different operating modes.

Operating mode	V_D range	I_D expression
Forward biasing	$V_D > -5V_T$	$I_D = I_S \left(e^{\frac{V_D}{nV_T}} - 1 \right)$
Reverse biasing	$-5V_T \geq V_D > -V_B$	$I_D = -I_S + GV_D$
Reverse biasing	$V_D < -V_B$	$I_D = -I_S \left(e^{-\frac{V_B + V_D}{V_T}} - 1 + \frac{V_B}{V_T} \right)$

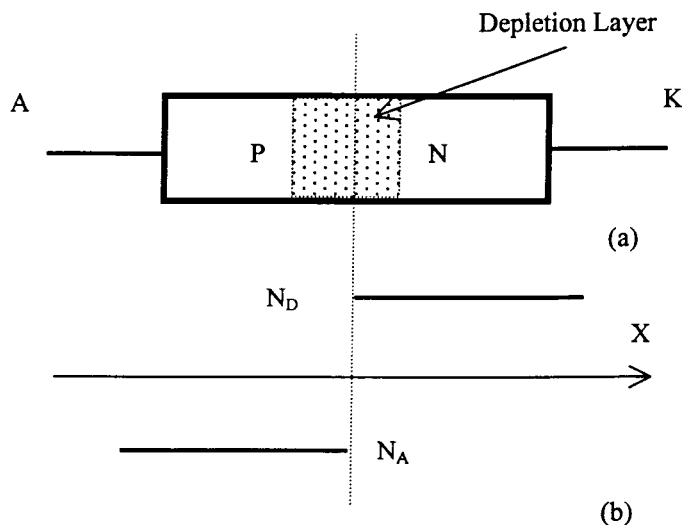


Figure 3.3.1.(a) PN junction under equilibrium conditions. (b) Doping profile .

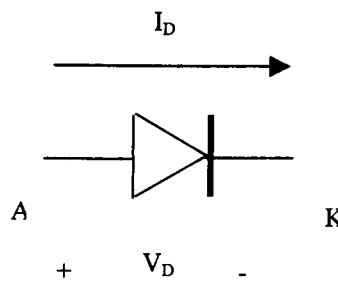


Figure 3.3.2. Circuit representation of the ideal diode

From the expression of the current when the diode is reverse biased, it can be shown that two additional parameters are to be considered. These parameters are related to the current value $-I_B$, when V_D is exactly equal to $-V_B$. A special care is to be considered for the value of I_B passed to the simulating program in order to ensure convergence. Indeed, at that special point, the following equation is to be verified:

$$\lim_{V_D \rightarrow V_B} I_D = -I_S \frac{V_B}{V_T} = -I_B$$

b) Large-Signal Model

The large signal model considers the charge-storage effect of the device. The importance of these effects is clear. If there were no charge storage, the device would be infinitely fast; that is, there would be no charge inertia, and currents could be changed in zero time. The two forms of charge storage are the minority-carrier injection Q_s and the space charge Q_d .

The minority-carrier injection charge storage results from excess minority carriers injected across the junction when the diode is forward biased. It can be shown theoretically [22,23] that Q_s is proportional to the forward current I_D .

$$Q_s = \tau_D I_D(V_D) \quad (3.3.1.5)$$

The proportionality constant τ_D between the current and the charge is a time constant which represents the minimum time required to either store or remove the charge; and is called the transit time of the diode.

The second charge storage Q_d can be explained if we assume the depletion layer to be a capacitor with a space charge region width modulated by the reverse applied voltage. The equivalent capacitance associated with a change dV_D of the applied voltage V_D is theoretically :

$$C_d = \frac{dQ_D}{dV_D} = \frac{C_d(0)}{\sqrt{1 - \frac{V_D}{\phi_0}}} \quad (3.3.1.6)$$

Where ϕ_0 , is known as the diode built-in voltage, and $C_d(0)$ is the zero-bias depletion capacitance.

Practically, equation (3.3.1.6) is often modified to fit the experimental results as:

$$C_d = \frac{dQ_D}{dV_D} = \frac{C_d(0)}{\left(1 - \frac{V_D}{\phi_0}\right)^m} \quad (3.3.1.7)$$

Where m is a parameter not necessary equal to 0.5.

Now two important observations can be made. For reverse bias and small forward bias, Qd is the dominant charge storage. For moderate forward bias, and beyond, the injected charge Qs dominates; hence the effects of Qd become negligible. This second observation is extremely important, since as V_D approaches ϕ_0 , the space-charge capacitance becomes infinite, where as charge Qd becomes zero and hence equations (3.3.1.6) and (3.3.1.7) are no longer valid. The large signal diode model is presented in figure 3.3.3. In this model C_D represents both Qs and Qd contributions in the total charge-storage element. In SPICE program C_D is defined as follows:

$$C_D = \frac{dQ_D}{dV_D} = \begin{cases} \tau_D \frac{dI_D}{dV_D} + C_d(0) \left(1 - \frac{V_D}{\phi_0}\right)^{-m} & \text{for } V_d < FC \times \phi_0 \\ \tau_D \frac{dI_D}{dV_D} + \frac{C_d(0)}{F_2} \left(F_3 + \frac{mV_D}{\phi_0}\right) & \text{for } V_d \geq FC \times \phi_0 \end{cases} \quad (3.3.1.8)$$

In the above equation, F_2 , F_3 and FC are SPICE constants whose values are:

$$\begin{aligned} F_3 &= 1 - FC(1 + m) \\ F_2 &= (1 - FC)^{1-m} \\ FC &= 0.5 \end{aligned} \quad (3.3.1.9)$$

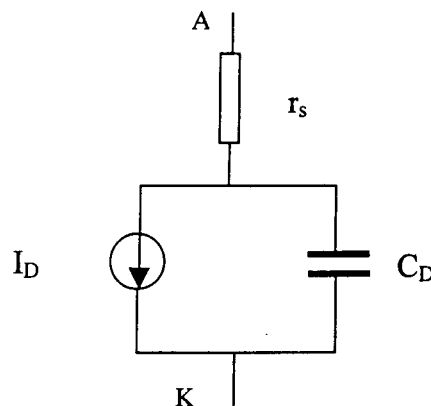


Figure 3.3.3. Diode large-signal model

c) Small-Signal Model

The small-signal model can be found by considering small-voltage variations of V_D around a given DC voltage V_{DQ} and writing $V_D = V_{DQ} + \Delta V_D$. The interest is in the corresponding small change of current, which is proportional to the change in the voltage change if this last is small enough. This linear relationship can be used to define a small-signal conductance $g_D = dI_D/dV_D$. The conductance is a DC or a low-frequency concept, hence, g_D can be approximated by expanding the current expression in a Taylor series about V_{DQ} .

$$I_D = I_S \left(e^{\frac{V_{DQ}}{nV_T}} - 1 \right) + I_S e^{\frac{V_{DQ}}{nV_T}} \left[\frac{\Delta V_D}{nV_T} + \frac{1}{2!} \left(\frac{\Delta V_D}{nV_T} \right)^2 - \dots \right] \quad (3.3.1.10)$$

The first term in the right side of equation (3.3.1.10) is the operating current I_{DQ} ; the second term is I_D , the small-signal component of the current, which is approximately linear related to V_D if the second term in the brackets is much less than the first one. Consequently, the small-signal conductance is:

$$g_D = \left. \frac{dI_D}{dV_D} \right|_Q = \frac{I_S}{nV_T} e^{\frac{V_{DQ}}{nV_T}} \quad (3.3.1.11)$$

Graphically, g_D is the slope of the static characteristic at the operating point. With moderate reverse bias, I_D is negative and approaches the saturation current I_S hence, the conductance is zero. On the other hand, for moderate forward bias, the current I_D is much larger than the saturation current, and the conductance is approximately proportional to I_D .

Further, the charge Q_D stored in the diode changes an amount dQ_D for a small voltage change dV_D ; so if $Q_D = Q_S + Q_d$, it can be written:

$$C_D = \left. \frac{dQ_D}{dV_D} \right|_Q = \begin{cases} \tau_D g_D + C_d(0) \left(1 - \frac{V_D}{\phi_0} \right)^{-m} & \text{for } V_d < FC \times \phi_0 \\ \tau_D g_D + \frac{C_d(0)}{F_2} \left(F_3 + \frac{mV_D}{\phi_0} \right) & \text{for } V_d \geq FC \times \phi_0 \end{cases} \quad (3.3.1.12)$$

Of course, g_D and C_D are evaluated at the DC operating point $(I_D, V_D)_Q$. The small-signal linearised model is then obtained as shown in figure 3.3.4.

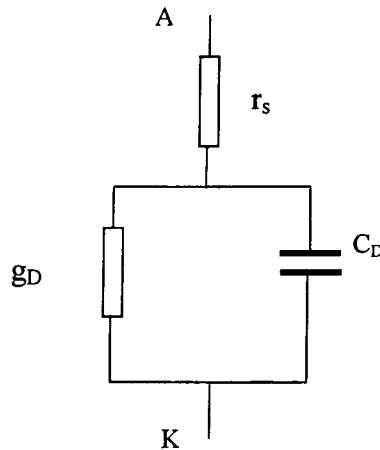


Figure 3.3.4. Diode linearised, small-signal model

The previous models used for PN junction diodes still valid for Schottky diodes, because a good electrical approximation of the Metal-Semiconductor contact (Schottky barrier) is the abrupt one sided P⁺N junction. However, important differences make these diodes attractive and useful.

First, the diode operates as majority-carrier device under low-level injection conditions. As a consequence, storage time (due to storage of minority carriers in the case of PN junctions) is eliminated and fast response is obtained [22,26].

Second, for a fixed voltage bias, the current through the device is typically more than two orders of magnitude greater than it is for junction device.

3.3.2. Bipolar Junction Transistors (BJTs)

The bipolar junction transistor can be considered to be an interacting pair of PN junctions, and the approach to the problem is basically the same as that used for the diode. Two diode solutions are hence needed, and the boundary conditions for one diode are the same as the boundary conditions for the other [25]. The model which is implemented in SPICE program is a more comprehensive version of the classic Gummel-Poon model [27] and in fact it is an extension to the Ebers-Moll model [28].

The original Ebers-Moll model, which is a non-linear DC model, has been modified by many people to include effects such as charge storage, β variation with current, base-width modulation, and so forth.

The Gummel-Poon model is originally based on the charge control Gummel-Poon model. However, the model can be treated as an extension of the Ebers-Moll model. Several secondary effects are implemented in the model, and each modification can be introduced independently to obtain greater accuracy over Ebers-Moll model [25].

3.3.2.1. Transistor Conventions and symbols

The well known circuit symbols for NPN and PNP BJTs are shown in figure 3.3.5. To define the circuit currents, and voltages, the emitter, base, and collector currents, as well as the emitter-base, emitter-collector, and base-collector voltages, must be specified. Figure 3.3.6 defines the current directions and the voltage polarities conventionally considered.

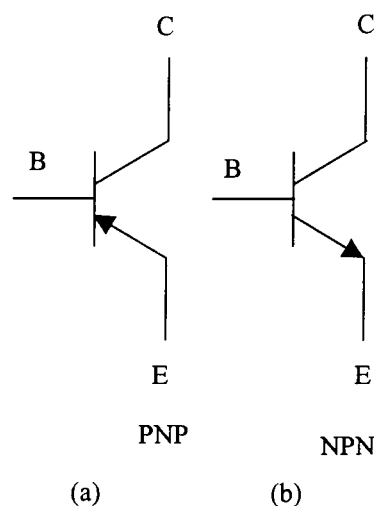


Figure. 3.3.5. Circuit symbols for BJTs
(a) PNP type, (b) NPN type

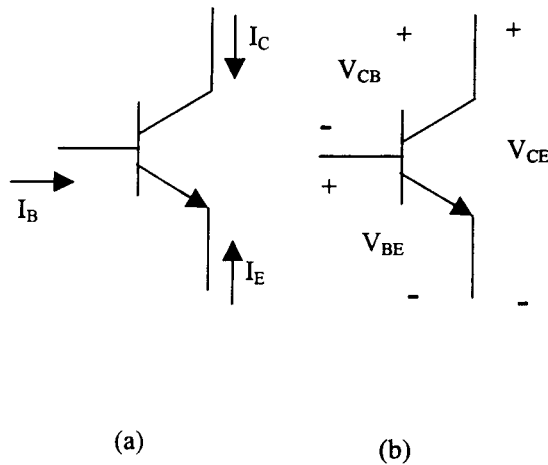


Figure 3.3.6. Terminal variables for BJT. (a) Terminal currents. (b) Terminal voltages

Currents and voltages are related through the basic Kirchhoff's circuit laws:

$$I_E + I_B + I_C = 0 \quad (3.3.2.1)$$

$$V_{CE} = V_{BE} + V_{CB} \quad (3.3.2.2)$$

The BJT device has actually four modes of operation in term of the applied junction voltages. Figure 3.3.7 summarises this modes.

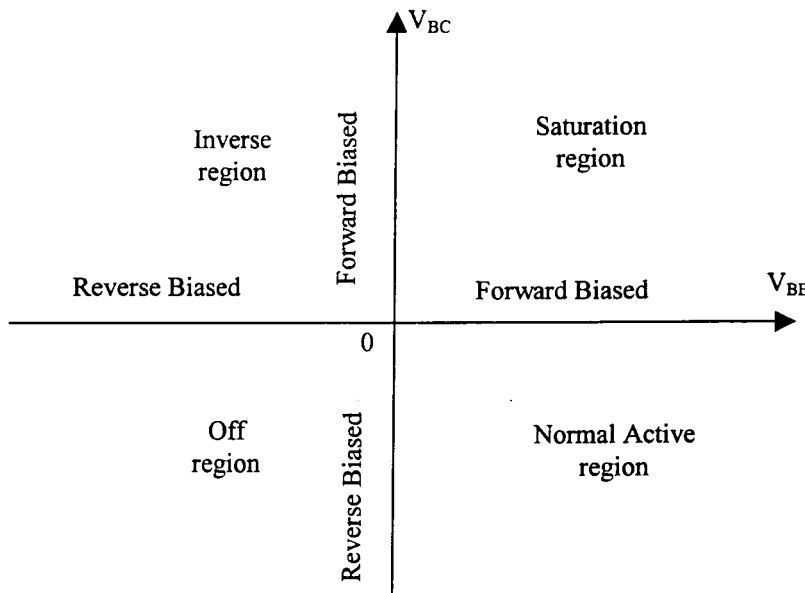


Figure 3.3.7. Regions of operation for BJT

3.3.2.2. Ebers-Moll Static Model

The Ebers-Moll equations express formally the of solution the interacting pair of PN junctions that form the BJT. They provide the emitter and collector currents I_E and I_C of the transistor in terms of the emitter and collector diode voltages V_{BE} and V_{BC} .

Currently there are two versions of the Ebers-Moll model; the injection version shown in figure 3.3.8.a and the transport version shown in figure 3.3.8.b. These

versions are mathematically equivalent; however, since the second version is preferred for computer simulation, it is considered the base for the analysis of BJT's behaviour.

In the injection version, the reference currents are I_F and I_R , the currents through the diodes. Thus, one may write:

$$I_F = I_{ES} \left(e^{\frac{V_{BE}}{V_T}} - 1 \right) \quad (3.3.2.3)$$

$$I_R = I_{CS} \left(e^{\frac{V_{BC}}{V_T}} - 1 \right) \quad (3.3.2.4)$$

Where, I_{ES} and I_{CS} are respectively the base-emitter and the base-collector saturation currents.

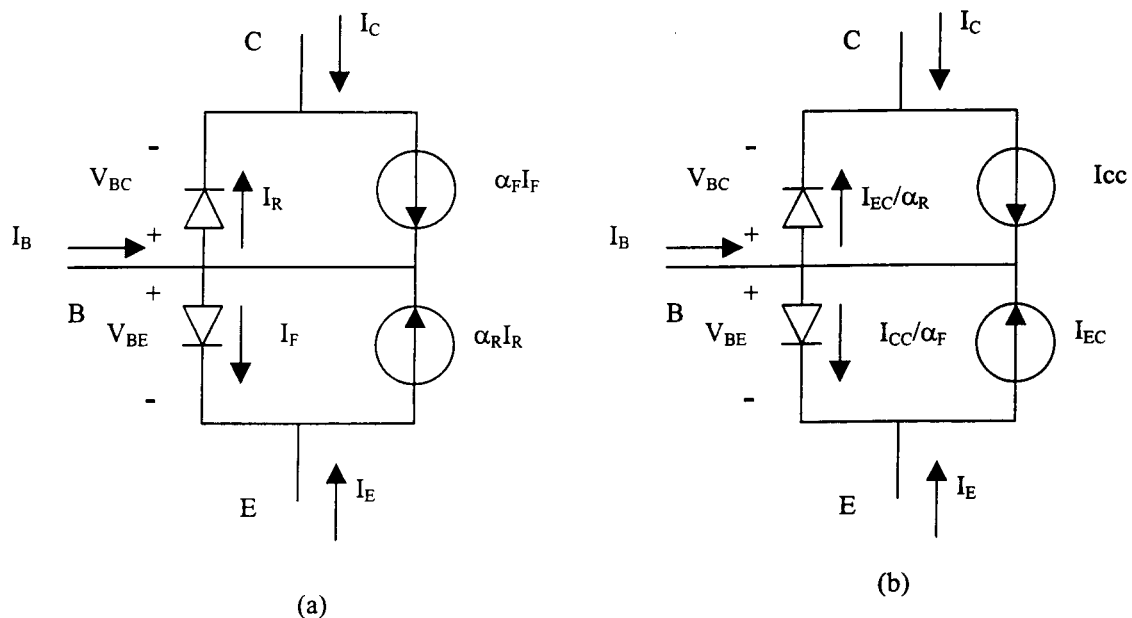


Figure 3.3.8. Ebers-Moll static model for NPN ideal BJT. (a) injection version, (b) transport version.

The terminal currents can be then expressed as follows:

$$\begin{aligned} I_C &= \alpha_F I_F - I_R \\ I_E &= -I_F + \alpha_R I_R \\ I_B &= (1 - \alpha_F) I_F + (1 - \alpha_R) I_R \end{aligned} \quad (3.3.2.5)$$

Where, α_F and α_R are, respectively, the large-signal forward and reverse current gains of a common-base BJT.

A dual consideration is valid for BJT operating in the reverse active region; it is sufficient to consider I_R and α_R instead of I_F and α_F and to change the role of the two junctions. Indeed, from equations 3.3.2.3 to 3.3.2.5, four parameters are needed to model the device, but this number can be reduced by one when the reciprocity property is applied. This property gives:

$$\alpha_F I_{ES} = \alpha_R I_{CS} = I_S \quad (3.3.2.6)$$

Where I_S is the BJT saturation current.

The last result allows an interesting change in the model topology as shown in figure 3.3.9, where the following familiar relations are considered :

$$\beta_F = \alpha_F / (1 - \alpha_F) \quad (3.3.2.7)$$

$$\beta_R = \alpha_R / (1 - \alpha_R)$$

In the transport version (Figure 3.3.8.b) the reference currents I_{CC} and the I_{EC} are those flowing through the model's current sources it can be easy to show that:

$$I_{CC} = I_S \left(e^{\frac{V_{BE}}{V_T}} - 1 \right) \quad (3.3.2.8)$$

$$I_{EC} = I_S \left(e^{\frac{V_{BC}}{V_T}} - 1 \right) \quad (3.3.2.9)$$

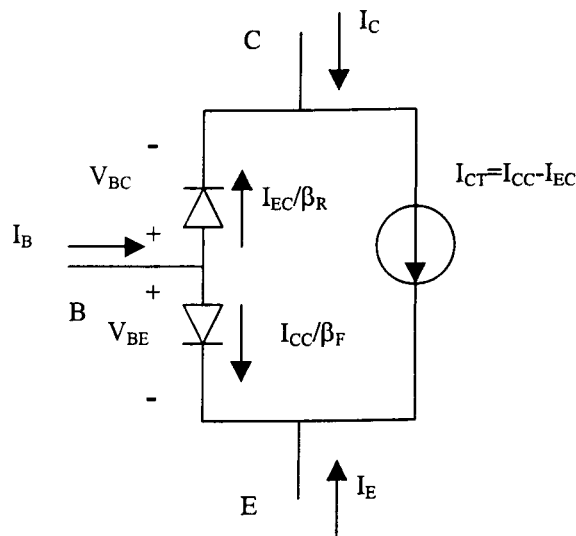


Figure 3.3.9. The modified Ebers-Moll static model

The BJT's terminal currents are then given by :

$$\begin{aligned} I_C &= I_{CT} - I_{EC} / \beta_R \\ I_E &= -I_{CT} - I_{CC} / \beta_F \\ I_B &= I_{EC} / \beta_R + I_{CC} / \beta_F \end{aligned} \quad (3.3.2.10)$$

Where I_{CT} is given by:

$$I_{CT} = I_{CC} - I_{EC} = I_S \left(e^{\frac{V_{BE}}{V_T}} - e^{\frac{V_{BC}}{V_T}} \right) \quad (3.3.2.11)$$

Hence, a complete description of the static Ebers-Moll model is obtained if the parameters I_S , β_F and β_R are known. Calculated terminal currents with respect to junction voltages are obtained using equations 3.3.2.10 and 3.3.2.11. Note that, when the junction voltage is less than $-5V_T$ the corresponding current is considered to be constant and equal to $-I_S$.

3.3.2.3. Ebers-Moll static model and second-order effects

Although it is very simple in form and requires, at most, three parameters, the Ebers-Moll model as described before is accurate and is recommended when the BJT is working as a DC switch or in a specific and narrow bias range. The limitation of this model lies mainly in its neglect of transistor charge storage and ohmic resistances to the terminals. This means that to increase the accuracy the model, modifications should be introduced to consider these effects. In general (and as it is the case in SPICE program) extra electrical elements (capacitors and resistors) are added to the ideal Ebers-Moll model (figure 3.3.9).

The inclusion of three constant resistors as shown in figure 3.3.10, improves the DC characteristics of the model. Each of the resistances models a specific phenomenon:

- The effect of r_C is to decrease the slope of the curves $I_C=f(V_{CE})$, in the saturated region for low collector-emitter voltages.
- r_E is mainly due to the ohmic contact at the emitter region, because, in present-day transistors this region is the most heavily doped one, in order to produce a high emitter-injection efficiency. The effect of this resistance is mainly the reduction of the voltage seen at the emitter junction by a factor of $r_E I_E$.
- r_B has an important impact on the small-signal and transient responses of the BJT. It is difficult to measure because it depends strongly on the operating point.

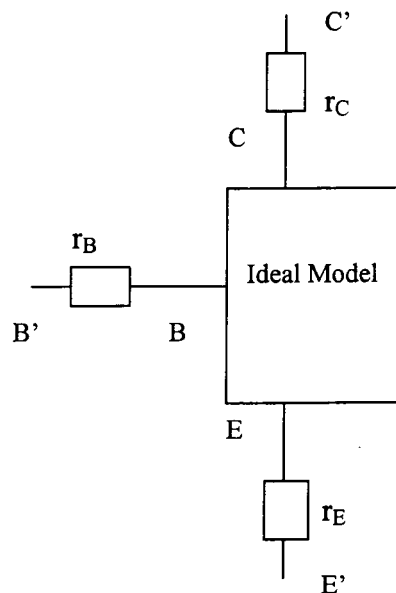


Figure 3.3.10 Effect of ohmic resistances

An other effect of great importance is what is known as the Early effect. This effect is due to the change of the width of the base region when the collector junction is reverse biased with high voltage value. This is why this effect is also referenced as the based-width modulation effect. This effect has a direct impact on the BJT saturation current and on the forward current gain and its characterised by the presence of a non zero slope value of the curves $I_C=f(V_{CE})$, in the normal active region and for large collector-emitter voltages. The analysis, which assumes that the transistor is

operated in the linear region, first determines the effect of base-width modulation on the base width and then on the model base-width related parameters. The result of analysis are as follows [25]:

$$I_S(V_{BC}) = \frac{I_S(0)}{1 + \frac{V_{BC}}{V_A}} \approx I_S(0) \left(1 - \frac{V_{BC}}{V_A} \right) \quad (3.3.2.12)$$

$$\beta_F(V_{BC}) = \frac{\beta_F(0)}{1 + \frac{V_{BC}}{V_A}} \approx \beta_F(0) \left(1 - \frac{V_{BC}}{V_A} \right) \quad (3.3.2.13)$$

Where V_A is known as the forward Early voltage.

As a result, the current source I_{CT} parameter of the ideal Ebers-Moll model will be affected and takes a new form:

$$I_{CT} = \frac{I_S(0)}{1 + \frac{V_{BC}}{V_A}} \left(e^{\frac{V_{BE}}{V_T}} - e^{\frac{V_{BC}}{V_T}} \right) \quad (3.3.2.14)$$

Similarly to the forward Early voltage, the reverse Early voltage V_B can be defined. In this case the collector and the emitter terminals interchange their roles.

3.3.2.4. Ebers-Moll large-signal model

In this model, which is shown in figure 3.3.11 capacitances due to charge storage effects at both junctions C_{DE} and C_{DC} are included and have exactly the same form of equation 3.3.1.8 obtained for the PN junction diode.

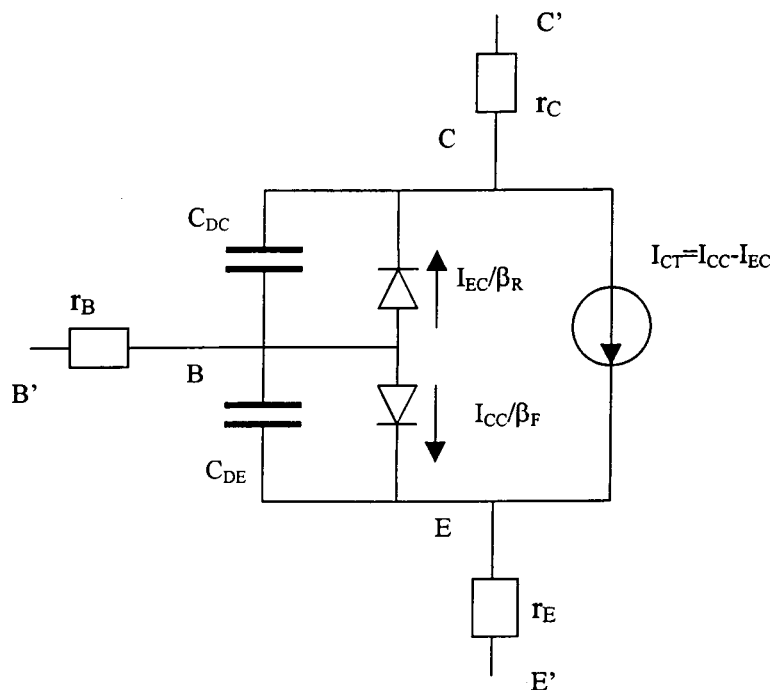


Figure 3.3.11 Ebers-Moll large-signal model

3.3.2.5. Small-signal Ebers-Moll model

When transistors are biased in the active region and used for amplification, it is often worthwhile to approximate their behaviour under conditions of small voltage variations at the base-emitter junction. If these variations are smaller than the thermal voltage V_T , it is possible to represent the transistor by a linear equivalent circuit. This representation can be of great help in the design of amplifying circuits. It is called the small-signal transistor model, and is represented in figure 3.3.12.

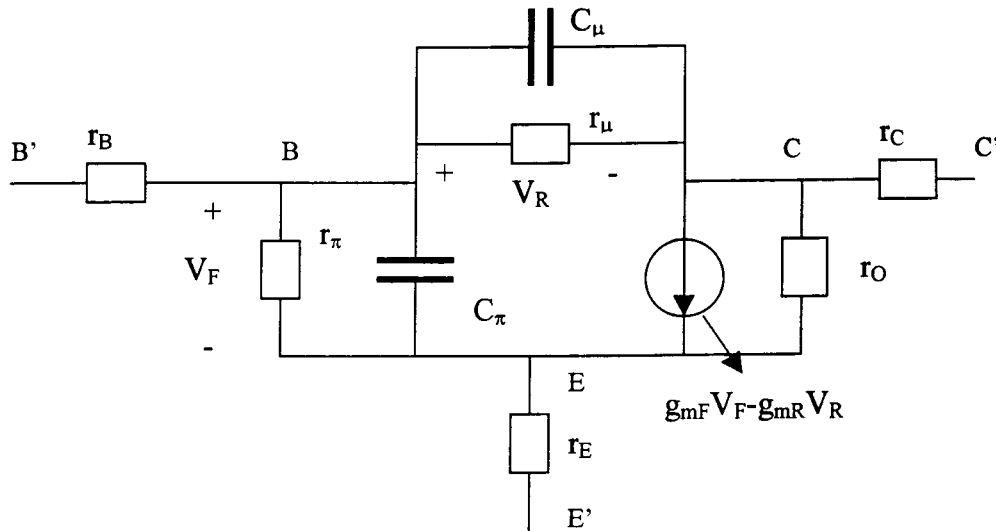


Figure 3.3.12. Linear hybrid- π model

The different extra parameters are defined as follows

$$g_{mF} = \frac{I_C}{V_T}$$

$$r_\pi = g_\pi^{-1} \text{, where, } g_\pi = \frac{dI_C}{dV_{BE}} = \frac{g_{mF}}{\beta_F}$$

$$r_\mu = g_\mu^{-1} \text{, where, } g_\mu = \frac{dI_B}{dV_{BC}} = \frac{g_O}{\beta_F} = \frac{g_{mR}}{\beta_R} \text{ and, } g_O = \frac{dI_C}{dV_{BC}} = \frac{I_C}{|V_A|} = r_o^{-1}$$

$$C_\pi = g_{mF} \tau_F + C_{JE}(V_{BE})$$

$$C_\mu = g_{mR} \tau_R + C_{JC}(V_{BC})$$

(3.3.2.15)

Where C_{JE} and C_{JC} , are the capacitances relative to the depletion regions and take the form of equation 3.3.1.8

3.3.2.5. The Gummel-Poon Model

The Ebers-Moll model lacks a representation of many important second order effects present in current devices; these effects are the result of the high level of integration of semiconductor devices in microelectronic industry.

The most important effects are those of low-current and high-level injection. The low-current effects result from additional base current due to recombination that degrades current gain. On the other hand, the effects of high-level injection reduce also

the current gain but in addition cause an increase in the transit time τ_F and τ_R , in both forward and reverse operating modes. The Gummel-Poon model has been established to take these main effects into account.

The static Gummel-Poon model is shown in figure 3.3.13.

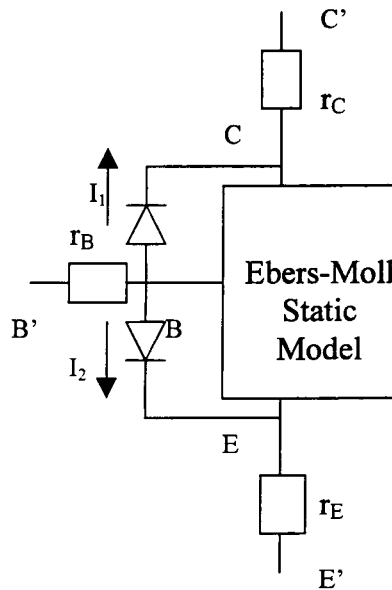


Figure 3.3.13. Gummel-Poon Static model

In this model additional currents are introduced:

$$I_1 = C_4 I_{SS} \left(e^{\frac{V_{BC}}{n_{CL} V_T}} - 1 \right) \quad (3.3.2.16)$$

$$I_2 = C_2 I_{SS} \left(e^{\frac{V_{BE}}{n_{EL} V_T}} - 1 \right) \quad (3.3.2.17)$$

Where the introduced model parameters are defined as:

- C_2 and C_4 are respectively, the forward and reverse low-current non-ideal base current coefficient.
- n_{CL} and n_{EL} are respectively the low-current emission coefficient in the forward region and the reverse region.
- I_{SS} depends only on the base doping profile and, it coincides with the I_S parameter of the Ebers-Moll model if the depletion approximation is assumed. The general expression of I_{SS} with respect to I_S is : $I_{SS} = q_b I_S$. q_b is the new factor introduced by Gummel and Poon analysis, which is a function of the bias conditions and is approximated by:

$$q_b = \frac{q_1}{2} + \sqrt{\left(\frac{q_1}{2} \right)^2 + q_2} \quad (3.3.2.18)$$

Where q_1 and q_2 are defined as:

$$q_1 = 1 + \frac{V_{BE}}{V_B} + \frac{V_{BC}}{V_A} \quad (3.3.2.19)$$

and,

$$q_2 = \frac{I_{SS}}{I_{KF}} \left(e^{\frac{V_{BE}}{V_T}} - 1 \right) + \frac{I_{SS}}{I_{KR}} \left(e^{\frac{V_{BC}}{V_T}} - 1 \right) \quad (3.3.2.20)$$

Where I_{KF} and I_{KR} are respectively corner for forward and reverse β high-current roll-off.

In SPICE program the Gummel-Poon model is used, and implemented so that by appropriate setting parameter values the model can be made equivalent to either Ebers-Moll model or Gummel-Poon one. Furthermore, other parameters are introduced to maximise the accuracy of the results. These parameters are n_F the forward, and n_R the reverse, emission coefficients (see section 3.3.1.a).

The terminal currents still have the same expression given by equation 3.3.2.10 but with a modified equation 3.3.2.11. Indeed the following equation for I_{CT} is used:

$$I_{CT} = I_{CC} - I_{EC} = \frac{I_{SS}}{q_b} \left(e^{\frac{V_{BE}}{n_F V_T}} - e^{\frac{V_{BC}}{n_R V_T}} \right) \quad (3.3.2.21)$$

where,

$$I_{CC} = \frac{I_{SS}}{q_b} \left(e^{\frac{V_{BE}}{n_F V_T}} - 1 \right) \quad (3.3.2.22)$$

and,

$$I_{EC} = \frac{I_{SS}}{q_b} \left(e^{\frac{V_{BC}}{n_R V_T}} - 1 \right) \quad (3.3.2.23)$$

The Gummel-Poon model equations (3.3.2.24) are then obtained in the different operating regions as :

Normal active region :
 $V_{BE} > -5n_F V_T$

$$I_C = \frac{I_S}{q_b} \left(e^{\frac{V_{BE}}{n_F V_T}} + \frac{q_b}{\beta_R} \right) + C_4 I_S$$

and

$$V_{BC} \leq -5n_R V_T$$

$$I_B = I_S \left[\frac{1}{\beta_F} \left(e^{\frac{V_{BE}}{n_F V_T}} - 1 \right) - \frac{1}{\beta_R} \right] + C_2 I_S \left(e^{\frac{V_{BE}}{n_{EL} V_T}} - 1 \right) - C_4 I_S$$

Inverse region :

$$V_{BE} \leq -5n_F V_T$$

and

$$V_{BC} > -5n_R V_T$$

$$I_C = -\frac{I_S}{q_b} \left[e^{\frac{V_{BC}}{n_R V_T}} + \frac{q_b}{\beta_R} \left(e^{\frac{V_{BC}}{n_R V_T}} - 1 \right) \right] - C_4 I_S \left(e^{\frac{V_{BC}}{n_{CL} V_T}} - 1 \right)$$

$$I_B = -I_S \left[\frac{1}{\beta_F} - \frac{1}{\beta_R} \left(e^{\frac{V_{BC}}{n_R V_T}} - 1 \right) \right] - C_2 I_S + C_4 I_S \left(e^{\frac{V_{BC}}{n_{CL} V_T}} - 1 \right)$$

$$I_C = \frac{I_S}{q_b} \left[\left(e^{\frac{V_{BE}}{n_F V_T}} - e^{\frac{V_{BC}}{n_R V_T}} \right) - \frac{q_b}{\beta_R} \left(e^{\frac{V_{BC}}{n_R V_T}} - 1 \right) \right] - C_4 I_S \left(e^{\frac{V_{BC}}{n_{CL} V_T}} - 1 \right)$$

Saturated region :

$$V_{BE} > -5n_F V_T$$

and

$$V_{BC} > -5n_R V_T$$

$$I_B = I_S \left[\frac{1}{\beta_F} \left(e^{\frac{V_{BE}}{n_F V_T}} - 1 \right) + \frac{1}{\beta_R} \left(e^{\frac{V_{BC}}{n_R V_T}} - 1 \right) \right] + \dots$$

$$C_2 I_S \left(e^{\frac{V_{BE}}{n_{EL} V_T}} - 1 \right) + C_4 I_S \left(e^{\frac{V_{BC}}{n_{CL} V_T}} - 1 \right)$$

Off region :

$$V_{BE} \leq -5n_F V_T$$

and

$$V_{BC} \leq -5n_R V_T$$

$$I_C = \frac{I_S}{\beta_R} + C_4 I_S$$

$$I_B = -I_S \left(\frac{\beta_F + \beta_R}{\beta_F \beta_R} \right) - C_2 I_S - C_4 I_S$$

It must be noticed that all parameters in the above expressions (n_{CL} , n_{EL} , n_F , n_R , V_B , V_A , I_{SS} , C_2 , C_4 , I_{KF} and I_{KR}) are model parameters that can be extracted from data measurements as it will be shown in the next chapter.

3.3.3. Junction Field Effect transistors (JFETs)

The Junction Field Effect Transistor (JFET) is one member of the Field Effect Transistors (FET) family, which includes several other types such as the MOSFETs.

Mainly this kind of transistors differs from the BJTs by the manner the device current is controlled. In the BJT, the collector current is controlled by the base current, while in the FET the drain current is controlled by the gate voltage.

The structure of an n-channel FET is shown in figure 3.3.14. It consists of a conductive channel that has two ohmic contacts, one acting as the cathode (source) and the other as the anode (drain), with an appropriate voltage applied between drain and source. The third electrode (gate) forms a rectifying junction with the channel. Thus the JFET is basically a voltage-controlled resistor, and its resistance can be varied by changing the width of the depletion region extending into the channel. As it is shown, the conducting process involves one type of carrier, hence the JFET (and most of FETs) is called sometimes a unipolar transistor at the opposite of the bipolar transistor, in which both types of carrier are involved. Note that the n-channel JFET requires zero or negative gate bias and positive drain voltage. The p-channel JFET requires opposite voltage polarities[23].

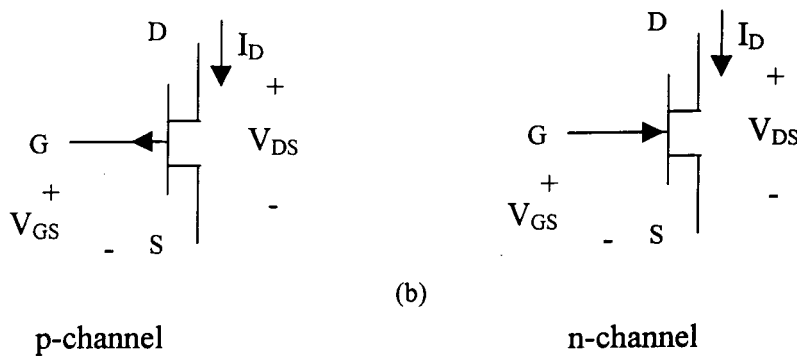
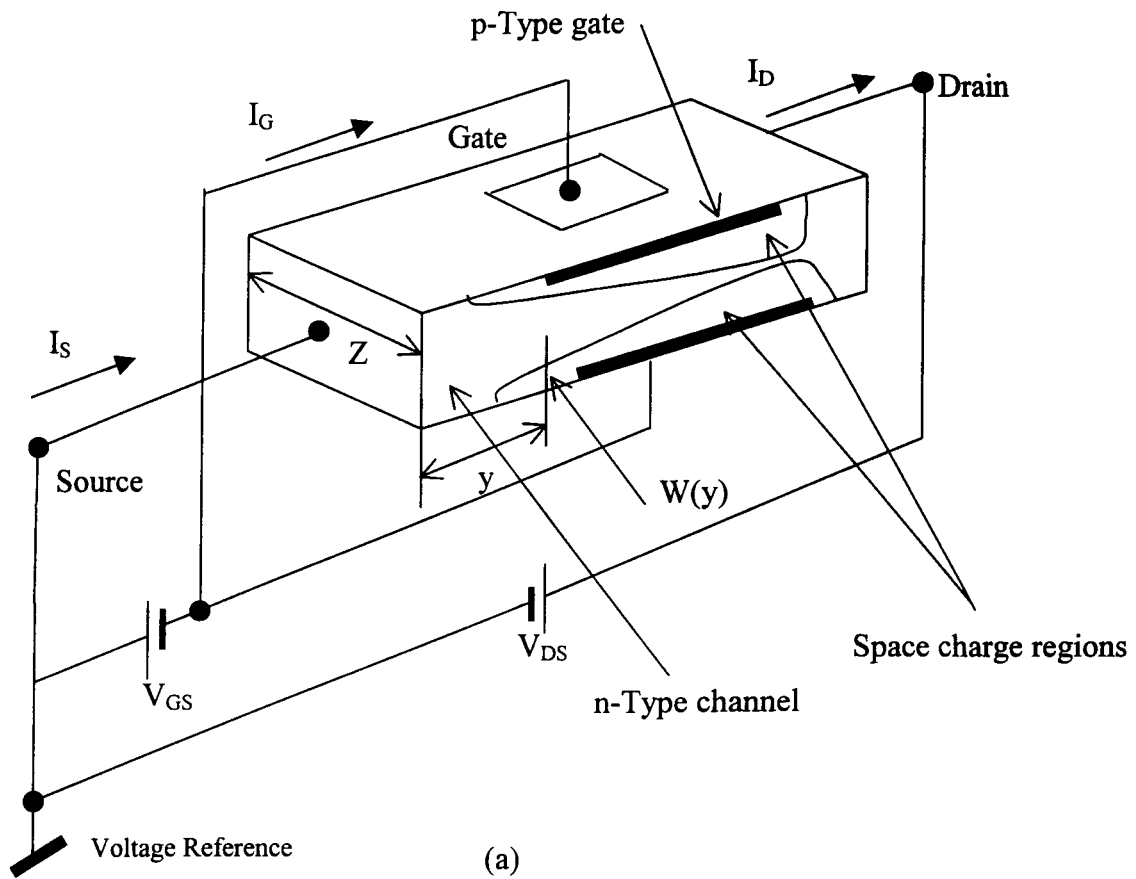


Figure 3.3.14 (a) Basic structure of an n-channel JFET, (b) JFET symbols and sign convention

3.3.3.1. JFET Static model

The JFET static model can be obtained by considering the channel resistance variation with respect to the space charge region by just using the well known equation, $R = \rho \frac{L}{x_W Z}$. x_W represents of course, the channel width.

A first approximation of the drain current as function of drain and voltages is hence obtained. This approximation is limited since it does not take into consideration second order effects such as, the channel-length modulation, the control of the depletion-layer width by the channel substrate junction, the drain and source series resistances and breakdown. A modified version of the idealised model is therefore

obtained, and implemented in SPICE program as the Shichman and Hodges model [21]. Figure 3.3.15, summarises this model.

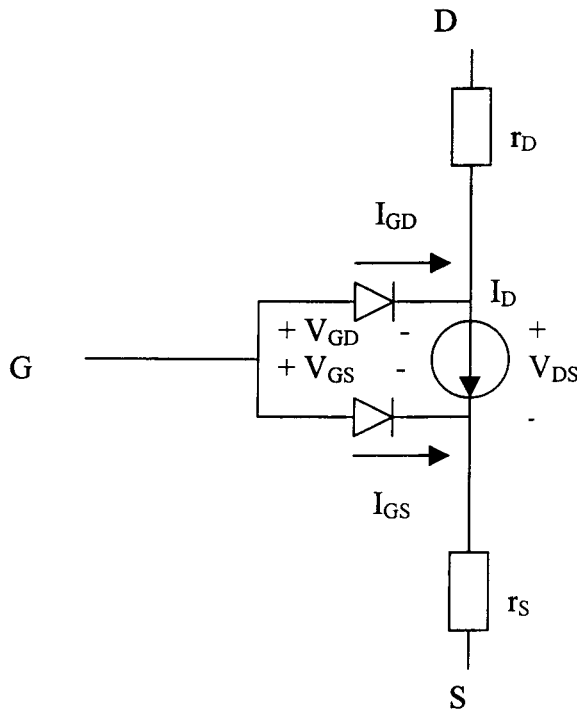


Figure 3.3.15 n-channel JFET static model

In this model the current I_D generated current drain-source takes the following form:

$$I_D = \begin{cases} 0 & \text{for } V_{GS} - V_{T0} \leq 0 \\ \beta(V_{GS} - V_{T0})^2(1 + \lambda V_{DS}) & \text{for } 0 < V_{GS} - V_{T0} \leq V_{DS} \\ \beta V_{DS} [2(V_{GS} - V_{T0}) - V_{DS}](1 + \lambda V_{DS}) & \text{for } 0 < V_{DS} < V_{GS} - V_{T0} \end{cases} \quad (3.3.3.1)$$

Where the parameter β , is the gain of the transistor (also known as the transconductance parameter) and depends on the geometry of the device. The parameter λ determines the effects of channel-length modulation.

The two diodes represents the gate-drain and the gate-source junctions, and they are modelled by the following equations:

$$I_{GD} = \begin{cases} -I_S & \text{for } V_{GD} \leq -5nV_T \\ I_S \left(e^{\frac{V_{GD}}{nV_T}} - 1 \right) & \text{for } V_{GD} > -5nV_T \end{cases} \quad (3.3.3.2)$$

$$I_{GS} = \begin{cases} -I_S & \text{for } V_{GS} \leq -5nV_T \\ I_S \left(e^{\frac{V_{GS}}{nV_T}} - 1 \right) & \text{for } V_{GS} > -5nV_T \end{cases} \quad (3.3.3.3)$$

The resistances r_D and r_S are considered to be the series resistances.

3.3.3.2. JFET Large-signal model

In the JFET large signal model, the charge storage effect of both gate-drain and gate-source junctions is considered. This will lead to the model of figure 3.3.16.

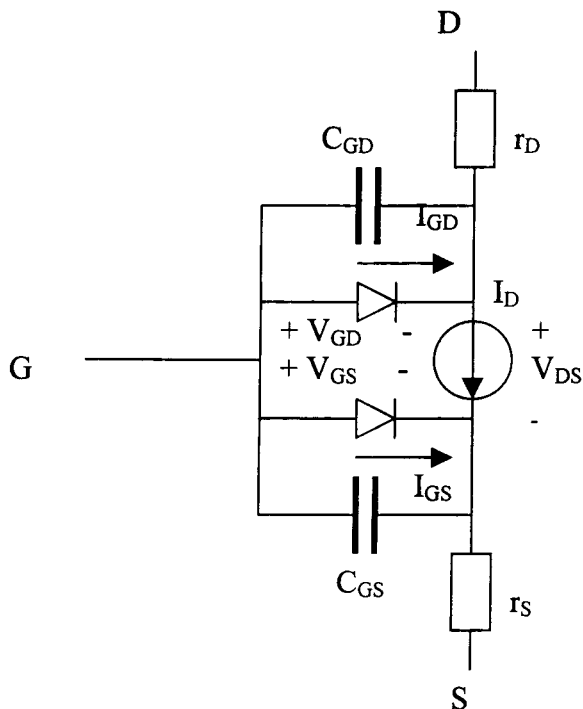


Figure 3.3.16 JFET large signal model

The capacitances introduced in this model take the same expression of equation 3.3.1.8.

3.3.3.3. JFET small-signal model

The small-signal linearised model for the JFET is given in figure 3.3.17. The conductances g_{GS} and g_{GD} are the conductances of the two gate junctions. Since neither gate junction is forward-biased in normal operation, both g_{GS} and g_{GD} usually are very small. The transconductance g_m and the output conductance g_{DS} are defined by the equations:

$$g_m = \left. \frac{dI_D}{dV_{GS}} \right|_Q \quad (3.3.3.4)$$

$$g_{DS} = \left. \frac{dI_D}{dV_{DS}} \right|_Q \quad (3.3.3.5)$$

$$g_{GS} = \left. \frac{dI_{GS}}{dV_{GS}} \right|_Q \quad (3.3.3.6)$$

$$g_{GD} = \left. \frac{dI_{GD}}{dV_{DS}} \right|_Q \quad (3.3.3.7)$$

The JFET small-signal equivalent circuit is quite similar to that of the BJT, and much of the theory developed for bipolar transistor circuits applies equally to JFET

circuits if the appropriate parameter values are used. One major difference is the absence of any input shunt resistance in the JFET model because of the reverse-biased PN junction in series with the gate electrode. This makes the JFET very attractive for circuits requiring high input impedance.

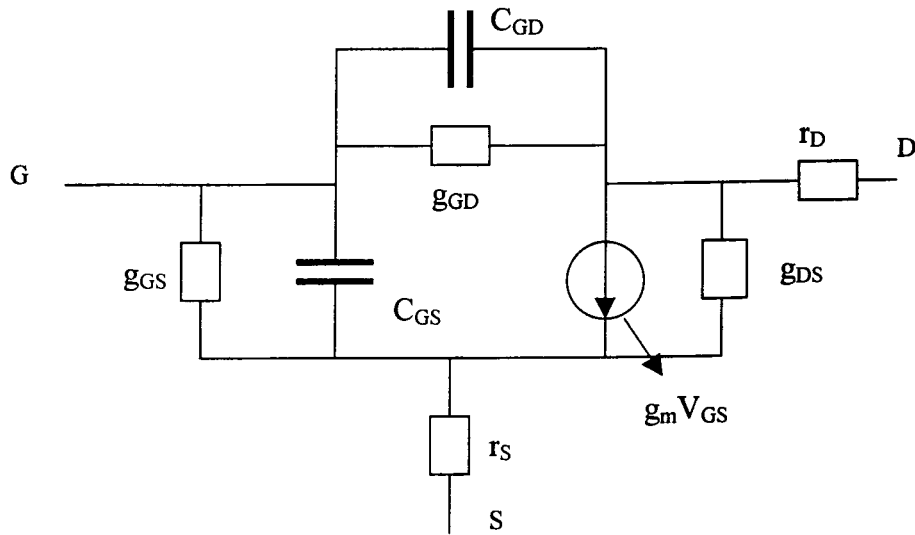


Figure 3.3.17 JFET small-signal model

Chapter 4

Extraction Methods of Model Parameters

4.1 Introduction

In The present chapter methods that have been developed to extract model parameters for both passive and active devices are described.

Traditionally, two different approaches have been used for parameter extraction. First there is a large number of local methods where the parameters are determined two by two as the slope and the intercept of a straight line [29]. The influence of other effects (parameters) is often ignored. The second approach is the use of general optimisation techniques [30]. In these methods , all parameters (or subsets thereof) are extracted simultaneously, sometimes even using data from several different device sizes. These methods show good agreement between measured an simulated data but they are CPU-intensive and require a relatively large number of data points[31]. As an alternative to these two approaches, least square fitting techniques on linearised model equations have been proposed [32]. An other alternative is so-called direct parameter extraction using only a small number of data points. This approach was first introduced by Hamer [33] an was then further developed by several research groups [34,35].

The parameter extracting methods we have developed in this work are based on the local methods and the optimisation approaches.

Extracting parameters using local methods (also known as graphical methods), depends on the equation forms on which the theory of the derived model is based. These methods are in no ways considered to be general ones, since for each device model the resulting equations are different. In general, by judicious handling of the model equations (sometimes using some assumptions) we end up with a linear form. Parameters are then determined (often two by two) by means of graphical methods as a slope and an intercept of a straight line. The slope and the intercept of the line are usually found using least square fitting techniques on a number of measured data points.

Optimisation techniques on the other hand, can be considered as universal methods and are used for many different kinds of optimisation problems. The main advantage of optimisation methods, is that the model parameters for new or modified models are easy to extract. This is because the optimiser can use the same modules as the circuit simulator to calculate the device terminal variables (currents and voltages). this hence guarantees that the same equations are used by the simulation and the extraction programs. All extraction algorithms that are based on optimisation techniques try to minimise an error function, also called objective function or cost function. The value of the error function is a measure of the distance between measured and calculated data points. Even after the error function has been minimised there will be a difference between measured and calculated data points since the model always is an approximation to reality and the data points contain measurement noise. In general three main categories of optimisation algorithms exist: Gradient following methods, direct searching methods and combined methods (combination of the to first ones) .

The algorithm we have chosen to build our parameters extraction programs using optimisation methods, is based on the gradient following approach and more precisely on the Levenberg-Marquardt algorithm [31].

4.2 Method of Extraction of passive devices parameters

The technique we have chosen to extract model parameters of the passive components described in chapter 3, is summarised in the flow chart of figure 4.1.

First, a graphical method related to the device type is used, on a set of DC and (or) AC measurement data, to extract the different model parameters. This step is necessary for two reasons: First, the extracted parameter values may be satisfactory enough so that no further refinements are needed. Second, the extracted parameter values are injected as an initial condition to the second bloc of extraction if necessary.

If the parameters obtained from the first step are not reliable enough, the user can try an improvement of the parameter values, using an optimisation method, which is in general more sophisticated than the graphical one.

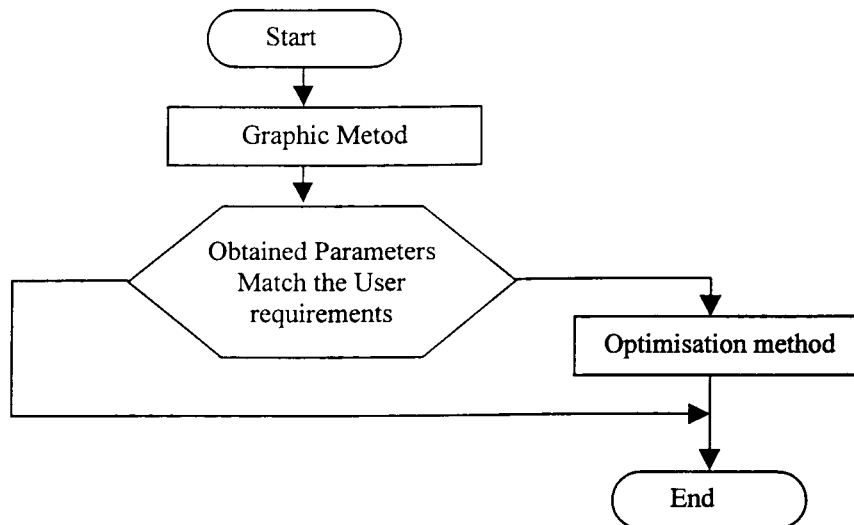


Figure 4.1 Technique of extraction of model parameters of passive devices

4.2.1 Method of Extraction of the Resistor Model Parameters

The details of the method of extraction of the resistor model parameters will now be presented. The analysis starts from the resistor equivalent circuit of figure 3.2.1. From that figure it is clear that the admittance of the device is : $Y(\omega) = G(\omega) + jB(\omega)$. Where:

$$G(\omega) = \frac{R_p}{R_p^2 + (L\omega)^2} \quad (4.2.1.1)$$

And,

$$B(\omega) = C\omega - \frac{L\omega}{R_p^2 + (L\omega)^2} \quad (4.2.1.2)$$

From (4.2.1.1) and (4.2.1.2) we can show that:

$$\frac{1}{G(f)} = R_p + \frac{(2\pi L)^2}{R_p} f^2 \quad (4.2.1.3)$$

Of course, here f , stands for the operating frequency ($\omega=2\pi f$).

At this level of analysis one may suggest two different methods of extraction.

Method 1:

- i) R_p is obtained from DC measurements, using an Ohm-meter for instance.
- ii) L is obtained by averaging values calculated using equation (4.2.1.3) at different frequency values.

$$L = \frac{R_p}{2\pi f} \sqrt{\frac{1}{G(f)R_p} - 1} \quad (4.2.1.4)$$

- iii) Once L obtained C is extracted similarly by averaging values calculated using equation (4.2.1.2), at different frequency values.

$$C = \frac{B(f)}{2\pi f} + \frac{G(f)L}{R_p} \quad (4.2.1.5)$$

Method 2:

- i) If we consider equation (4.2.1.3) and we let $a_2 = R_p$ and $a_1 = \frac{(2\pi L)^2}{R_p}$ then:

$$\frac{1}{G(f)} = a_1 f^2 + a_2 \quad (4.2.1.6)$$

The last equation states that $\frac{1}{G(f)}$ is a linear function of f^2 . Fitting $\frac{1}{G(f)}$ with respect to f^2 by a polynomial of degree one, gives the coefficients a_1 and a_2 and hence:

$$R_p = a_2 \quad (4.2.1.7)$$

and

$$L = \frac{1}{2\pi} \sqrt{a_1 a_2} \quad (4.2.1.8)$$

One important remark should be made. The set of measurement points does not ensure that the values of $\frac{1}{G(f)}$ are perfectly correlated with f^2 . Hence, a suitable choice of the frequency range is to be made to maximise the precision of L and R_p extraction. Therefore a plot of $\frac{1}{G(f)}$ versus f^2 for different frequency intervals is recommended as a decision criteria.

- ii) To extract C the same technique of method 1 is used.

We believe that the second method is better for different reasons:

- 1) In the second method no DC measurements to obtain R_p are needed. In fact such measurements are sometimes difficult to achieve, especially when R_p is of small value (non stable readings due to the heating of the device with the internal Ohm-meter current source, is a typical difficulty).
- 2) According to equation (4.2.1.4), the extraction of L in the first method, requires that the condition $\frac{1}{G(f)R_p} \geq 1$ is to be satisfied. Therefore, some measurement points may be missed in the calculation of L .

Note however, that a similar inconvenient exists in both methods when C is extracted, because for each frequency value, the calculated $C(f)$ in equation (4.2.1.5) must be positive.

4.2.2 Method of Extraction of the Capacitor Model Parameters

Let us consider the capacitor's equivalent circuit of figure 3.2.2. The impedance of the element can be expressed as $Z(\omega) = R(\omega) + jX(\omega)$. Where:

$$R(\omega) = R_S + \frac{R_P}{(CR_P)^2 \omega^2 + 1} \quad (4.2.2.1)$$

And,

$$X(\omega) = \left(L - \frac{CR_P^2}{(CR_P)^2 \omega^2 + 1} \right) \omega \quad (4.2.2.2)$$

From the two previous equations, it is easy to proof that

$$\frac{X(f)}{f} = -2\pi CR_P R(f) + 2\pi(L + R_S R_P C) \quad (4.2.2.3)$$

The method of extraction is as follows:

- i) From DC measurements $R_{Eq} = R_S + R_P$ can be obtained. We can assume that $R_{Eq} = R_P$ since in almost all situations R_P is much greater than R_S . Due to the high value of R_P , to achieve such measurements one resistor of known resistance R is connected in parallel to the device under test as shown in figure 4.2. Then R_P is obtained from the following equation:

$$R_P = \frac{1}{\frac{1}{R_{Eq}} - \frac{1}{R}} \quad (4.2.2.4)$$

- ii) To extract the remaining parameters we consider equation (4.2.2.3). If we let:

$$a_1 = -2\pi CR_P \quad (4.2.2.5)$$

And,

$$a_2 = 2\pi(L + R_S R_P C) \quad (4.2.2.6)$$

Then,

$$\frac{X(f)}{f} = a_1 R(f) + a_2 \quad (4.2.2.7)$$

That is, $\frac{X(f)}{f}$ is a linear function of $R(f)$.

The coefficients a_1 and a_2 are obtained from fitting $\frac{X(f)}{f}$ with respect to $R(f)$. And hence,

$$C = -\frac{a_1}{2\pi R_P} \quad (4.2.2.8)$$

And,

$$L = \frac{1}{2\pi} (a_2 + R_S a_1) \quad (4.2.2.9)$$

As it is shown in equation (4.2.2.9), to obtain L , R_S must be known. R_S can be obtained by averaging calculated values using equation (4.2.2.1) at different frequency values as follows:

Equation (4.2.2.1) implies that, $R_S = R(f) - \frac{R_P}{(2\pi CR_P)^2 f^2 + 1}$, and taking into consideration equation (4.2.2.5) we will end up with the following result,

$$R_S = R(f) - \frac{R_P}{a_1^2 f^2 + 1} \quad (4.2.2.10)$$

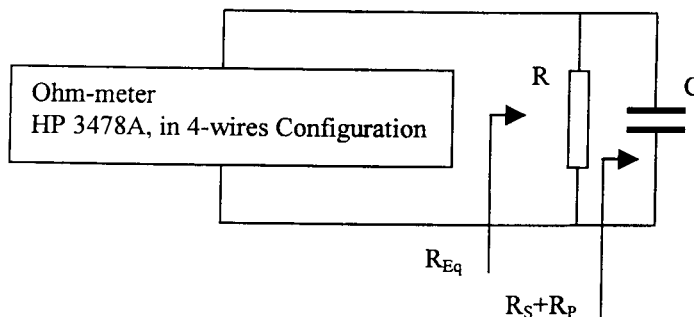


Figure 4.2 Measurement of $(R_S + R_P)$ for a capacitor device.

4.2.3. Method of Extraction of the Inductor Model Parameters

Let us consider the inductor model given in figure 3.2.3. From this figure one may calculate the total impedance of the considered circuit $Z(\omega) = R(\omega) + jX(\omega)$ where:

$$R(\omega) = R_S + \frac{G_P}{G_P^2 + \left(C\omega - \frac{1}{L\omega}\right)^2} \quad (4.2.3.1)$$

And,

$$X(\omega) = \frac{\frac{1}{L\omega} - C\omega}{G_P^2 + \left(C\omega - \frac{1}{L\omega}\right)^2} \quad (4.2.3.2)$$

Of course, G_P stands for R_P^{-1} .

From equation 4.2.3.1 we can write:

$$\frac{1}{R(f) - R_S} = G_P + \frac{R_P}{(2\pi L)^2 \left(\alpha f + \frac{1}{f}\right)^2} \quad (4.2.3.3)$$

Where,

$$\alpha = -(2\pi)^2 LC \quad (4.2.3.4)$$

On the other hand from equations 4.2.3.1, 4.2.3.2 and 4.2.3.4, it is easy to show that:

$$\frac{fX(f)}{R(f) - R_S} = \frac{R_P}{2\pi C} (1 + \alpha f)^2 \quad (4.2.3.5)$$

The steps involved to extract inductor model parameters are then presented as follows:

- i) R_S is obtained from DC measurements.
- ii) From equation 4.2.3.5, it is clear that by letting $a_1 = \alpha \frac{R_p}{2\pi C}$ and $a_2 = \frac{R_p}{2\pi C}$, then, equation 4.2.3.5 transforms to $\frac{fX(f)}{R(f) - R_S} = a_1 f^2 + a_2$. Therefore, a polynomial fitting of $\frac{fX(f)}{R(f) - R_S}$ with respect to f^2 gives the value of a_1 and a_2 . Note that :

$$\alpha = \frac{a_1}{a_2} \quad (4.2.3.6)$$

- iii) Once α obtained, its value will be used in equation 3.2.3.3. This equation shows that $\frac{1}{R(f) - R_S}$ is linearly dependent on $\left(\alpha f + \frac{1}{f}\right)^2$. Thus, using a polynomial fitting coefficients of $\frac{1}{R(f) - R_S} = b_1 \left(\alpha f + \frac{1}{f}\right)^2 + b_2$, can be obtained.

$$b_1 = \frac{R_p}{(2\pi L)^2} \quad (4.2.3.7)$$

and,

$$b_2 = G_p \quad (4.2.3.8)$$

And hence, R_p , L and then C can be deduced from equations 4.2.3.7, 4.2.3.8 and 4.2.3.4.

$$R_p = \frac{1}{b_2} \quad (4.2.3.9)$$

$$L = \frac{1}{2\pi\sqrt{b_1 b_2}} \quad (4.2.3.10)$$

$$C = -\frac{\alpha}{2\pi} \sqrt{b_1 b_2} \quad (4.2.3.11)$$

2.4. Implementation of the routine of extraction

The methods of extraction of the three passive component model parameters described above, have been implemented in one MATLAB routine. The developed program offers a comfortable user interface and all calculated parameters are displayed on the same frame as shown in figure 4.3. An other routine was also implemented in order to compare the calculated impedance magnitude and phase values with respect to measured ones. Figure 4.4 gives an example of comparison.

Characterisation of nonlinear capacitors was also implemented and an example is shown in figure 4.5. In fact, according to equation 3.2.4.2, it consists just on a polynomial fitting of the measured capacitance values with respect to applied voltage. The nonlinear inductor characterisation is not possible due to the limitation in the external current capability of the used HP 4275A model LCR meter.

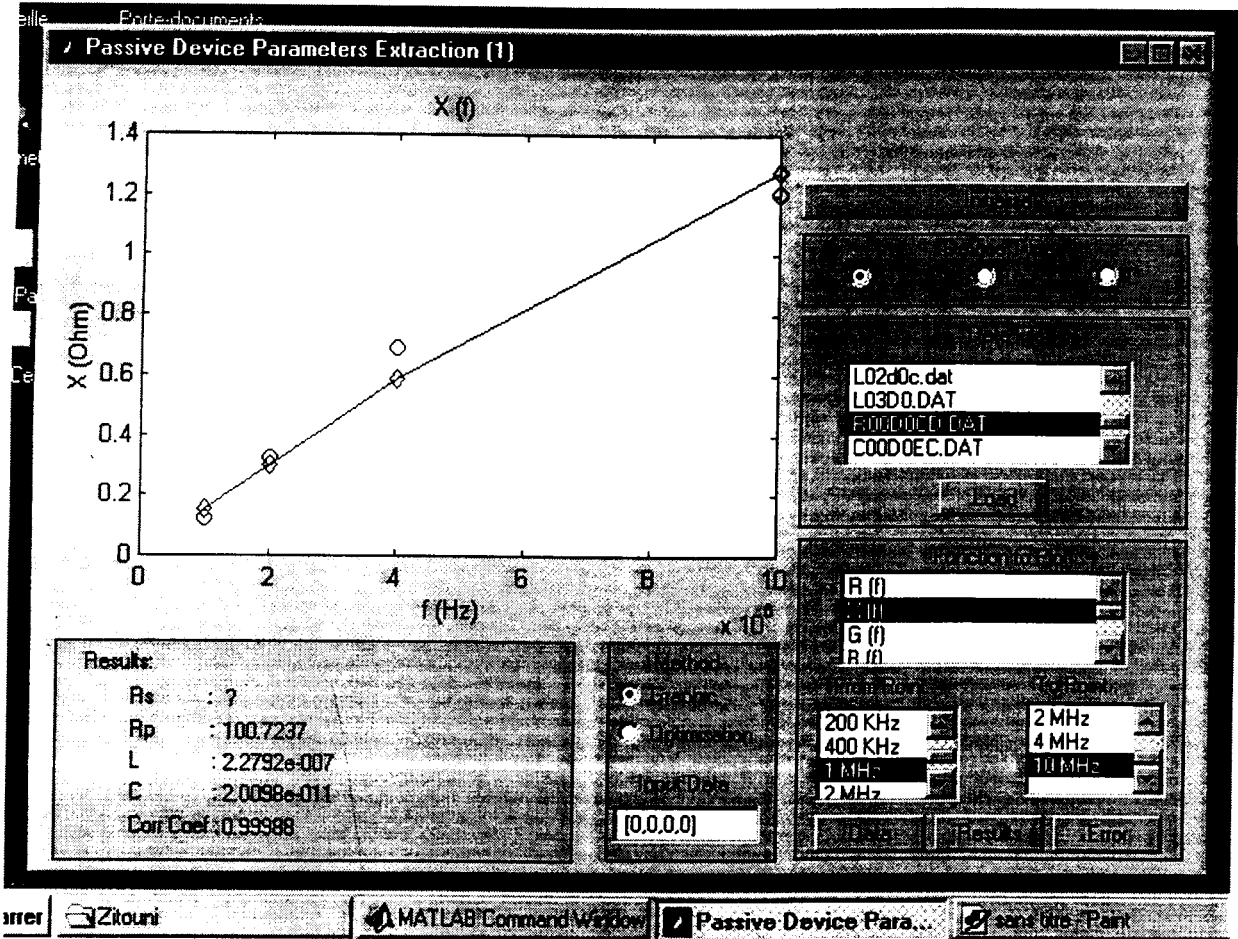


Figure 4.3. The implemented routine of extraction of passive components model parameters

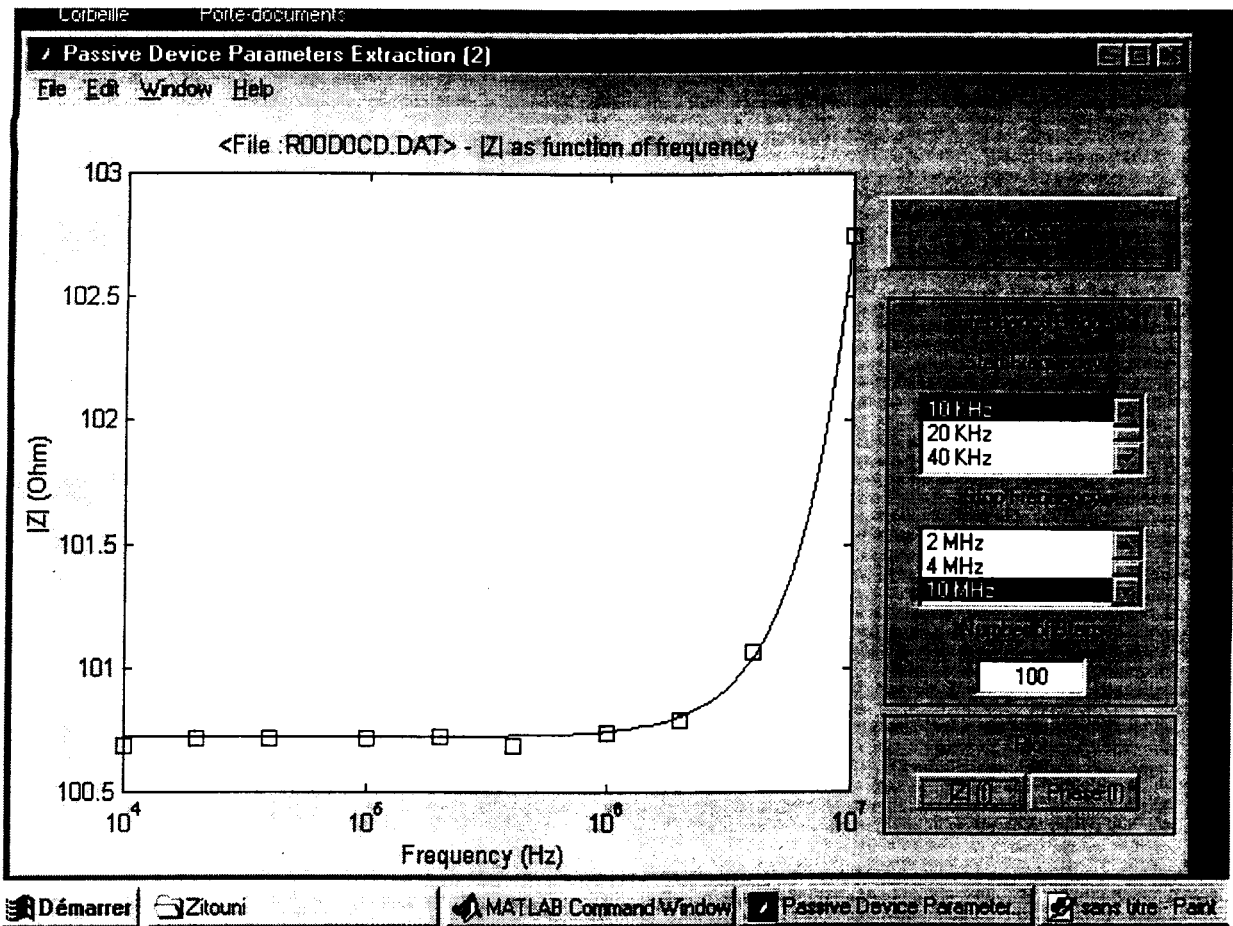


Figure 4.4 The routine of comparison between simulated data and measured data.
 Squares : Measurement points
 Solid line : Simulated impedance from extracted parameters

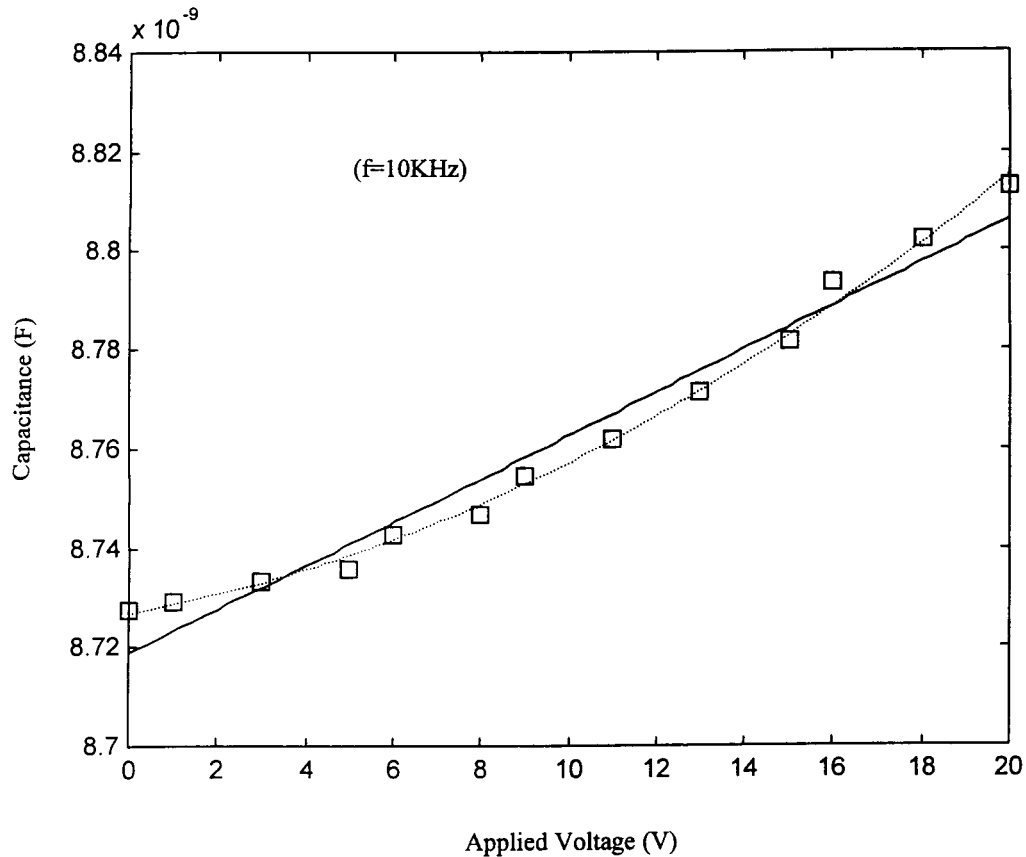


Figure 4.5 Capacitance as function of applied voltage of a 10nF ceramic capacitor
 Squares : Measurement points
 Solid line : First order polynomial fitting
 Dashed line : Second order polynomial fitting

4.3 Extraction of diode model parameters

4.3.1. Static model parameters measurement

As described in the previous chapter the model used by SPICE program to approximate the junction or Schottky diode needs four parameters, that are:

In the forward mode:

IS (I_S) : The saturation current.

N (n) : The emission coefficient

In the reverse mode:

BV (V_B) : The break down voltage

IBV (I_B) : The break down current

GMIN (G) : The reverse conductance just before break down.

- To extract the forward mode parameters, the plot of $\text{Log}(I_d)$ with respect to V_d is used. This plot shows a linear region where the relation $\text{Log}(I_d) = \text{Log}(I_S) + \frac{1}{nV_T}V_d$ is valid. Hence, fitting $\text{Log}(I_d)$ with respect to V_d gives the value of both n and I_S straight forward. If we let $\text{Log}(I_d) = a_1V_d + a_2$ then :

$$n = \frac{1}{a_1 V_T} \quad (4.3.1)$$

and,

$$I_s = e^{a_2} \quad (4.3.2)$$

- To extract the parameter G the slope of the curve of I_d with respect to V_d in the reverse mode (before the breakdown) is calculated. The breakdown voltage and current parameters are calculated also from curve fitting but in the breakdown region as shown in figure 4.6.

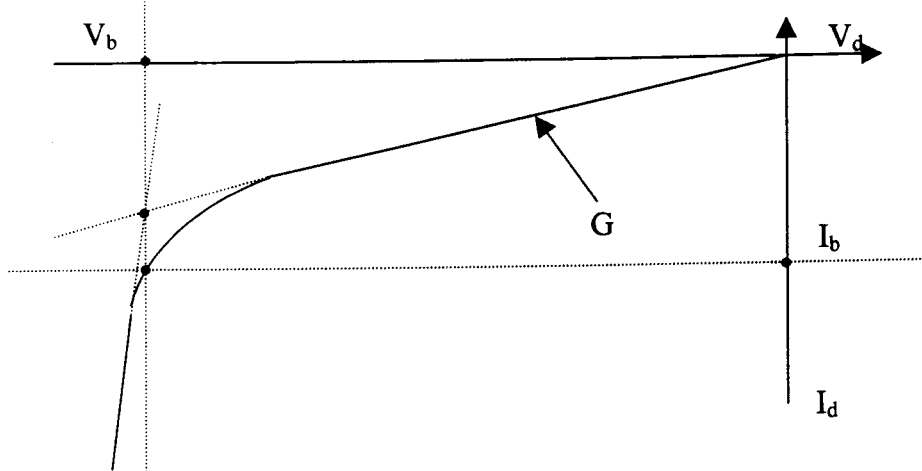


Figure 4.6. Extraction of the diode reverse parameters

A routine of static parameters extraction from measured data was implemented in MATLAB and, is presented in figure 4.7. In this routine the only input argument that must be introduced is the temperature value, which is set by default to 25 °C. An additional routine for comparison between simulated data using the extracted parameters and data measurement was also implemented. Figure 4.8 shows this routine at run time.

4.3.2. Dynamic model parameters measurement

In both large and small-signal dynamic models presented in the previous chapter, the main parameters that are necessary to know are: τ_D the transit time of the diode, ϕ_0 , the diode built-in voltage, $C_d(0)$ the zero-bias depletion capacitance and m the coefficient used in equation 3.3.1.7 to calculate the depletion capacitance.

- $C_d(0)$ is obtained from measurement of the junction capacitance at zero bias condition
- ϕ_0 and m are extracted using optimisation method using equation 3.3.1.7.

The measurement of the diode transit time is not possible with our system, since it requires other measuring devices and techniques of measurement, such as the transistor's unity-gain band-width for integrated diodes [25].

An example of dynamic model parameters extraction is given in figure 4.9. Note on this example the power of the optimisation technique.

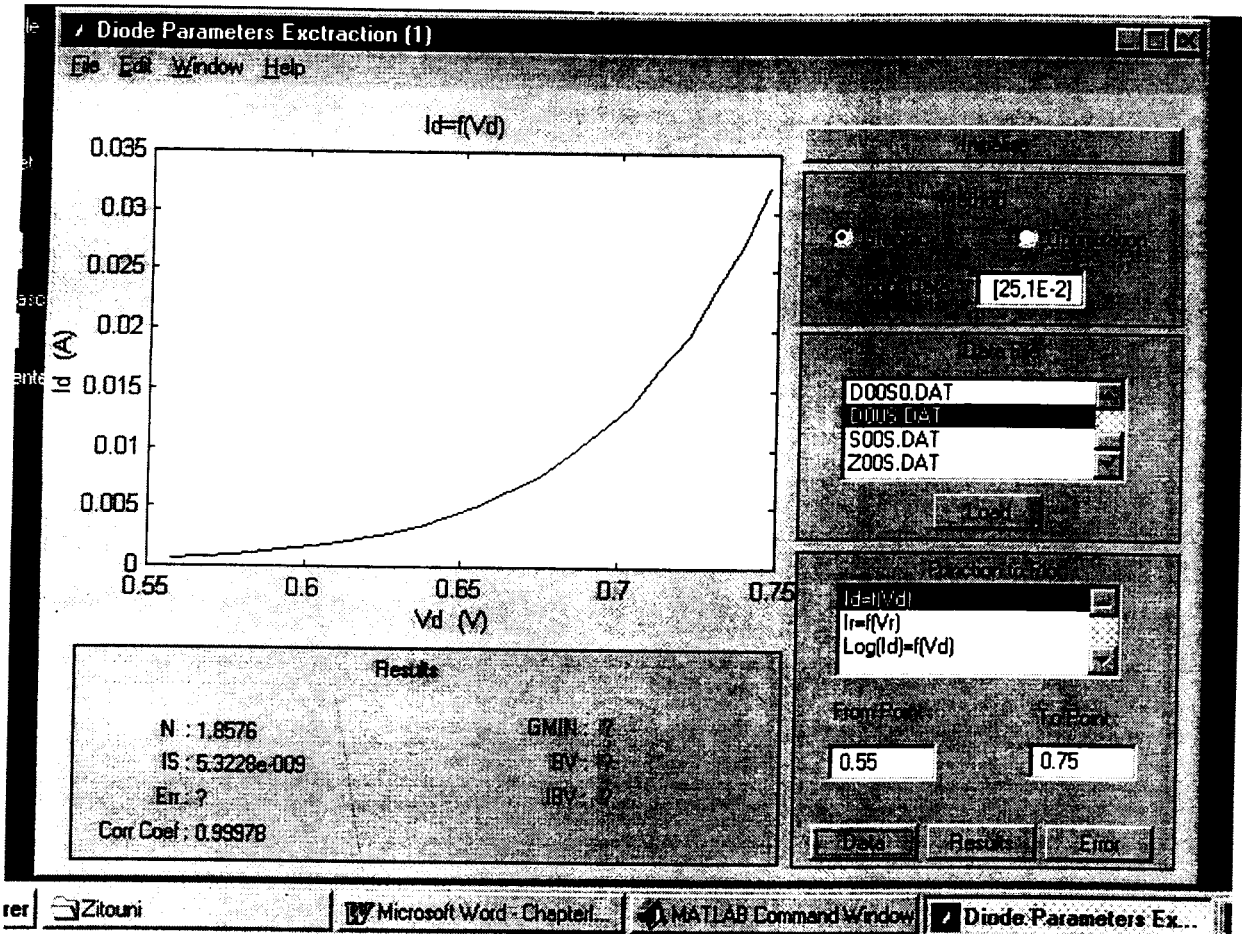


Figure 4.7 the implemented Diode model parameters extraction routine. The above example is for the 1N4003 diode model.

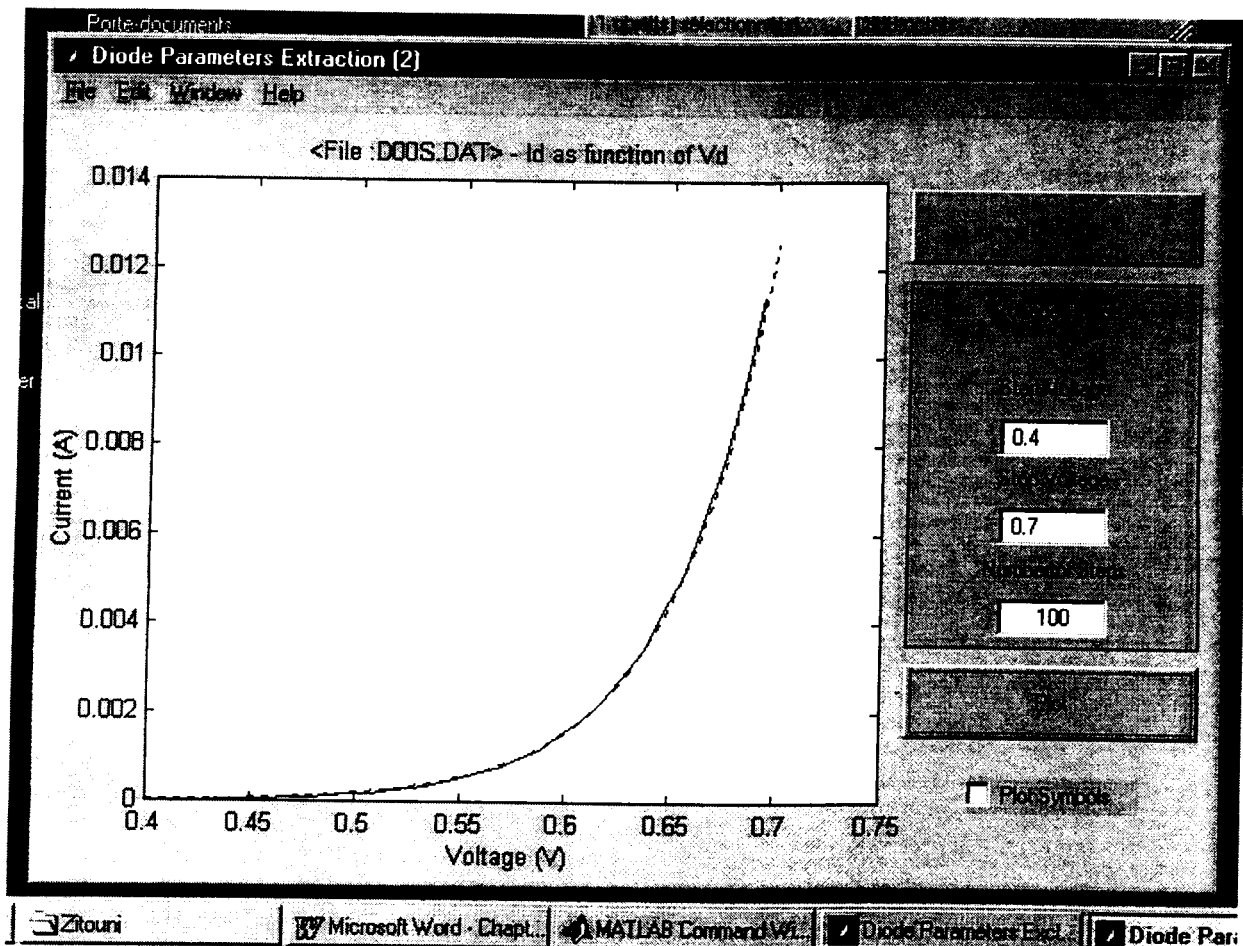


Figure 4.8. Comparison routine between simulated data from extracted parameters and data measurement for the 1N4003 diode model. Solid line: measurements, dashed line: simulated data.

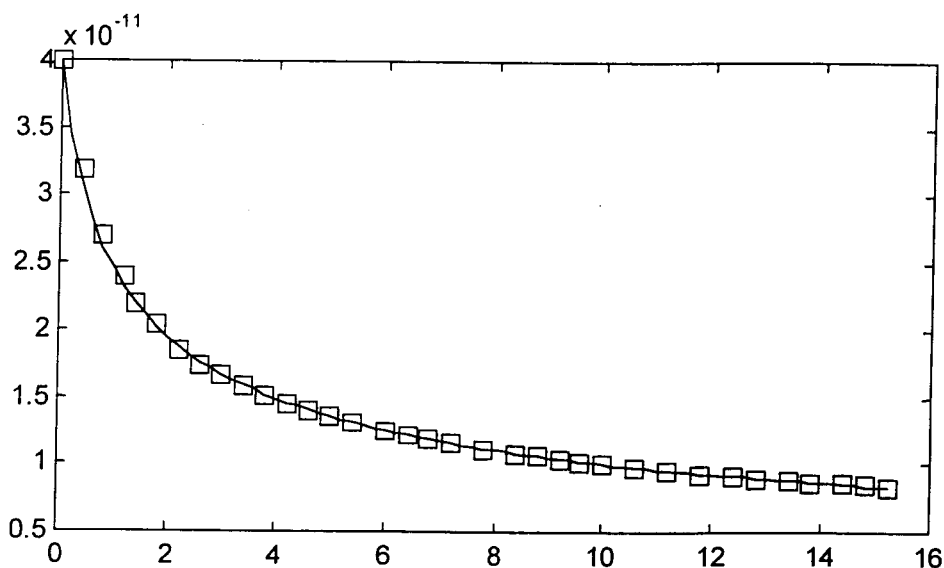


Figure 4.9. The depletion capacitance versus reverse voltage of the 1N4003 diode model.
 Squares : Measurement points
 Solid line : Estimated capacitance from extracted parameters ($m=0.462$, $\phi=0.529$ Volt)

4.4. Extraction of JFET model parameters

The model used to approximate the electric behaviour of the junction field effect transistor described in the previous chapter shows that eleven (11) parameters are to be defined.

1. for the equation of the drain currents (3.3.3.1), three parameters (β , V_{T0} and λ) are required.
2. for the equations of the gate-drain and the gate-source junctions (3.3.3.2,3.3.3.3), two parameters (I_S and n) should be known.
3. For the equations (3.3.1.8) used in approximating the large signal behaviour of the gate-drain and the gate-source junctions, four parameters ($m, \phi, C_{GD}(0)$ and $C_{GS}(0)$) are needed.
4. In addition to the above parameters, the drain and source series resistances (r_D and r_S) can be added.

In this section the extracting methods of these parameters will be developed. Note that the method of extraction of the parameters related to the two gate-drain and gate-source PN junctions, are exactly the same of those used to extract PN junction model parameters.

4.4.1. Extraction of $C_{GD}(0)$ and $C_{GS}(0)$:

These two parameters are obtained by direct measurement at zero bias of the gate-drain and gate-source junctions capacitance using the HP 4275A model LCR metre (see chapter 2) at a given frequency value and oscillator voltage level.

4.4.2. Extraction of m and ϕ :

They are obtained as for the PN junction diode, using optimisation method on the equation of the depletion capacitance with respect to the applied reverse voltage (3.3.1.7). Since SPICE program uses the same parameters for both junctions then the average values of extracted parameters from the two junctions are considered..

4.4.3. extraction of I_S and n :

the same technique used for the PN junction diode is used (see section 4.3.1), and as it is the case for m and ϕ parameters, average values of extracted parameters from both junctions are considered.

4.4.4. Extraction of β and V_{T0} :

β and V_{T0} are obtained at the same time from the curve of $\sqrt{I_D}$ with respect to V_{GS} for a large enough value of V_{DS} to ensure the transistor operating in the saturation region. Indeed, in this region we can consider that the drain current is:

$$I_D \approx \beta(V_{GS} - V_{T0})^2 \quad (4.4.1)$$

And hence,

$$\sqrt{I_D} \approx \sqrt{\beta}(V_{GS} - V_{T0}) \quad (4.4.2)$$

Therefore, fitting $\sqrt{I_D}$ with respect to V_{GS} by a straight line gives β as the square value of the obtained curve slope and V_{T0} as the intercept with the V_{GS} axis.

4.4.5. Extraction of λ :

the extraction of λ requires the measurement of the output conductance of the device in the saturation region for a given value of V_{GS} . This is shown by considering the definition of the output conductance as follows:

$$g_0 = \frac{dI_D}{dV_{DS}} = \beta(V_{GS} - V_{T0})^2 \lambda \approx \lambda I_D \tag{4.4.3}$$

Thus, by measuring g_0 at different values of I_D we may estimate the value of λ as the slope of the curve of g_0 vs. I_D as shown in figure 4.4.1.

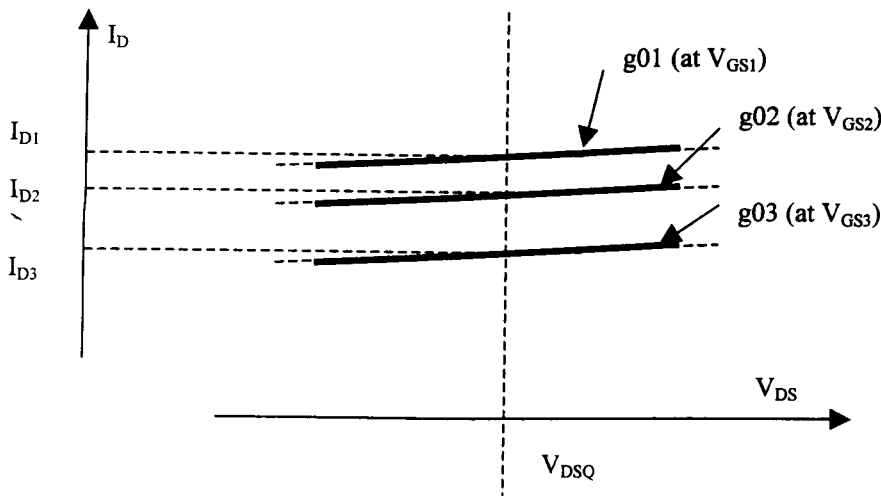


Figure 4.4.1. Extraction of λ

4.4.6. Extraction of r_S and r_D :

From the static model of the junction diode (equation 3.3.1.3), it is clear that the effect of the series resistances r_S and r_D is to shift the ideal characteristics $I_D = f(V_D)$ by an amount of $\Delta V_D = rI_D$, as shown on figure 4.4.2.

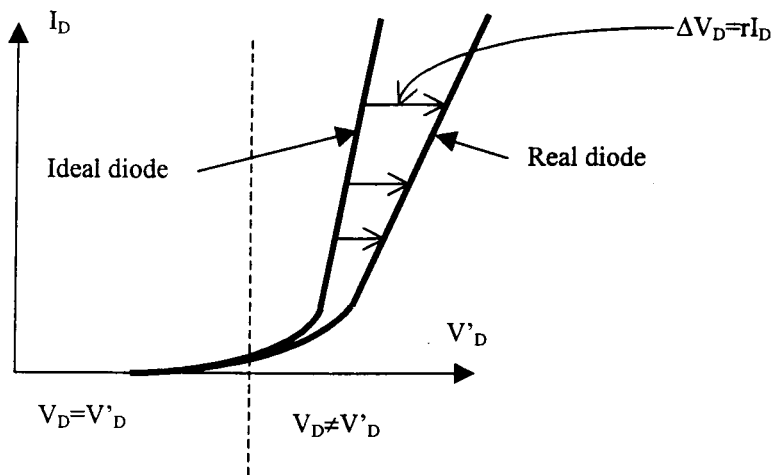


Figure 4.4.2. Extraction of the drain and source series resistances

Here, r stands for r_S or r_D depending on the considered junction, and can be extracted using the previous equation as :

$$r = \frac{\Delta V_D}{I_D} \tag{4.4.4}$$

Several values are calculated and the average value is considered.

• Remark:

The extraction of the series resistances in the case of JFET devices is possible because of their relatively high values in comparison with the junction diodes.

Practically we have noticed that the effect of the series resistances of the JFET becomes significant before the maximum current limit of the HP 4145B model (100mA) is reached. This is not the case of the PN junction and Shottky diode.

A MATLAB routine of JFET model parameters extraction was implemented, figure 4.4.3 shows this routine during run time.

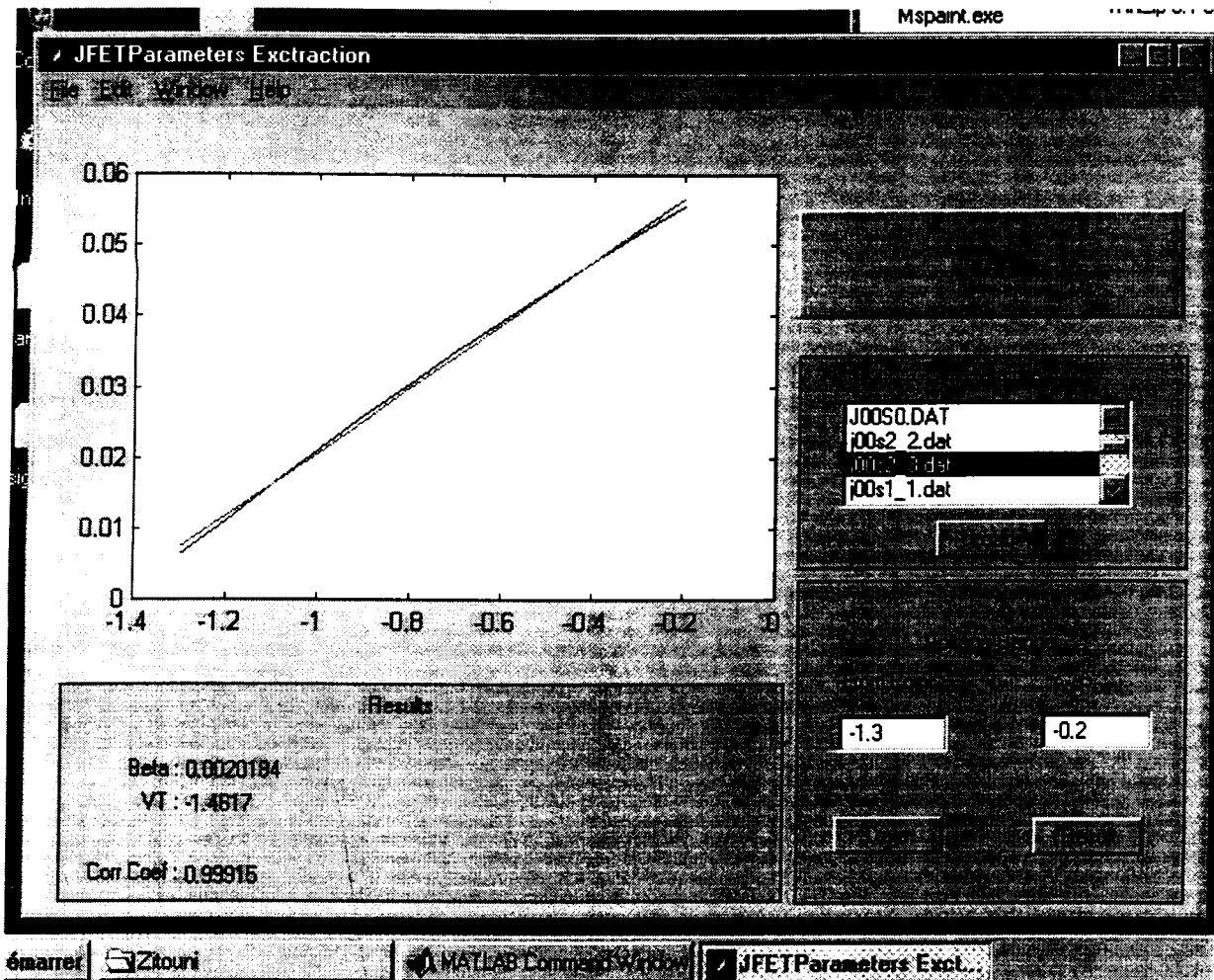
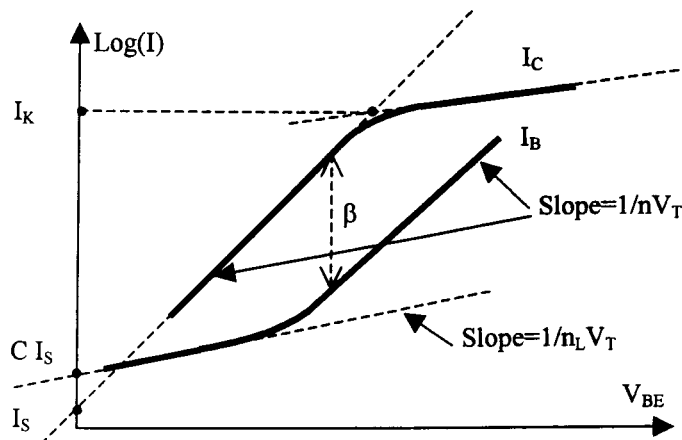


Figure 4.4.3. The implemented routine for JFET model parameters extraction

4.5. Parameters extraction of BJT model

The Gummel-Poon model parameters described previously, can be obtained for their majority by investigating the curves of $\log(I_C)$ and $\log(I_B)$ with respect of V_{BE} in both normal and reverse operating modes, for a given value of V_{BC} [25]. These curves are shown in figure 4.5.1.

In the normal mode; C is C_2 , I_K is I_{KF} , n is n_F , n_L is n_{EL} and β is β_F , while in the reverse mode (the collector and the emitter interchange their roles); C is C_4 , I_K is I_{KR} , n is n_R , n_L is n_{CL} and β is β_R , see the Gummel-Poon equations in the previous chapter. In addition to those parameters, two others should be also extracted, they are respectively the early voltage in normal and reverse mode (V_A and V_B), which are used to approximate the currents I_{CC} and I_{EC} .

Figure 4.5.1. Plot of $\log(I_C)$ and $\log(I_B)$ vs. V_{BE}

4.5.1. Extraction of I_S and n :

I_S is the transistor saturation current. With regard to the curve for I_C , by extrapolating the region with slope $1/nV_T$, the value of I_S is obtained. On the other hand the emission factor n is obtained from the curve slope as shown previously for the PN junction diode.

4.5.2. Extraction of I_K :

I_K is the knee current; it models the drop in β at high collector currents due to high-level injection. If we assume that low-level and high-level injection effects could be distinguished by regions, a value of I_K could be obtained by the intersection of the two asymptotes as shown in the above figure.

4.5.3. Extraction of C and n_L :

With regard to the curve of I_B , by extrapolating the region with a slope of $1/n_L V_T$ at low current levels, the value of C can be determined and, by determining this slope, n_L can be found. These parameters describe the nonideal component of I_B which is dominant at low currents. This component is responsible for the drop in β at low currents.

4.5.4. Extraction of β :

β is the maximum value of the ratio I_C to I_B when the transistor is in the normal active region. β can be determined by the regions of the two curves where they are parallel. In this region, both I_C and I_B have dominant ideal components, and hence I_C can be considered to be proportional to I_B .

4.5.5. Extraction of V_A and V_B :

V_A (or V_B in the reverse mode) is the early voltage that models the effect on the transistor characteristics of the base-width modulation.

The simplest method of obtaining V_A is from the slope of I_C vs. V_{CE} curve in the linear region. The base voltage should be constant and the transistor should be biased to its normal operating point. In the forward mode the collector current can be simplified as:

$$I_C = \frac{I_S}{q_b} e^{\frac{V_{BE}}{n_F V_T}} \quad (4.5.1)$$

Therefore by keeping the base voltage constant, the collector current would be proportional to $1/q_b$ and, if V_{BE} is small enough so that V_{CE} is approximately equal to

V_{BC} then from equations 3.3.2.18 to 3.3.2.20, we can neglect q_2 in the expression of q_b and hence we will end up with the following result [25]:

$$I_C \approx \frac{I_S}{q_1} e^{\frac{V_{BE}}{n_F V_T}} = I_S e^{\frac{V_{BE}}{n_F V_T}} \left(1 + \frac{V_{CE}}{V_A} \right) \quad (4.5.2)$$

The parameter V_A can now be calculated as the intersection of the extrapolated I_C curve with the V_{CE} axis, as shown in figure 4.5.2.

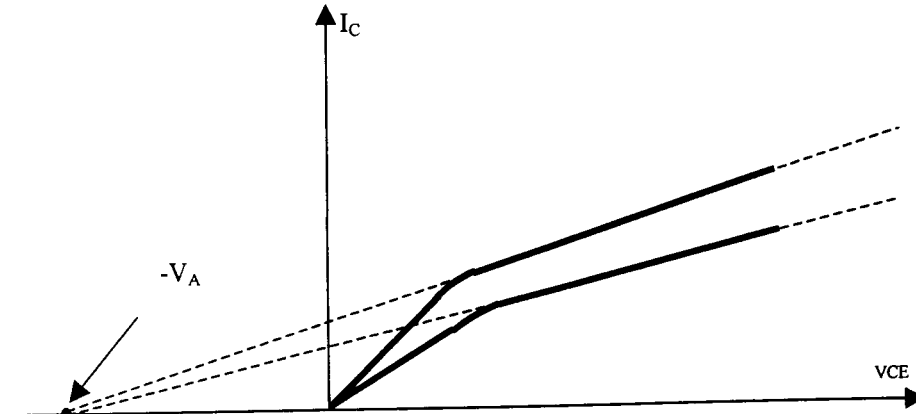


Figure 4.5.2. Approximate definition of V_A from I_C vs. V_{CE} curve

It is best to repeat the extraction at few base-emitter voltages and average the obtained V_A .

In the previous method, to determine V_A we have assumed the voltage V_{BC} small enough so that q_b is dependent only on V_A and V_{BE} . This is why in practice obtained values of V_A for different values of V_{BE} are often very different.

A more accurate method to determine V_A and V_B at the same time is, the use of the curve $\log(I_C)$ vs. V_{BE} (and $\log(I_E)$ vs. V_{BC}) in both normal and reverse modes, for two distinct values of V_{BC} (V_{BE}). For a given value V_{BE0} of V_{BE} , we can obtain in the normal mode the following equation:

$$\frac{I_C(V_{BC} = 0)}{I_C(V_{BC} = V_{BC1})} = \frac{1 + \frac{V_{BE0}}{V_B} + \frac{V_{BC1}}{V_A}}{1 + \frac{V_{BE0}}{V_B}} \quad (4.5.3)$$

And for a given value V_{BC0} of V_{BC} , in the reverse mode :

$$\frac{I_E(V_{BE} = 0)}{I_E(V_{BE} = V_{BE1})} = \frac{1 + \frac{V_{BC0}}{V_A} + \frac{V_{BE1}}{V_B}}{1 + \frac{V_{BC0}}{V_A}} \quad (4.5.4)$$

Equations (4.5.3) and (4.5.4) can be solved for V_A and V_B .

A MATLAB routine has been implemented to extract Gummel-Poon model parameters, figure 4.5.3 shows this routine at run time.

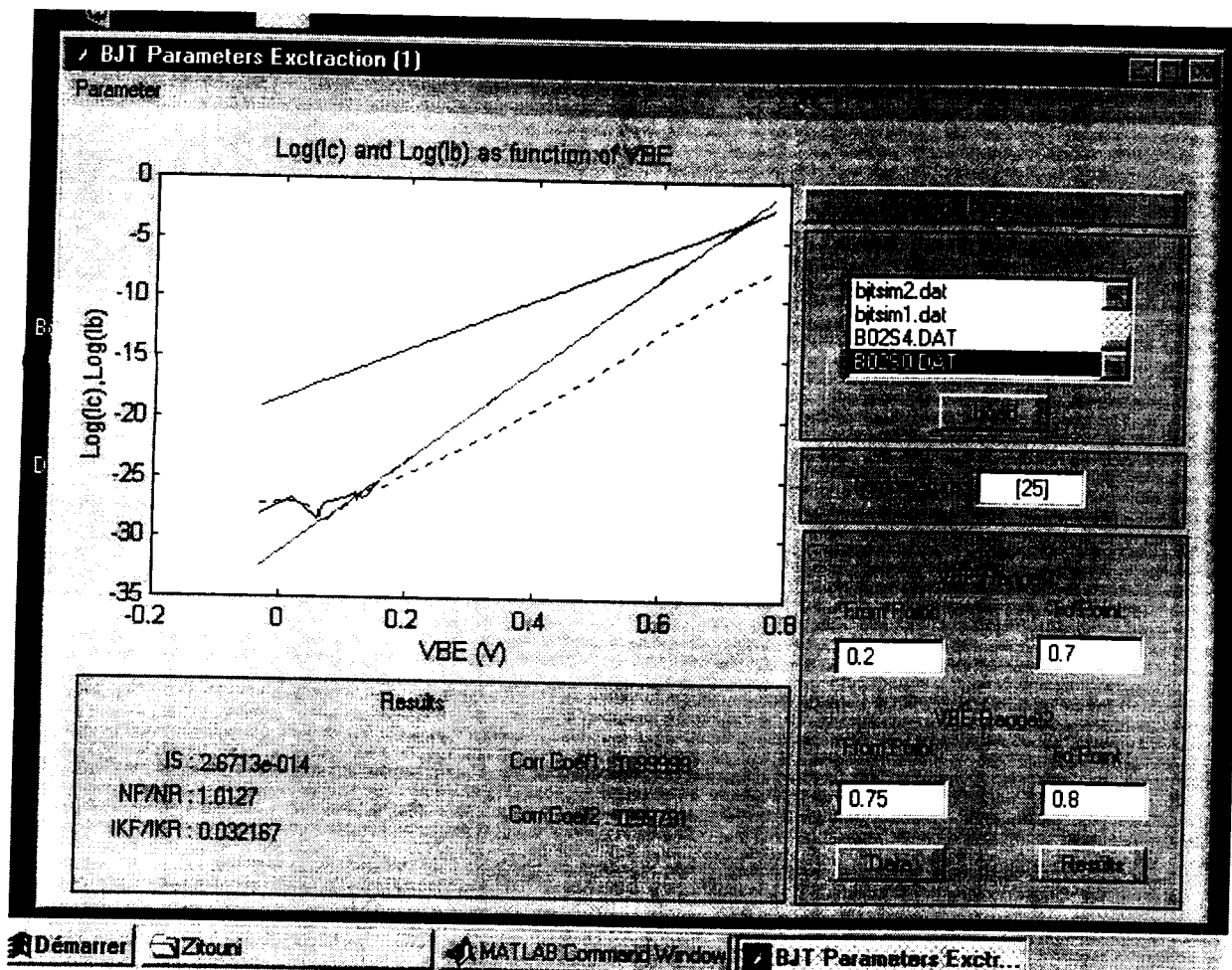


Figure 4.5.3. the implemented routine of extraction of the Gummel-Poon Model parameters

Chapter 3

The Integrated System Testing

5.1. Introduction

In chapter 2, we have described how the integrated system can perform automated measurements on electronic components. In chapter 4, methods of extraction of model parameters of different kind of devices have been presented. Through the present chapter results obtained using the implemented routines of model parameters extraction, on measurement data from the integrated system, are presented. A large amount of commercial devices including both passive and active types have been tested. For reason of convenience, some of them only have been selected in this chapter. In fact the main objective of this chapter is to justify the need of such integrated system by extracting actual device parameters in order to improve the simulated results accuracy, and the discussion on the obtained results is not the aim of our work. This is the included discussions on the obtained results are brief and may be not complete. We prefer to let then this task for specialists that are working in this area.

5.2. Testing of passive devices

Different types of resistors, capacitors and inductors have been tested. The results obtained are of different types.

a) Dynamic circuit model parameters:

The parameters of circuit models described in chapter 3 can be extracted with different degrees of difficulty.

- The resistor circuit parameters are obtained easily even with graphical methods (see chapter 4), and optimisation methods do not give significant improvement. The result can be considered very good. As an example results obtained on a 10 ohms wire-wound resistor are shown in figure 5.2.1 while those obtained on a thick film silicon type of the same resistance value are shown in figure 5.2.2. To compare the two devices, extracted circuit parameters are presented in table 5.2.1. Note that the second type of resistors is used mainly in control circuits of power machines, because it is supposed to be a low inductive device. As it is shown on table 5.2.1, this fact is proved.
- The capacitor and inductor circuit parameters are more difficult to obtain and the use of optimisation methods are necessary. Many initial condition trials should be done before obtaining satisfactory result. Figures 5.2.3 and 5.2.4 show examples of obtained results.

b) Non-linear capacitor model parameters:

The parameters related to the modelling of non-linear capacitors are simply coefficients of polynomial fitting, as described in chapter 3. An example of 10 nF ceramic capacitor is illustrated in figure 5.2.5. As it is shown on this figure polynomial of degree two fits better the measured data points, in comparison to a polynomial of degree one. This justify the use of terms of order two in SPICE program model [21].

c) Leakage currents in capacitors dielectric:

The measurement of leakage currents in the capacitor dielectric is possible using either the HP 4140B or the HP 4145B model, since current values as small as 1fA (10^{-15} A) can be measured. This allow the characterisation of capacitor dielectric (especially

electrolytic ones) and hence find any degradation by ageing or after operating in wrong conditions. Figure 5.2.6 shows the dielectric degradation of an electrolytic capacitor caused after wrong biasing conditions during a period of time equal to 10 minutes.

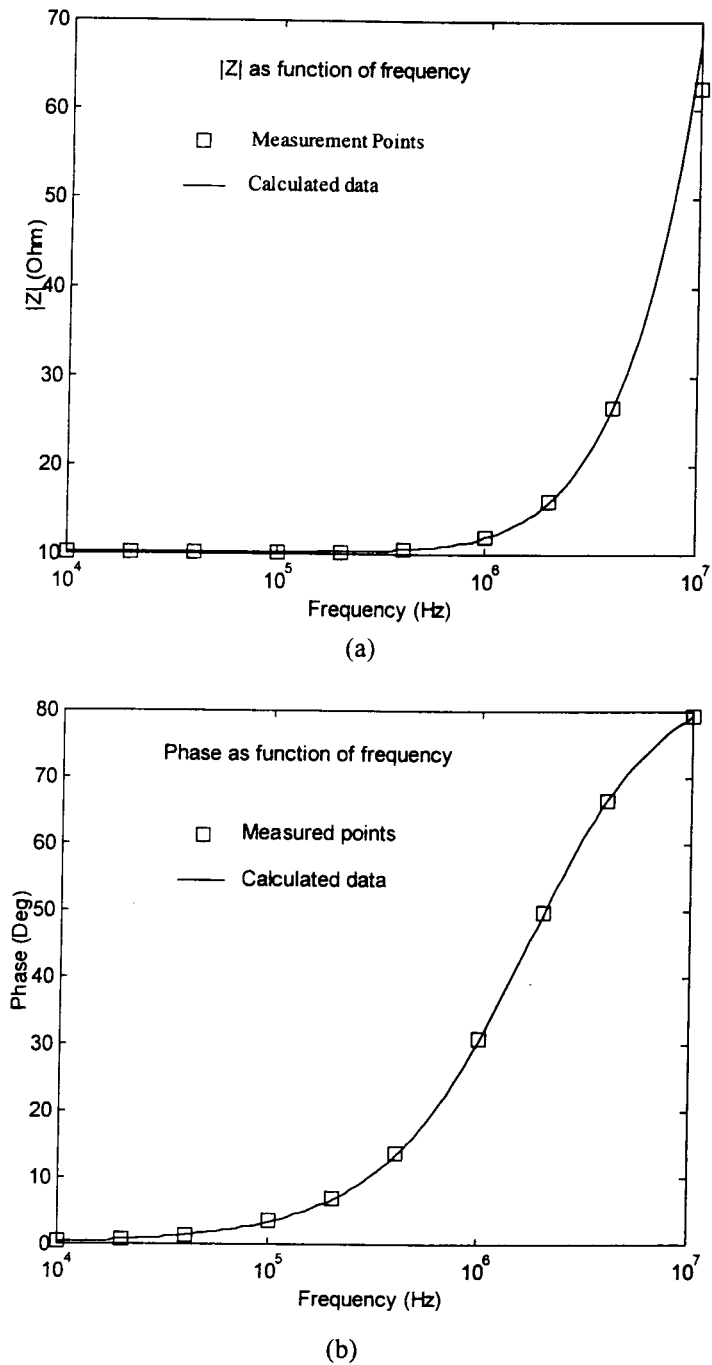
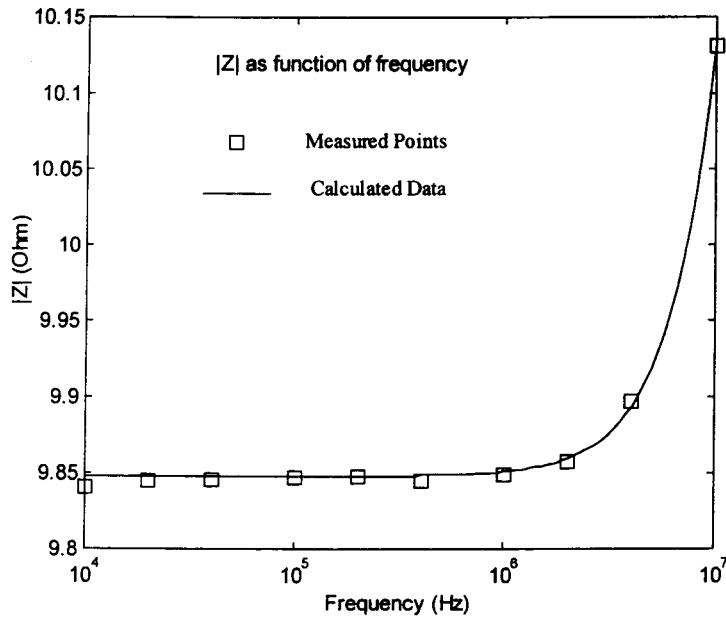
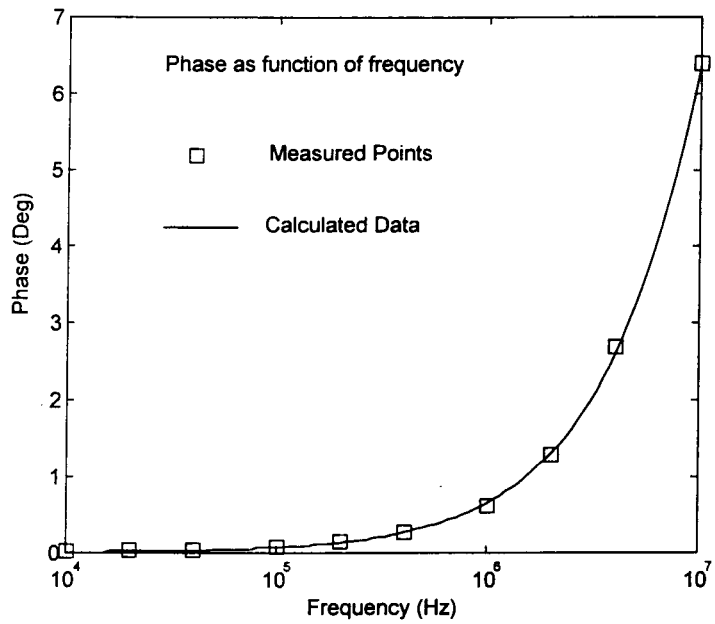


Figure 5.2.1 Calculated impedance magnitude (a) and phase (b) from extracted parameters of a 10 ohms wire-wound resistor type.



(a)



(b)

Figure 5.2.2 Calculated impedance magnitude (a) and phase (b) from extracted parameters of a 10 ohms thick film silicon resistor type.

Parameter	Wire-wound resistors	Thick Film Resistors
Rp(Ω)	10.223	9.848
L(nH)	958.51	29.42
C(pF)	26.49	119.34

Table 5.2.1 Extracted parameters from two different types of resistors

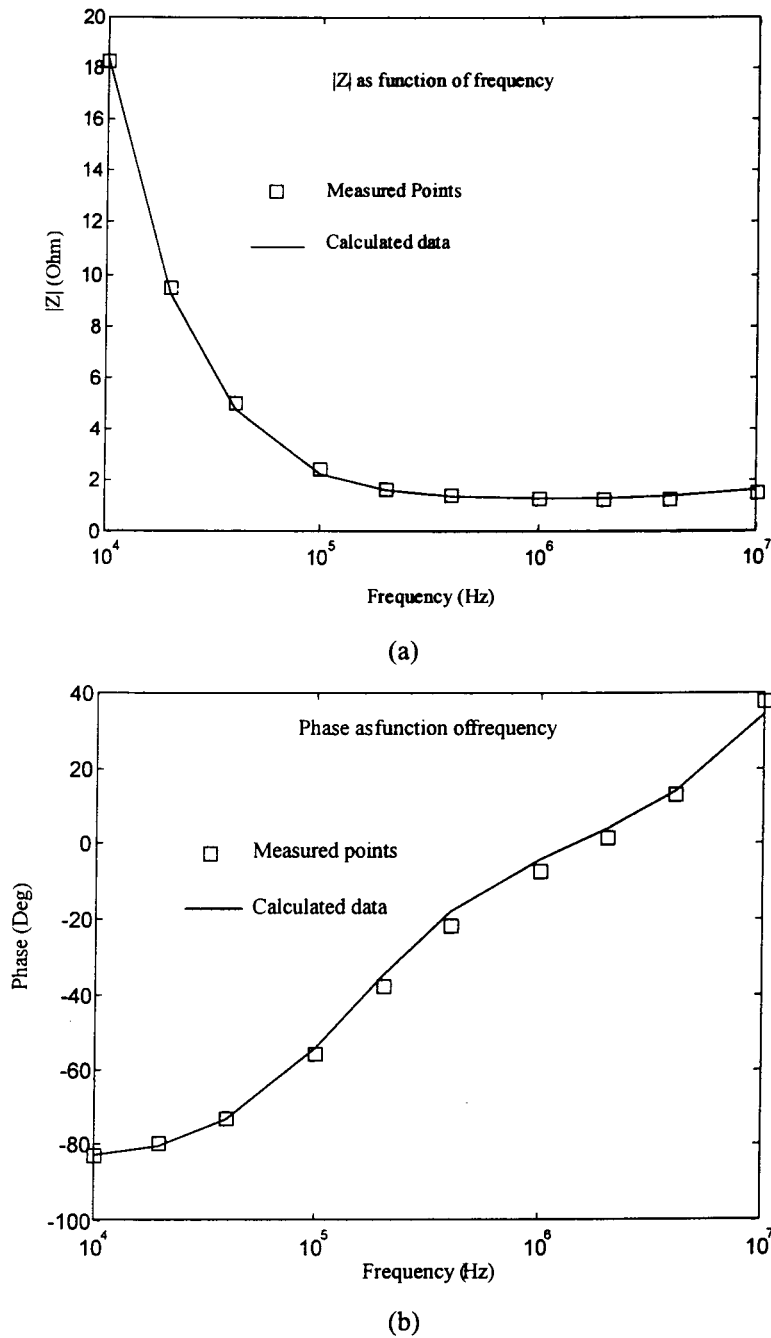


Figure 5.2.3
 Calculated impedance magnitude (a) and phase (b) from extracted parameters of a 1µF electrolytic capacitor.

Obtained parameters in this example are:

$$R_s=1.29\Omega, R_p=330.58\Omega, L=14.27nH \text{ and } C=0.867\mu F.$$

Note the unexpected low value of R_p .

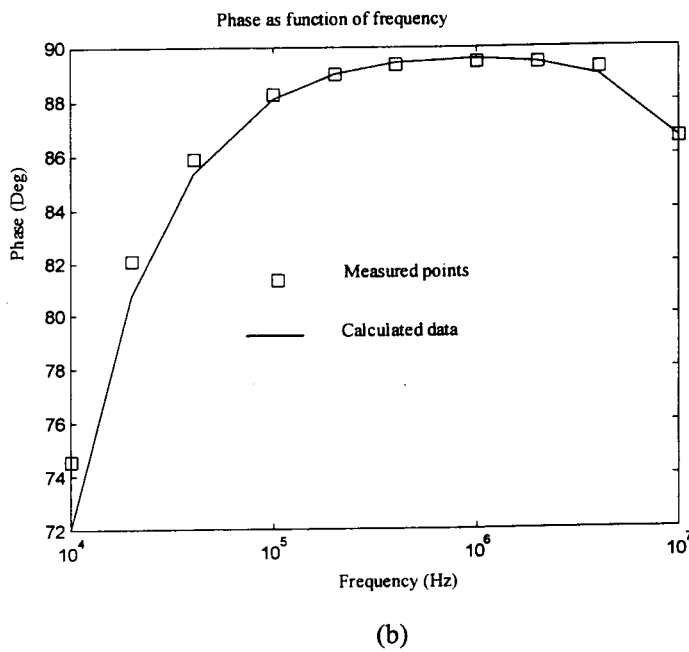
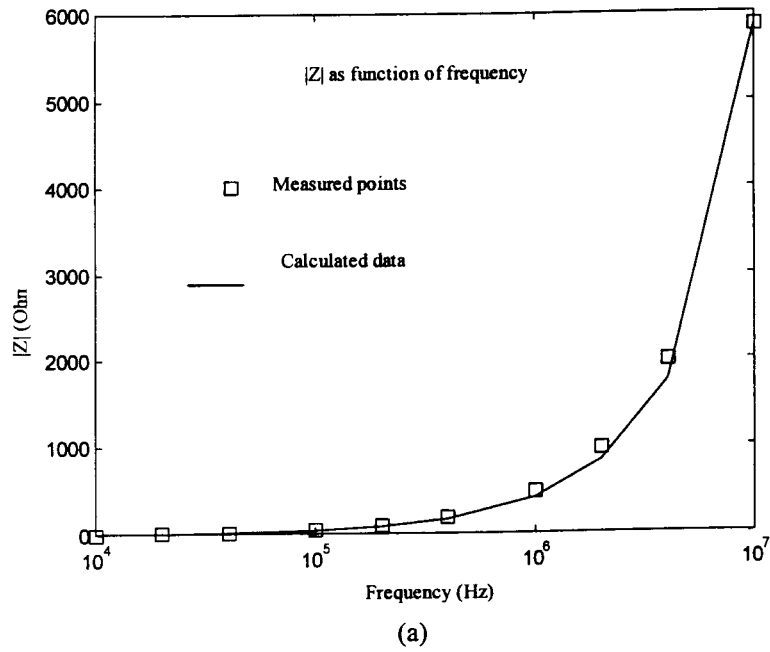


Figure 5.2.4
 Calculated impedance magnitude (a) and phase (b) from extracted parameters of a 70 μ H inductor.

Obtained parameters in this example are:
 $R_s=1.36\Omega$, $R_p=100K\Omega$, $L=66.67\mu H$ and $C=1.09pF$.

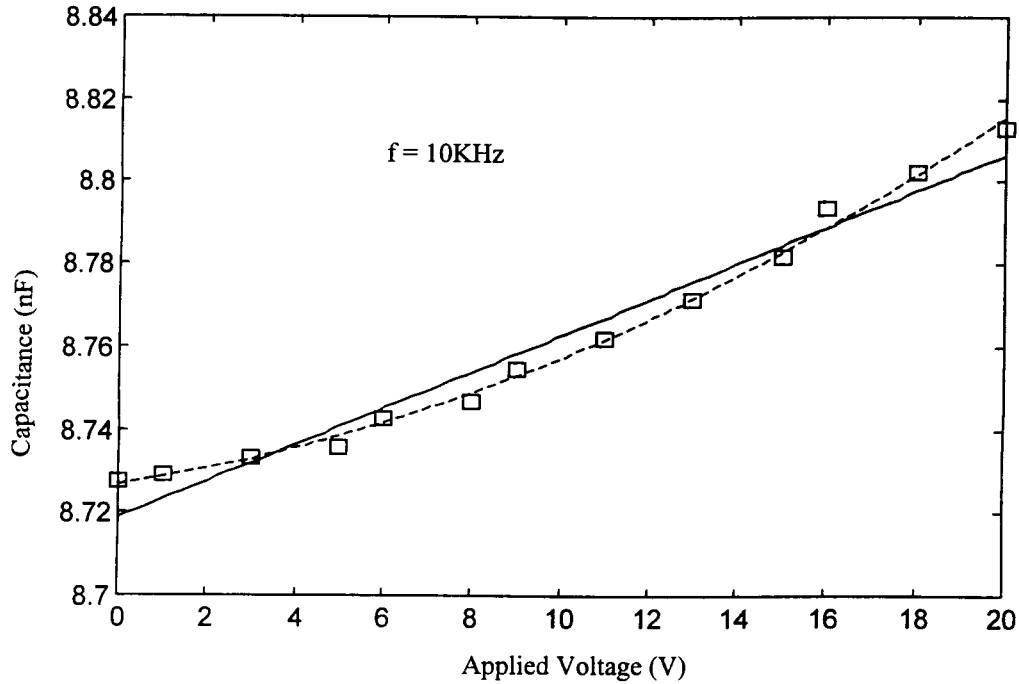


Figure 5.2.5 Capacitance vs. Applied voltage of a 10nF ceramic capacitor
 Squares : Measured points, Solid line : First order polynomial fitting, Dashed line : Second order polynomial fitting.
 According to SPICE program: $C(V) = C_0 (1 + C_1 V + C_2 V^2)$. In this example, $C_0 = 8.72 \text{ nF}$, $C_1 = 18.92 \cdot 10^{-5} \text{ V}^{-1}$ and $C_2 = 1.60 \cdot 10^{-5} \text{ V}^{-2}$.

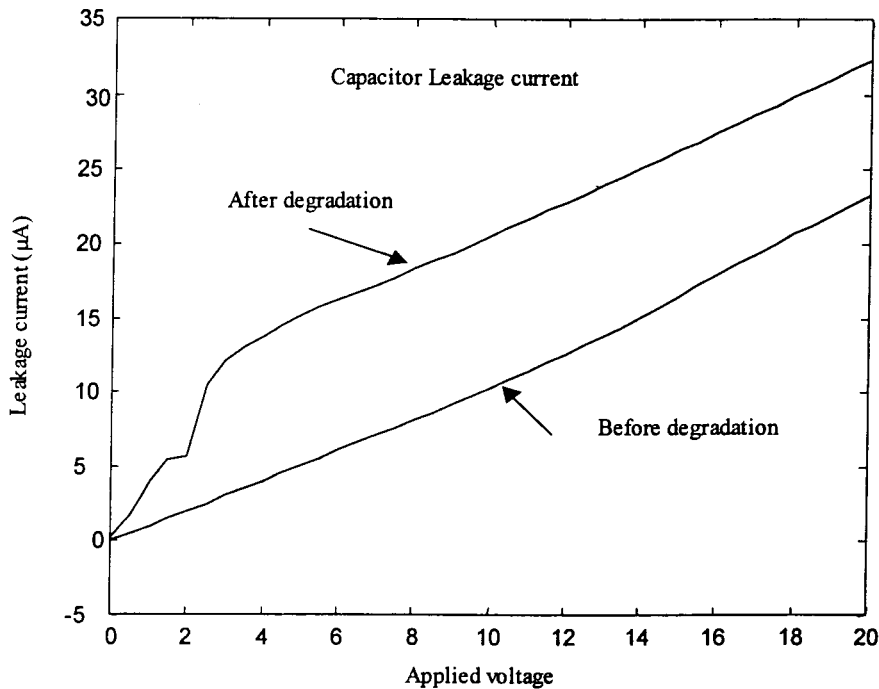


Figure 5.2.6 Degradation of an electrolytic capacitor after 10 minutes of wrong biasing conditions.

5.3. Testing of PN junction and Shottky diodes

In the following section results extracted from the PN junction 1N4003 model and the Shottky ITS 7818 model diodes are presented.

The presented results are obtained from measurements of the forward and reverse diodes DC characteristics, and junction depletion capacitances at ambient temperature (around 25°C).

The obtained model parameters in the forward biasing conditions can be considered very good as indicated in figures 5.3.1 and 5.3.2. However in the reverse biasing conditions the Shottky diode fits better the theoretical model as shown in figure 5.3.3. Summarised results are presented in table 5.3.1. The results shown in this table agree with the expected ones. For example, practical values of the emission coefficient for PN junction diodes are between 1 and 2, while it is close to 1 for Shottky diode [25].

The same table shows the extracted parameters related to the depletion capacitance of the large signal model. As it is indicated on figure 5.3.4 the model fits perfectly the experimental data.

Diode	I_s	n	C_j	C_{js}	C_{js0}
1N4003	$5.32 \cdot 10^{-9}$	1.86	42.26	0.432	0.452
ITS 5818	$1.27 \cdot 10^{-6}$	0.9985	428.5	0.382	0.463

Table 5.3.1 Extracted parameters of both PN junction and Shottky diodes

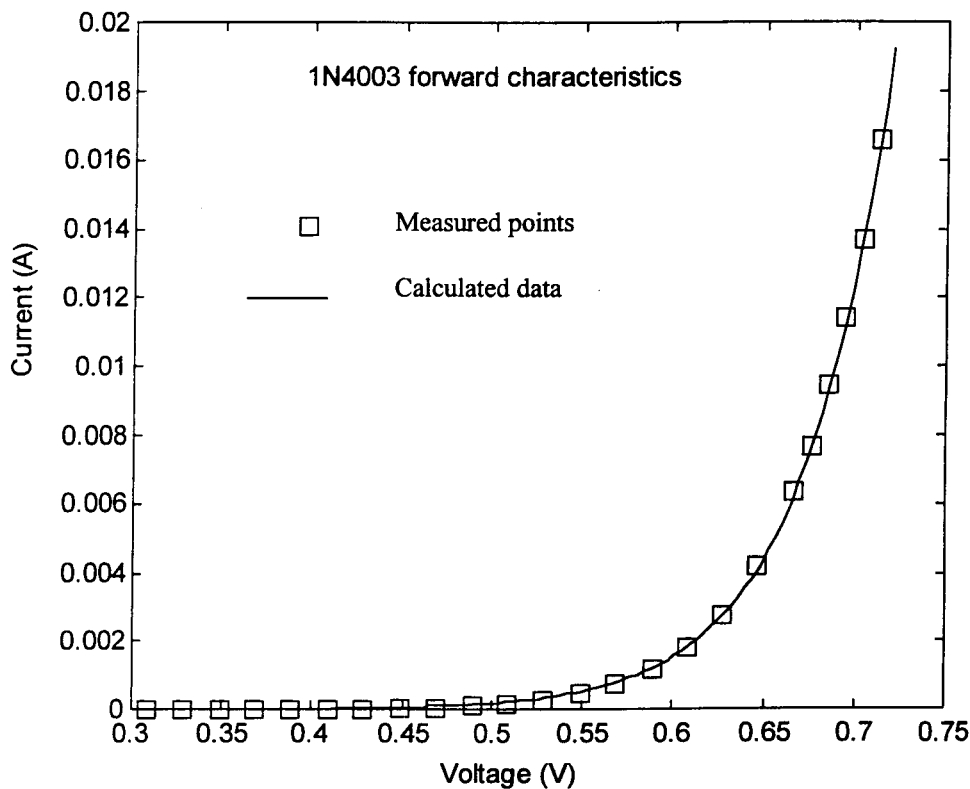


Figure 5.3.1 1N4003 diode model DC characteristics

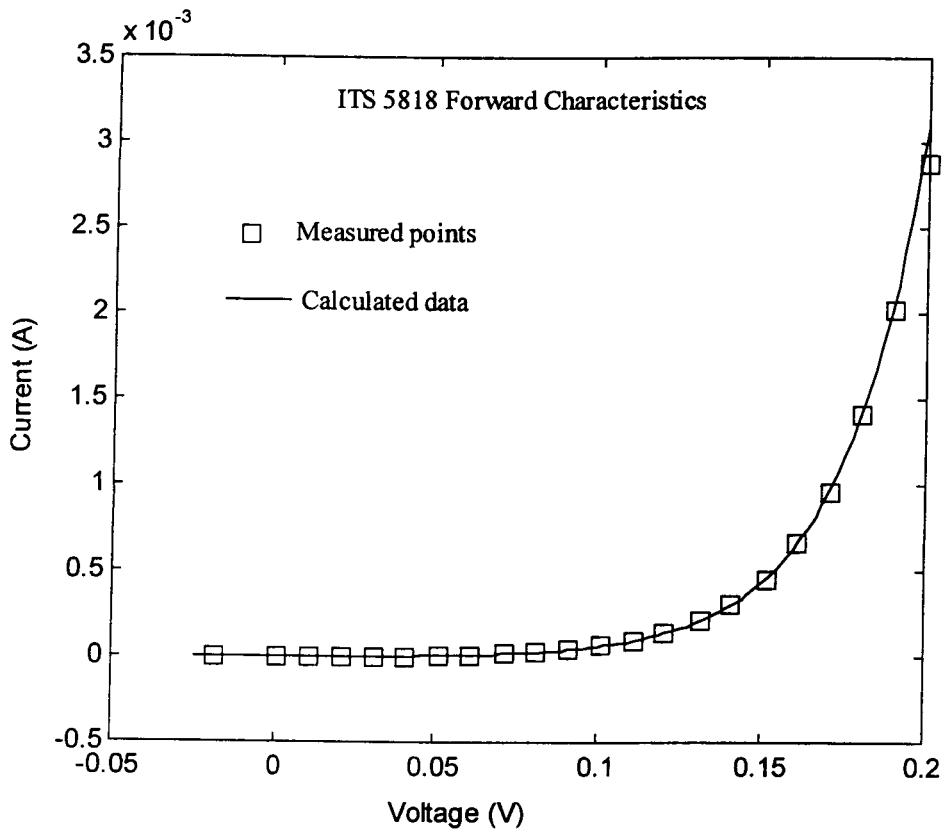


Figure 5.3.2 ITS5818 Shottky diode DC characteristics

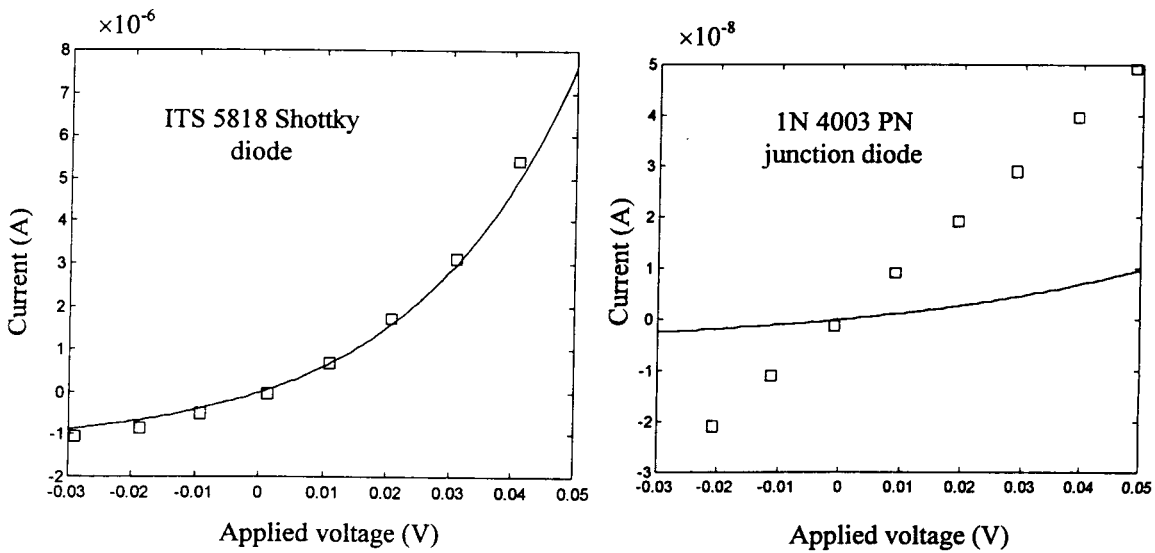
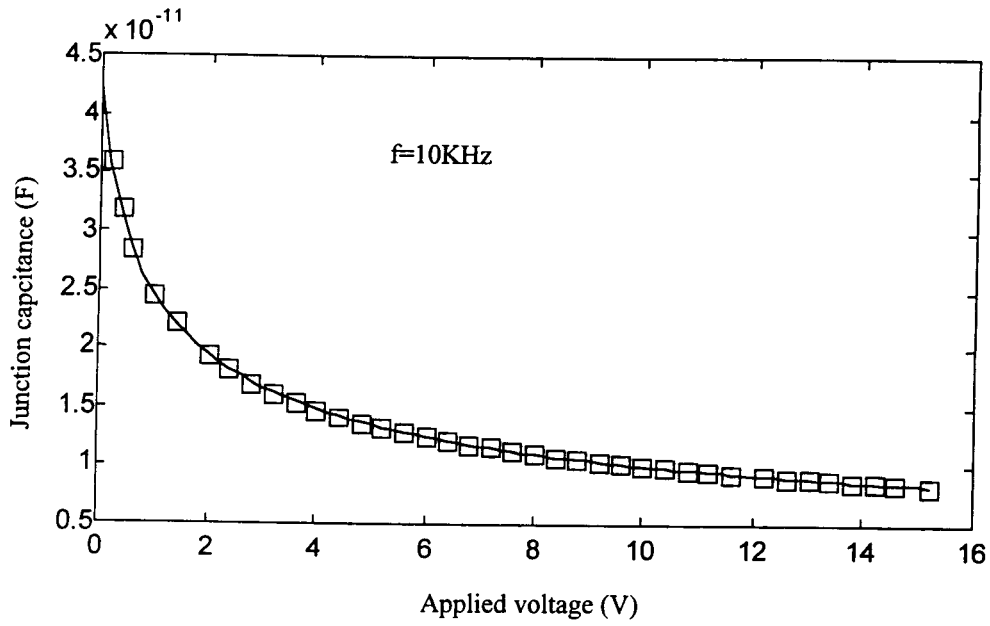
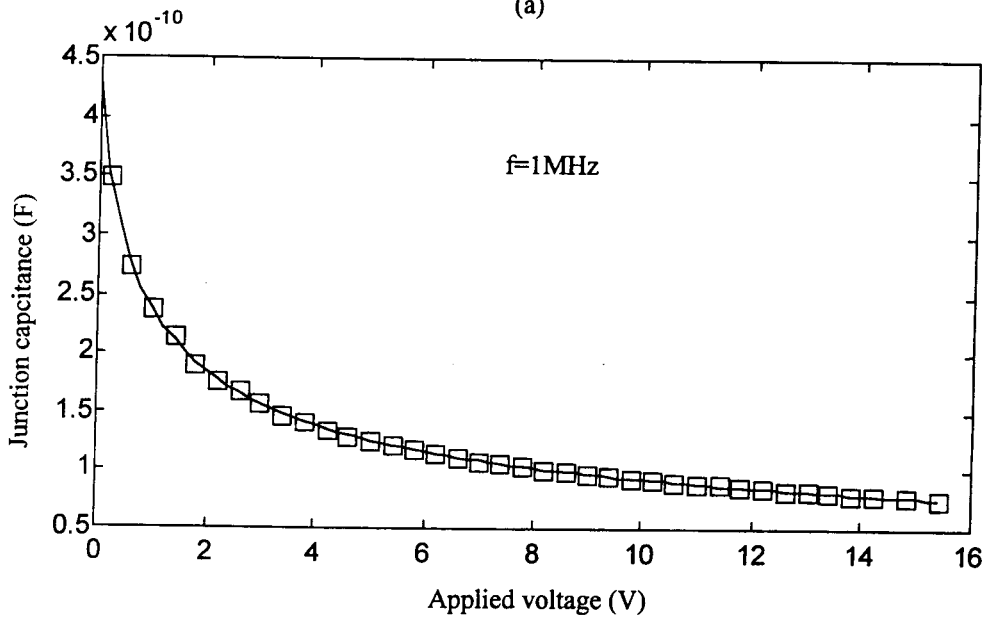


Figure 5.3.3 PN junction and Shottky diode in reverse biasing mode. Squares : measured points, Solide lines : calculated data.



(a)



(b)

Figure 5.3.4 Depletion capacitance as function of applied reverse voltage. (a) PN junction diode, (b) Shottky diode.

5.4. Testing of junction field effect transistors (JFETs)

In this section results extracted from the JFET 2N3823 model are presented.

In order to obtain meaningful results, let us first, compare drain current I_D vs. the drain voltage V_{DS} for several values of V_{GS} by simulation using the MicroSim PSPICE program, with measured data. The obtained results are shown in figure 5.4.1.

As it is noticed on this figure the data obtained by simulation are considerably different from measured ones, even if the used model is known to be very accurate one (see chapter 3). This example shows clearly that accurate models is not sufficient to obtain accurate simulated data.

The difference between simulated and experimental data in our example can be explained by the fact that the simulation program uses default model parameters to carry out its results. These parameters are defined the first time the software is installed, and can be modified according to the user application. A list of some default parameters is presented in table 5.4.1 [21].

We have calculated model parameters from measured data using methods of extraction presented in the previous chapter, they are also presented in table 5.4.1. We run again the simulation program but with the extracted parameters this time the obtained results are shown in figures 5.4.2 and 5.4.3. As we can show in this figure, the simulation results are improved significantly .

Hence, from this simple example we can deduce that first, results obtained from simulation are more accurate when actual model parameters are used, second, the developed methods of extraction of JFET parameters model described in the previous chapter are valid.

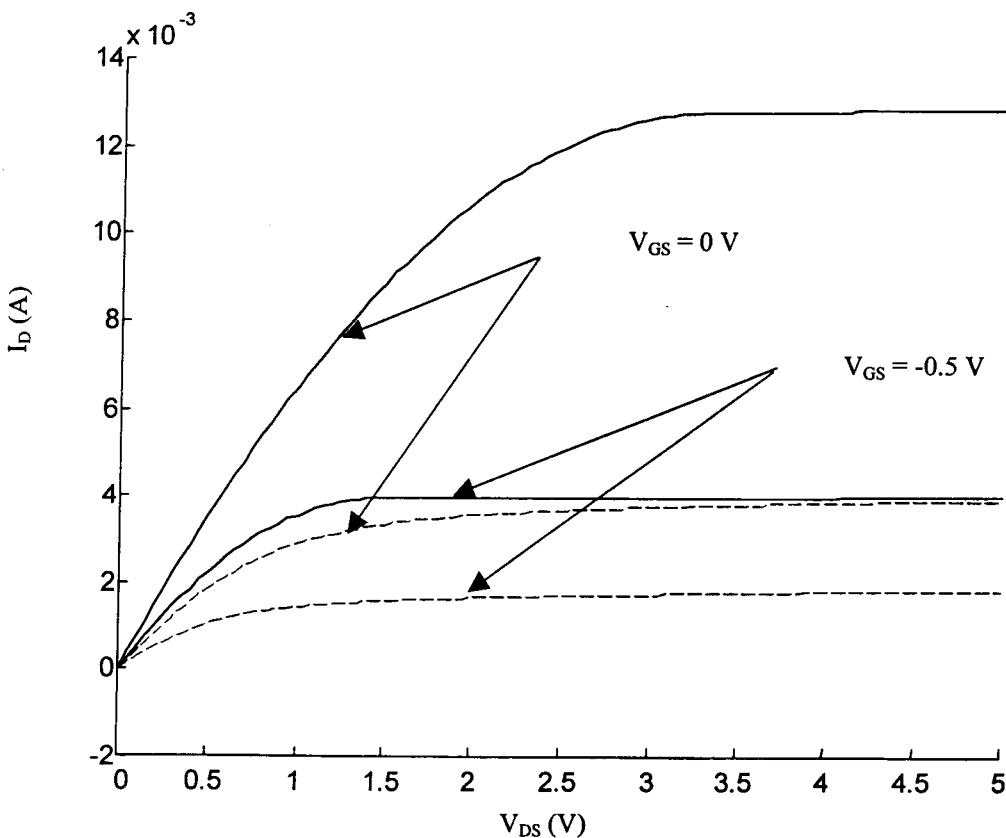


Figure 5.4.1 Comparison between simulation data (solid lines) using default parameters and experimental data (dashed lines)

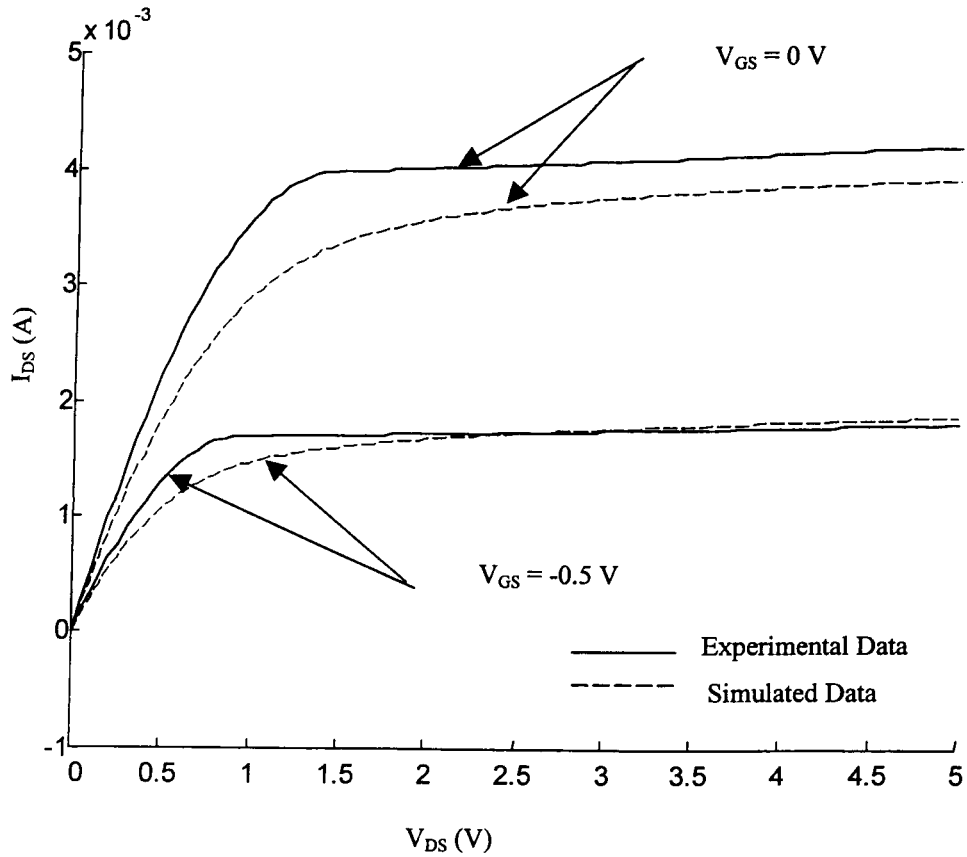


Figure 5.4.2 Comparison between simulation data with extracted parameters using graphical method, and experimental data

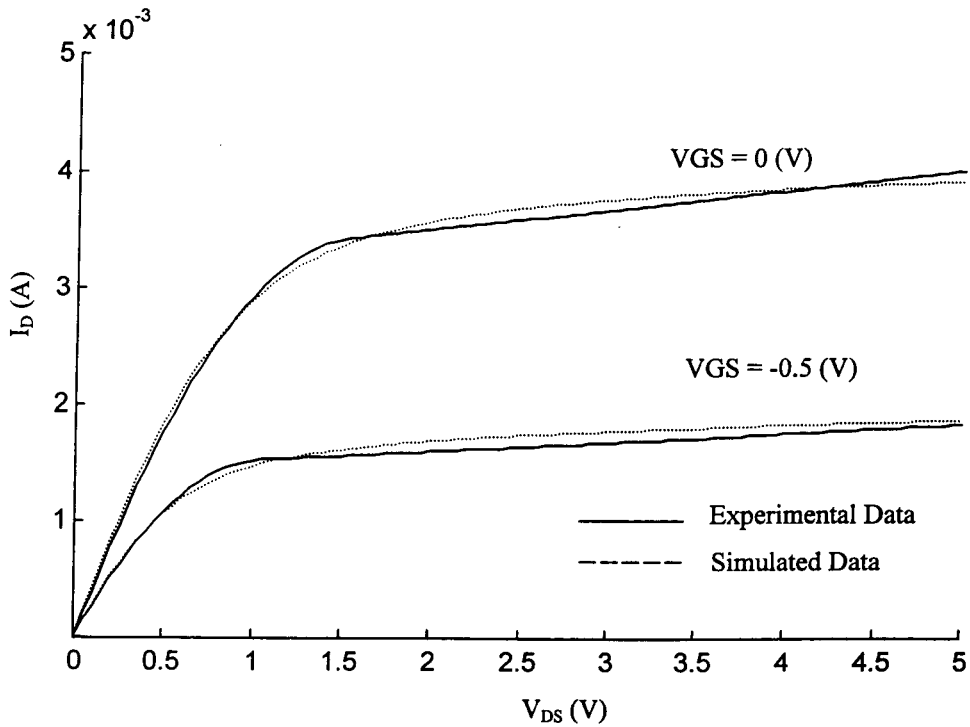


Figure 5.4.3 Comparison between simulation data with extracted parameters using optimisation method, and experimental data

β (AV^{-2})	$1.17 \cdot 10^{-3}$	$1.8925 \cdot 10^{-3}$	$1.3627 \cdot 10^{-3}$
r_D (Ω)	1	2.34	2.34
r_S (Ω)	1	2.27	2.27
λ (V^{-1})	$4 \cdot 10^{-3}$	$16.844 \cdot 10^{-3}$	$54.155 \cdot 10^{-3}$
V_{T0} (V)	-3.3	-1.443	-1.533
I_S (fA)	33.57	$1.5060e-14$	$1.5060e-14$
N	1	1.1934	1.1934
C_{GD} (pF)	1.6	4.59	4.59
C_{GS} (pF)	2.414	4.62	4.62
M	0.3622	0.7914	0.7914
ϕ (V)	1	1.0682	1.0682

Table 5.4.1 2N3823 model parameters

5.5. Bipolar junction transistor testing

The device we have selected to present testing results of BJTs, is the 2N2219A model.

The same approach used for the JFET testing is used. The simulation data that consist on the collector current I_C with respect to collector-emitter voltage V_{CE} for different values of I_B using default model parameters are shown on figure 5.5.1. On the other hand, the simulation data obtained using calculated model parameters from measured data, are shown on figure 5.5.2. table 5.5.1 presents some default and extracted device parameters.

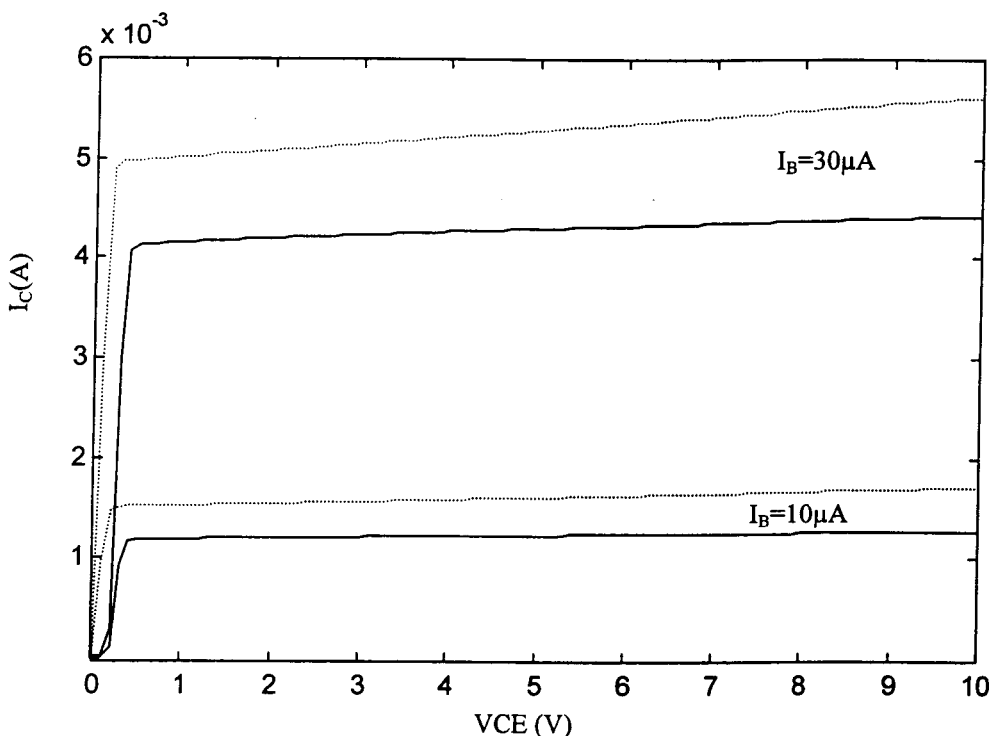


Figure 5.5.1 Comparison between simulation data (dashed lines) using default parameters and experimental data (solid lines)

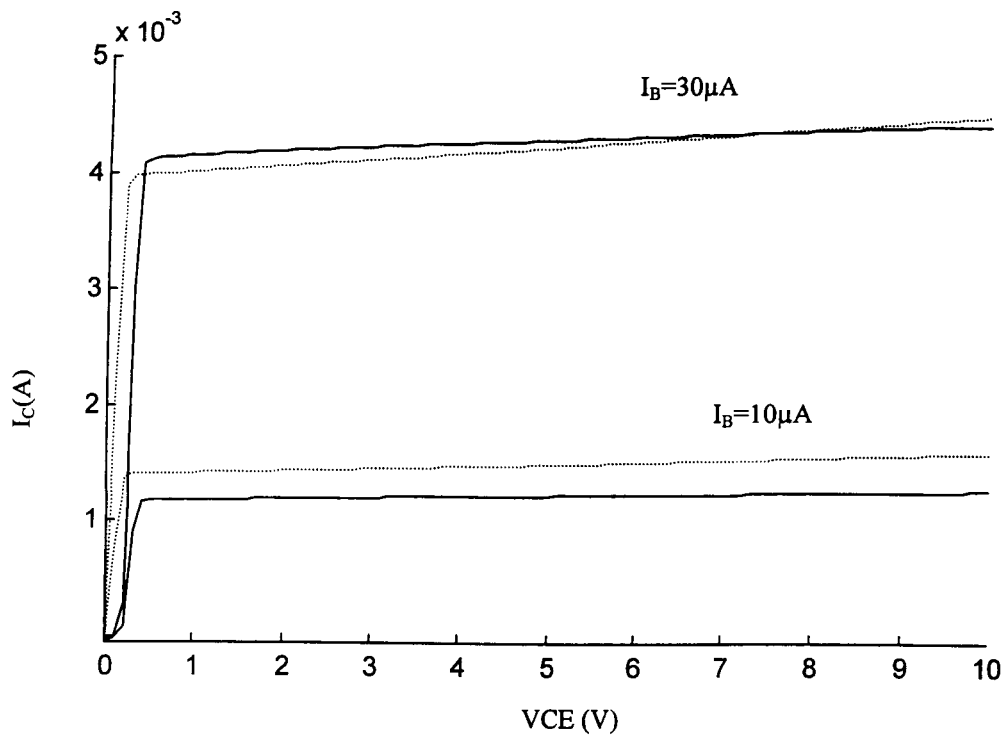


Figure 5.5.2 Comparison between simulation data (dashed lines) using extracted parameters and experimental data (solid lines)

I_S (fA)	14.34	4.774
n_F	Not Defined	1.019
IK_F (A)	$24.47 \cdot 10^{-2}$	$4.015 \cdot 10^{-2}$
C_2	1	6.43
n_{EL}	1.307	2.05
β_F	255.9	148.26
n_R	0	1.012
IK_R (A)	Not Defined	$1.59 \cdot 10^{-2}$
C_4	0	6.84
n_{CL}	2	1.50
β_R	6.092	3.78
V_A (V)	74.03	105.4
$C_{BE}(0)$ (pF)	22.01	23.34
$C_{BC}(0)$ (pF)	7.306	14.63
ϕ_E (V)	0.75	0.77
m_E	0.377	0.323
ϕ_C (V)	Not Defined	0.44
m_C	Not Defined	0.27

Table 5.5.1 Default and Extracted BJT model parameters

From the obtained curves of figures 5.5.1 and 5.5.2, it appears that results using extracted parameters are better than those using default parameters but are not very accurate. This is due to the difficulty of calculating some parameters, specially those related to the drop in β at low current levels (C_2 and C_4). This difficulty is in our opinion related to the thermal noise that are not negligible at low current levels. We think that improved results can be obtained from measurements at low temperature value in an isothermal environment. In such conditions effect of disturbing currents can be reduced or eliminated.

Chapter 6

Conclusion

In this work an integrated PC-based system for the characterisation of integrated and discrete electronic devices has been implemented. The system can carry out experimental data from electronic devices through the GPIB bus using a set of high quality HP model test instruments, with the help of an appropriate GPIB interface card housed in the PC slot. Automated measurements of electrical quantities (currents, voltages, impedances, ...) on a wide range of current, voltage and frequency are possible.

For reason of validation a set of MATLAB routines were also implemented. These routines permit the extraction of SPICE model parameters of different types of commercial electronic components, they are mainly based on two type of extraction methods: Graphical methods and Optimisation methods.

According to the results presented in chapter 5, it can be noticed that in general optimisation methods are more accurate than graphical methods. However, careful definition of initial conditions is required to ensure convergence of the algorithm. This is why even less accurate, graphical methods are used as first trial to provide the optimisation algorithm with appropriate initial conditions.

The results obtained from the characterisation of the basic passive components (resistor, capacitor and inductor) are very good and the circuit models can be considered to be good in the 10KHz to 10MHz frequency range. To obtain this result, optimisation methods are necessary especially for the capacitor and inductor models. Good results can be obtained for the resistor element even using graphical methods, this is due to the developed method which does not need any additional DC measurement.

Extracted PN junction and Schottky diode model parameters are also very good. The comparison of the experimental data with the simulated one proves the accuracy of both the DC model and the used method of extraction. Here again, the power of the optimisation technique to extract depletion capacitance parameters is demonstrated.

When testing JFET devices the importance of good parameters extraction methods is clearly shown by comparison of experimental data with the MicroSim PSpice software (evaluation version 6) simulated data using first, model parameter default values, second, parameter values graphically extracted and third, parameter values extracted using optimisation techniques.

The extraction of some of the BJT Gummel-Poon model parameters (such as C_2 and C_4) is more difficult and the obtained results for this device are less accurate than those found for the other type of devices. We believe strongly that this is due to presence of disturbing currents that are generated at low biasing levels by thermal noise. This effect can be normally reduced by lowering the temperature value. This means that measurements in isothermal conditions are recommended.

We can conclude then, that our system has been successfully tested on a wide range of components and the obtained results are considered to be very good within the

experimental conditions (such as non control of temperature, limited range of currents and frequency ...).

Further, many engineer final projects and research works [13-16] exploited (and still exploiting) the facilities that the system offers, and the users found it a very useful and versatile tool.

Because most (and may be all) of electronic device models are temperature dependent, the control of the temperature value is very important. Such control is not available in our system, and this can be considered to be the main barrier that make the system not complete. In fact a temperature control loop is available in our laboratory but we still miss a vacuum pump to see it working. Hopefully we are expected to get this important piece in the near future.

Finally, we hope that the developed product will be of great utility in industrial environments as well as for further workers in the electronic devices characterisation field.

Appendix A

Appendix A: Installation of The Pro488 Device Driver

There exists two types of device drivers; **RESIDENT** device drivers and **INSTALLABLE** device drivers. A resident device driver is loaded automatically with the operating system at boot time and hence are included with the operating system. For example, DOS controls the standard PC ports such as, **LPT1:** and **COM1:** by **RESIDENT** device drivers. An **INSTALLABLE** device driver is furnished by the constructor if any extra device or port is to be installed to the PC, and hence is external to the operating system and should be installed following a special procedure. Image scanners and kinds of pointing devices (such as mouse) are controlled using **INSTALLABLE** device drivers.

As it is the case for all **INSTALLABLE** device drivers, the **PRO488** is invoked from the **CONFIG.SYS** DOS system file at boot time. The **DEVICE=PRO488.SYS** line should exist in **CONFIG.SYS** file to load the **PRO488** device driver. In this case it is assumed that the **PRO488.SYS** file is located in the root directory otherwise, the path where the **PRO488.SYS** file is actually located in the system file, should be added.

The **PRO488** parameters

Once **PRO488.SYS** has been successfully loaded the **HPIB** port is an integral part of the personnel computer. As well as loading the **PRO488** device driver into memory DOS calls the driver at its initialisation point, the "Hello" message appears then on the screen. In the message is listed the default configuration (assuming that no parameter is added to the **DEVICE=PRO488.SYS** line). This configuration can be changed by adding parameters to the **DEVICE=PRO488.SYS** line in the **CONFIG.SYS** file as it is illustrated in the following example.

```
DEVICE=PRO488.SYS /"IEEE","IEEEDATA","IEEECTRL",4,BASE=02E1H,IFC ...
```

As its indicated in this example, comma "," sign is used to separate different parameters. The slash "/" character specifies that parameters are going to follow. The device driver parameters are of two types:

a) The **IEEE** port names

These are the file names to be recognised as the **HPIB** port names. This is the only way to specify them at boot time. Three filenames are provided by **PRO488** device driver.

a.1) The **ORIGINAL** file name

The **ORIGINAL** file name defined by default as "**IEEE** " (see last example), is an optional parameter and it holds the file name that DOS recognises as the **IEEE** original port. This filename is the one to be changed when redirecting **LPT1:** or **COM1** to **IEEE** port. This is this way that an **HPIB** interfaced device, for example a printer or

a plotter, can be made as output device instead of a parallel printer connected to LPT1: port or a serial plotter connected to COM1: port. This file name can be any valid DOS file name consisting of 8 characters from the following list:

A-Z 0-9 \$ & # @ ! % () - { } _ . If the name is less than 8 characters long, then it should be padded with spaces. Both leading and trailing double cotes thus " must be used.

a.2) The DATA file name

This optional parameter holds the file name that DOS recognises as IEEE DATA port. It obeys the same DOS file name conventions as indicated before.

When output is sent to this port the current device is addressed and sent the data. When input is requested from this port the current device is addressed to send data back to the PC. The DATA file name is set by default to IEEEEDATA and may be changed to any valid DOS name that is found convenient e.g. HPIBDATA or GPIBDATA.

a.3) The CONTROL file name

This optional parameter holds the file name that DOS recognises as the IEEE CONTROL port. This file name obeys the same DOS file name conventions as before. ASCII strings may be sent to this port, each string consists of one or more of the IEEE control functions or bus interface messages that the PC ELLITE interface card recognises. A full list is given in annex A.

b) Other parameters

The PRO488 device driver can accept many commands under program control. These include ABORT, TRIGGER, LOCAL, SPOLL and so on (see annex A). It is possible to have the PC automatically execute any of these bus commands when it powers on, by just adding them to the DEVICE=PRO488.SYS line. Any number of IEEE commands can be sent this way. This feature allows many exciting possibilities for IEEE bus control and give PRO488 tremendous flexibility. For example, the user can put the IEEE bus into a initial state at boot time by including the ABORT command to the DEVICE=PRO488.SYS command.

If The first parameter after the filenames and before any bus command parameter is an integer number, then it is treated as the new current device number which by default the device with address 4.

Appendix B

Appendix B: The AssignIeee procedure and The Rebuffer function

AssignIeee is different from the standard Turbo Pascal Assign in two ways; first, it forces the file to be opened in raw data mode. DOS treats files as either cooked data or raw data. The former, which is the default, only ever transfers one byte at a time, and also performs checks on certain control characters. Raw data is transferred as many bytes as possible at a time (so is quicker), and does not check for control characters. The second difference is that, Turbo Pascal creates for files an internal buffer, usually of 128 bytes. Reads and writes go to this buffer, and periodically sent to the file itself. This has an unfortunate side-effect, that Read statement in a program will often read in more bytes from a file than are actually returned by the Read statement. The user cannot easily tell how many bytes there are still in the input buffer, and consulting the control status string may give a false answer when the driver has returned all the data read but some remains in the input buffer, unread by the program. AssignIeee therefore sets the input buffer, to one byte, so that the program is always up to data with the driver. Although safe reading from a file one byte at a time is potentially slow.

RebufferIeee is a function which can set the size of the input or output buffer of a file opened via AssignIeee. RebufferIeee will accept a file that was created via the standard Assign procedure, but its effects will be unpredictable. The operands are the file and a Word indicating the length of buffer required. The function knows whether to set the input or output buffer size by whether the file has been reset (input buffer) or is closed, ReWritten or Appended (output buffer). The Boolean value returned is set true if the function was able to make the size adjustment, and false if it could not for lack of memory. Buffers up to 128 bytes are allocated in the space used by the default buffer, so these calls will always succeed. Buffers from 129 bytes to 65535 bytes are allocated in the heap via the GetMem procedure. If RebufferIeee fails to reallocate the buffer, the buffer is left as it was. The contents of the buffer are lost whatever the outcome of the call. reset, Rewrite and Append procedures call RebufferIeee, so switching from input to output changes the buffer length to that last user on output, and vice versa.

References

References

- [1] Flight Electronics PC ELITE IEEE 488 Interface card. Reference manual.
- [2] X. M. Li and M. J. Deen, "*Determination of Interface State density in MOSFETs Using the Spatial Profiling Charge Pumping Technique*", Solid-State Electronics Vol.35, No. 8, 1059-1063, 1992.
- [3] V. Mitra, R. Bouderbala, A. Benfdila, H. Bentarzi and A. Amrouche, "*Charge-Extraction Technique for Studying the Surface States in MOS Devices*". IEEE Trans. On Electron Devices. Vol. 40. No. 5. 1993.
- [4] HP 4140B pA Meter/DC Voltage Source. Operation and Service Manual.
- [5] E. H. Nicollian and J. R. Brews, "*MOS Physics and technology*", Wiley, New York, 1981.
- [6] S. C. Witzcak, J. S. Suehle and M. Gaitan , "*An Experimental comparison of Measurement Techniques to Extract Si-SiO₂ Interface Trap density*" , Solid-State Electroniques Vol. 35, No. 3,pp. 345-355, 1992.
- [7] HP 4275A Multifrequency LCR meter. Operation Manual.
- [8] HP 8116A 50 MHz Programmable Pulse/Function generator. Operating and Programming Guide.
- [9] HP 5384A Frequency meter. Operating and Service Manual
- [10] HP 3478A Multimeter. Operator's Manual.
- [11] HP 4145B Semiconductor Parameter Analyzer. Operational manual.
- [12] Flight Electronics Professional IEEE 488 Device Driver. Reference manual.
- [13] A. Zitouni, M. Dehmas and H. Bourdoucen, "*An Integrated PC-Based system for Electrical Measurements and Analysis of Electronic Components*", International 93 Orlando Conference, Modelling, measurement and Control, A, Vol. 58, No. 1, 1994, pp. 1-9.
- [14] Y. Kribes, "*Optical and Electrical Characterisation of GaN Grown by MBE*", PhD thesis, University of Nottingham, Spt. 1998.
- [15] F. Rahmoune, "*Experimental Investigation of the Charge Pumping Current in Integrated MOS Transistors*", Magister Thesis , INELEC (Boumerdes), 1998.
- [16] A. Merabet, "*Modeling and Characterization of Electronic Components*", "Ingénieur d'état" Thesis, INELEC (Boumerdès), 1996.
- [17] C. M. Snowden, "*Semiconductor Device Modeling*", Word scinetific publishing, Co pte ltd, 1988.
- [18] Theo Smedes, "*Compact Modelling of the Dynamic behaviour of MOSFETs*", Ph.D. thesis, University of Eindhoven, Nederlands, 1991.
- [19] L. W. Nagel, PhD thesis, University of California, Berkley, 1975.
- [20] T. W. Thrope, "*Computerized Circuit Analysis with SPICE*", John Wiley and sons, Inc, 1992.
- [21] MicroSim PSPICE A/D, Circuit Analysis Software. Reference Manual.
- [22] A. S. Grove, "*Physics and Technology of Semiconductors Devices*" , John Wiley and sons, Inc, 1967.
- [23] S. M. Sze, "*Physics of semiconductor Devices*" , Jhon Wiley and sons, Inc, 1981.
- [24] R. M. Warner Jr., B. L. Grung "*Transistors Fundamentals for the integrated-Circuit Engineer*", Jhon Wiley and sons, Inc. 1983.
- [25] Paolo Antognetti and Giuseppe Massobrio, "*Semiconductor Device Modeling with SPICE*", Mc Graw-Hill Book Company, 1988.
- [26] A. B. Gaser and Subak-Sharpe, "*Integrated Circuit Engineering*", Addison-Wesley, Reading. Mass., 1979.
- [27] H. K. Gummel and H. C. Poon "*An Integral Charge Control Model of Bipolar Transistors*", Bell Syst. Tech. J.,49, 1970.

- [28] J. J. Ebers and J. L. Moll, "Large Signal Behavior of Junction Transistors", Proc. IRE, **42**, 1954.
- [29] S. L. Wong and C. A. T. Salama, "Improved Simulation of p- and n- channel MOSFET's Using an Enhanced SPICE MOS3 Model", IEEE Trans. Computer-Aided Design, Vol. CAD-6, No. 4, pp. 586-591, 1987.
- [30] D. E. Ward and K. Doganis, "Optimized Extraction of MOS Model Parameters", IEEE Trans. Computer-Aided Design of Integrated Circuits and Systems, Vol. CAD-1, No 4, pp. 163-168, 1982.
- [31] Peter R. Karlsson, "Direct Extraction of MOS Transistor Current Model Parameters", Technical Report No. 248, Department of Solid State Electronics, School of Electrical and computer Engineering, Chalmers University of Technology, Göteborg.
- [32] F. M. Klaassen, W. de Groot, and F. L. van de Markt, "Computer Algorithm to determine MOS Process-Parameters", Philips Res. Repts. **31**, pp 84-92, 1976.
- [33] M. F. Hamer, "First-order parameter extraction on enhancement silicon MOS transistors", IEE Proceedings, Vol. **133**, Pt. I, No. 2, pp. 15-22, 1986.
- [34] H. P. Tuinhout, S. Swaving, and J. J. M. Joosten, "A fully Analytical MOSFET Model Parameter Extraction Approach", IEEE Proc. Microelectronic Test Structures, Vol. **1** No. 1, pp. 79-84, 1988.
- [35] P. R. Karlsson and K. O. Jeppson, "An Efficient Parameter Extraction Algorithm for MOS Transistor Models", IEEE Trans. Electron Devices, Vol. **39**, No. 9, 1992.
- [36] Hewlett Packard Characterization Solutions, A quarterly Publication of Semiconductor Systems Center, Winter 1992.
- [37] M. Upadhy and A. P. Sathe, "An Integrated PC-based System for measurement of various Parameters for Two-Terminal Devices Used in Industry", IEEE Trans. On Instrumentation and Measurement; Vol. **41**, No. 5, Oct 1992.